THESIS APPROVAL

GRADUATE SCHOOL, KASETSART UNIVERSITY

Doctor of Engineering (Chemical Engineering)

DEGREE

Chemical Engineering	Chemical Engineering
FIELD	**DEPARTMENT**

TITLE: Reduction of NO over Copper Containing Silica-Aluminosilicate Catalysts: Effect of Chitosan Addition, Core-Shell Structure and Metal Incorporation Techniques

NAME: Miss Busaya Chamnankid

THIS THESIS HAS BEEN ACCEPTED BY

THESIS ADVISOR

(Associate Professor Paisan Kongkachuichay, Ph.D.)

THESIS CO-ADVISOR

(Associate Professor Metta Chareonpanich, D.Eng.)

DEPARTMENT HEAD

(Associate Professor Apinya Duangchan, Ph.D.)

APPROVED BY THE GRADUATE SCHOOL ON _____

DEAN

(Associate Professor Gunjana Theeragool, D.Agr.)

THESIS

REDUCTION OF NO OVER COPPER CONTAINING SILICA-ALUMINOSILICATE CATALYSTS: EFFECT OF CHITOSAN ADDITION, CORE-SHELL STRUCTURE AND METAL INCORPORATION TECHNIQUES

BUSAYA CHAMNANKID

A Thesis Submitted in Partial Fulfillment of
the Requirements for the Degree of
Doctor of Engineering (Chemical Engineering)
Graduate School, Kasetsart University
2012

Busaya Chamnankid 2012: Reduction of NO over Copper Containing Silica-Aluminosilicate Catalysts: Effect of Chitosan Addition, Core-Shell Structure and Metal Incorporation Techniques. Doctor of Engineering (Chemical Engineering), Major Field: Chemical Engineering, Department of Chemical Engineering. Thesis Advisor: Associate Professor Paisan Kongkachuichay, Ph.D. 114 pages.

This research focuses on the synthesis, characterization and activity of porous materials. The purpose of these works is to investigate the novel method to synthesize the mesoporous silica/aluminosilicate composites within one step via a sol-gel process. The pH condition of the hydrolysis-condensation process was found to be the main factor which affected the formation of core-shell structure or infiltration structure of silica and aluminosilicate materials. The mesoporous silica matrix was first developed in a strong acidic condition after that the pH of the solution was adjusted to 6.5 or 11.5. Since the silica solubility was significantly increased with the increasing pH therefore in a strong basic condition (pH 11.5), silica matrix was dissolved back into silicate form and reacted with the tetrahedral aluminates to form an aluminosilicate. Under this condition, the composite of aluminosilicate uniformly infiltrated in silica framework was established. On the other hand, in a slightly acidic condition of pH 6.5, the dense silica matrix could be dissolved only at the edge of the cluster. Therefore the aluminates could be formed and subsequently corner-linked with the unbound silicate starting from the outer layer of the dense silica matrix. As a result, a core-shell structure of silica and aluminosilicate shell was formed.

The synthesized materials were used as catalytic supporters composed of copper metal for NO_x removal process using H_2 as a reducing agent. Furthermore, two different techniques to introduce Cu species into the support including an incipient wetness impregnation method and a substitution technique were also studied. The amount of metal used in this work was also studied, and it was found that the maximum amount of copper was 1.5 wt% that could be incorporated inside the silica/aluminosilicate framework. By using the substitution technique, the copper species were expected to replace aluminum atoms of aluminosilicate. As a result, the tetrahedral coordination of Cu^{2+} atoms were surrounded with four framework oxygen atoms, at this position the Cu^{2+} atoms were being in the most stable site and were difficult to be reduced. On the contrary, in case of impregnation method was used, the Cu species were mainly existed at the outer surface of clusters and were easily reduced into Cu^{+1}. The Cu^{+1} species were considered to be the active sites for converting NO to N_2. When the effect of chitosan was investigated, it was found that the addition of chitosan created macropores and small domains which provided a higher capillary force between clusters of silica-aluminosilicate composites leading to a higher amount of Cu atoms which were trapped inside the pores. However, the excess Cu atoms and the macropores seem not to be necessary for the enhancing of NO conversion.

_____ / / _____

Student's signature Thesis Advisor's signature

ACKNOWLEDGEMENTS

I would like to express my sincere gratitude to my thesis advisor, Assoc. Prof. Dr. Paisan Kongkachuichay for his advice, knowledge, encouragement and support throughout this research. I am very thankful to Assoc. Prof. Dr. Metta Chareonpanich for her kindly giving the time to revise and fulfill my research. I am greatly indebted to Prof. Dr. Günther Rupprechter and Dr. Karin Föttinger who are my thesis co-advisor and give me a warm welcome at Institute of Materials Chemistry, Vienna University of Technology, Austria. Their suggestions on research work are sincerely acknowledged.

I gratefully acknowledge the financial support from the Thailand Research Fund (TRF) under the Royal Golden Jubilee Ph.D. Program (Grant No. PHD/0182/2008). This work was supported in part by grants from the National Science and Technology Development Agency (NSTDA Chair Professor and NANOTEC Center of Excellence), the Kasetsart University Research and Development Institute (KURDI), the Commission on Higher Education as well as the Ministry of Education, under the Postgraduate Education and Research Programs in Petroleum and Petrochemicals, and Advanced Materials.

I would like to thank for the help of my colleagues and for the assistance and valuable suggestion from administrative staffs and technical staffs at Department of Chemical Engineering, Kasetsart University. I also thank to members of Dr. Paisan's research group and Dr. Chareonpanich' s research group for their kind helps and supports. Finally, my appreciation devotes to my family who always give me supports and for their love, encouragement, and their understanding during the whole period of my education.

Busaya Chamnankid

April 2012

TABLE OF CONTENTS

LIST OF TABLES

LIST OF FIGURES

LIST OF FIGURES (Continued)

LIST OF FIGURES (Continued)

LIST OF FIGURES (Continued)

LIST OF ABBREVIATIONS

ASC	=	Silica-aluminosilicate composites prepared with the chitosan addition
ASP	=	Silica-aluminosilicate composites prepared without the chitosan addition
IASC	=	Silica-aluminosilicate composites prepared with the chitosan addition and loaded copper by impregnation method
IASP	=	Silica-aluminosilicate composites prepared without the chitosan addition and loaded copper by impregnation method
MCM-41	=	Mobil Composition of Matter No. 41
SASC	=	Silica-aluminosilicate composites prepared with the chitosan addition and loaded copper by substitution method
SASP	=	Silica-aluminosilicate composites prepared without the chitosan addition and loaded copper by substitution method

REDUCTION OF NO OVER COPPER CONTAINING SILICA-ALUMINOSILICATE CATALYSTS: EFFECT OF CHITOSAN ADDITION, CORE-SHELL STRUCTURE AND METAL INCORPORATION TECHNIQUES

INTRODUCTION

During the last decade a growing interest in the pollution problems by the scientific community, engineers or politicians has arisen, since identification of nitrogen oxide gas is considered as a participant in the destruction of the stratospheric ozone layer and in the greenhouse effect (Kramlich, 1994). Nitrogen monoxide (or Nitric oxide: NO) is one of the most prominent air pollutants, not only affects the environment but also results in health problems such as carcinomas, sclerosis, tissue toxicity, arthritis and ulcerative colitis (Tylor, 1997). In addition, it was found that the main source of NO is the combustion of fossil fuels such as petroleum in the engines of vehicles or coke in the electrical power plants (Klingstedt, 2006; Helms, 1993).

Nowadays, the increasing of NO_x which are gaseous pollution has been concerned significantly due to their toxicity which considerably affected both living and non-living organism. Due to the noxious effect of nitric oxide, many researchers attempt to decrease the level of nitrogen oxide emission by the decomposition of this toxic gas into other products via several methods. However, presently, only two main methods for removal of NO_x from emission gases are employed namely the three ways catalysts (TWC), which has been developed for mobile sources and the selective catalytic activity (SCR), which has been applied for stationary sources such as power plants and for lean-burn engines (Roy, 2009).

In order to increase the catalytic activity and selectivity for the reduction of NO, many developments and designs of catalyst have been investigated such as the using of bimetallic catalyst, supported transition metals and supported noble metals,

as well as controlling the activity and selectivity of such reactions by changing the architecture of nanoparticles. It was found that acidic supports, e.g. zeolites with Brønsted acid sites, were helpful to stabilize active metallic, as a result, high activity and selectivity were achieved on metallic catalysts (Yahiro and Iwamoto, 2001; Shibata *et al*., 2004). However, the possessed microporous structure is a limitation of the mass transfer also the strong acidic site of zeolite may cause a deactivation in the gas phase, thus the mesoporous materials having medium acidity could be applied in the abatement of NO_x (Karthik *et al*., 2009). The aluminosilicate is a material combining the advantages of two types of molecular sieves including the intrinsic acidities of zeolite and a better mass transfer as well as high abrasive resistance of mesoporous silica. Moreover, it was found that these composite materials exhibited more advantageous and higher activity than the mechanical mixtures.

In order to prepare the composite materials there are several techniques being used such as a two-template system presenting the simultaneous synthesis of MFI/MCM-41 phases (Karlsson *et al.*, 1999), a top-down and bottom-up synthesis of zeolite on a mesoporous silica wall (Ogura, 2008), and a plasma-spray technique for synthesis of the silica–aluminosilicate composites (Cipri *et al.*, 2007). However, most of these techniques were carried out by means of a two-step process, starting with the preparation of a zeolite precursor and then following by the use of surfactant micelles to assemble aluminosilicate species. By using the two-step process and controlling synthesis conditions such as hydrothermal temperature and crystallization period, the aggregation of ZSM-5/MCM-41 (Huang *et al.*, 2000; Feng *et al.*, 2008) and Beta/MCM-41 (Li, 2008; Zhang and Li, 2008) were achieved in each thermodynamically metastable region. In addition, it was shown that the core–shell structure of composite materials could be prepared by using the two-step process, e.g., the growth of silicalite shell on the surface of HZSM-5 core (Vu *et al.*, 2009), the composite of ordered mesoporous aluminosilicate core and wormhole structure of aluminosilicate shell (Zhai *et al.*, 2005).

The synthesis of the novel structure or the unique assembly of composite materials was supposed to enhance the catalytic properties, for instance, zeolite with

different topologies showed the significantly differences in NO reduction activities (Sultana *et al.*, 2008), the metal oxide–support interaction affects both the redox properties and the dispersion of the active metals (Auroux, 2000), also the use of co-precipitation method to prepare mixed metal-support can improve the sulfur resistance and increase the activity at low-temperature (Spassova *et al.*, 1999; Si, 2010). Li *et al.* 2005, synthesized Cu-ZSM-5 on the surface of honeycomb cordierite substrate to enhance the thermal and hydrothermal stability of ZSM-5/cordierite for the conversion of NO_x. However, only few researchers reported the synthesis of the catalysts having core-shell nanostructures to use as selective catalysis and membrane separation. Zhou *et al.* 2005 synthesized Pt–Cu bimetallic core–shell nanoparticles and tested their performance in the removal of NO, the results showed high activity and selectivity for NO reduction by H_2.

In this work, the mesoporous silica/aluminosilicate composites having core-shell structure and uniform infiltration were prepared by using one-pot synthesis. The effect of pH alternation and chitosan addition on the morphology and the development of large pores were investigated. After that the synthesized products were used as a support for deNO_x reaction by using copper and H_2 as an active metal and a reactant, respectively.

OBJECTIVES

1. To synthesize composites of silica/aluminosilicate with different morphology including silica-core aluminosilicate-shell and uniform infiltration of silica-aluminosilicate.

2. To study the effect of loading techniques including substitution technique and incipient wetness impregnation method.

3. To study the catalytic activity and selectivity of the synthesized catalysts via NO reduction by using H_2 as a reducing agent over copper active metal.

Scopes

1. To synthesize the mesoporous silica-aluminosilicate composites by using TEOS and aluminum nitrate as silica and alumina source, respectively, and CTAB-chitosan as binary templates, and also study the effect of the pH value on phase arrangements.

2. To characterize physical properties of catalyst; structure and morphology, surface area, nature and state of metal etc.

3. To incorporate copper metal into the silica-aluminosilicate composites support by using different procedures including substitution technique and incipient wetness impregnation method.

4. To determine the influence of core-shell structure on the activity and selectivity of NO reduction by using H_2 as a reducing agent at moderate reaction temperature range.

LITERATURE REVIEW

Mesoporous silica/aluminosilicate composites synthesis

In the past decades until now, mesoporous materials were synthesized to be used as the catalytic supporters in many reactions such as selective separation, CO_2 hydrogenation, stream reforming, water gas shift reaction, and NO_x reduction due to their high surface area and controllable pore size distribution. Especially, mesoporous silica, inert materials possess a high resistant after severe aging at high temperature.

In order to increase the catalytic activity, the synthesis of catalyst supporter which contains active metals within the framework was considered. In 1997, Corma synthesized mesoporous aluminosilicate material and found that the present of alumina metals inside the mesoporous silica framework would be increased the acidity of the catalysts. The acid catalyst gives satisfying performances in many reactions especially in catalytic cracking reaction. In 2004, Chao *et al*. clarified the mechanism to incorporate the metals into the silica framework by using an inorganic which was the precursor of silica and hydrolyzed metal salts in acidic condition (pH ~ 0). After that an ammonia solution was added, making the solution became alkaline (pH ~ 9.0) and co-condensation process was occurred rapidly as shown in Figure 1.

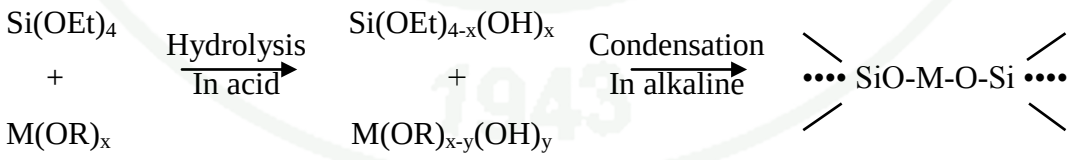

Figure 1 The incorporation mechanism of metals inside the silica framework

Source: Chao *et al.* (2004)

Since there are widely advantages, therefore many researchers have concentrated on the synthesis of these mesoporous materials. Many researches involve with the synthesis of silica/aluminosilicate material were found that pore size distributions, particle sizes, morphology or structure of framework and other properties all depended on types of precursors, surfactants and also the synthesis condition (Barrer, 1982). In this part, the background theories of the silica and/or aluminosilicate synthesis consisting of the preparation of mesoporous material via sol-gel process, the particle size control and the formation of large mesopores (macropores) by chitosan addition were described below.

1. The preparation of silica and aluminosilicate porous materials

Basically, there are three main steps to synthesize the mesoporous materials including micelle chemistry, sol-gel process and calcination. Beak *et al.* (1992) proposed two different mechanisms to form mesoporous silica as shown in Figure 2. The first one was based on the Liquid Crystal Templating (LCT) theory, by using this technique the molecules of surfactant working as a precursor of a silica framework preparation. The surfactants are dissolved in the solvent and then aggregated to form a rod structure called micelles which the hydrophilic head regions are in contact with surrounding solvent and the hydrophobic tail regions are in the micelle centre. When the solution is heated during the synthesis process, the micelles assemble and rearrange to form hexagonal arrays which then are attached with the following added silicate species. After the hydrolysis and condensation reaction occur the ordered hexagonal silica is formed. The second mechanism, Beck *et al.* (1992) proposed that the formation of hexagonal arrays is formed from the interaction of the added silicate species, making the micelles rearrange to structure a hexagonal shape.

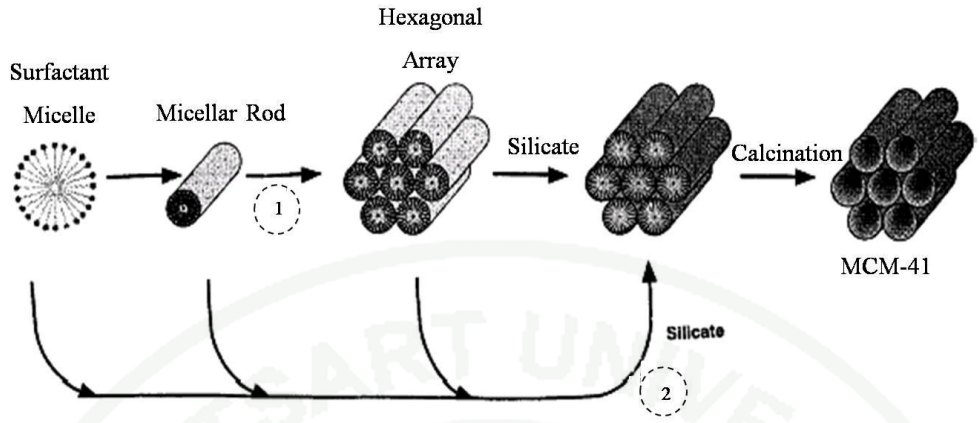

Figure 2 Possible mechanistic pathways for the formation of MCM-41: (1) liquid crystal phase initiated and (2) silicate anion initiated.

Source: Beak *et al.* (1992)

In 1993, Chen *et al*. also proposed the mechanism to form the mesoporous silica that it causes from the rearrangement of organic micelle rods which then are reacted with the silicate species, creating the thin layers surrounded the outer surface of micelles. After that the silanol groups (Si-OH) will interact with each other through a condensation reaction forming a long-range ordered silica framework with very high thermal stability. The illustration of proposed mechanism is shown in Figure 3.

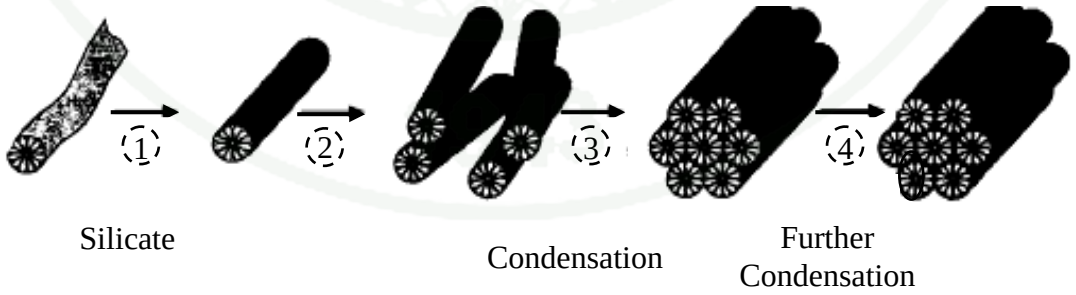

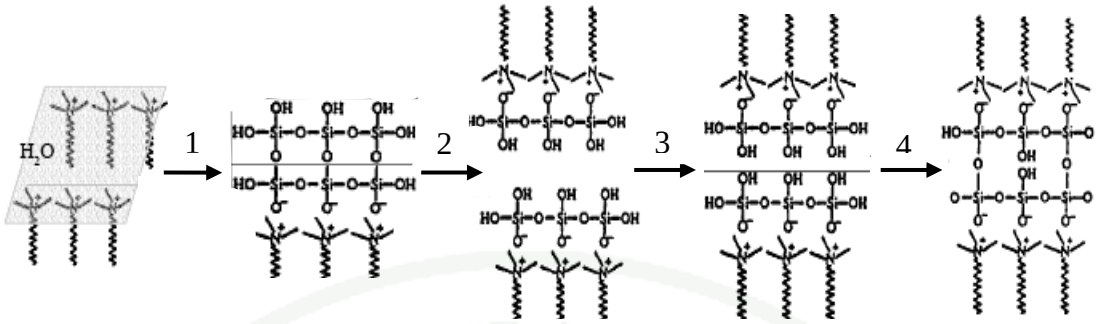

Figure 3 Mechanism of silica's mesopore formation

Source: Chen *et al.* (1993)

Commonly, there are four interaction patterns of surfactants and precursors as shown in Figure 4.

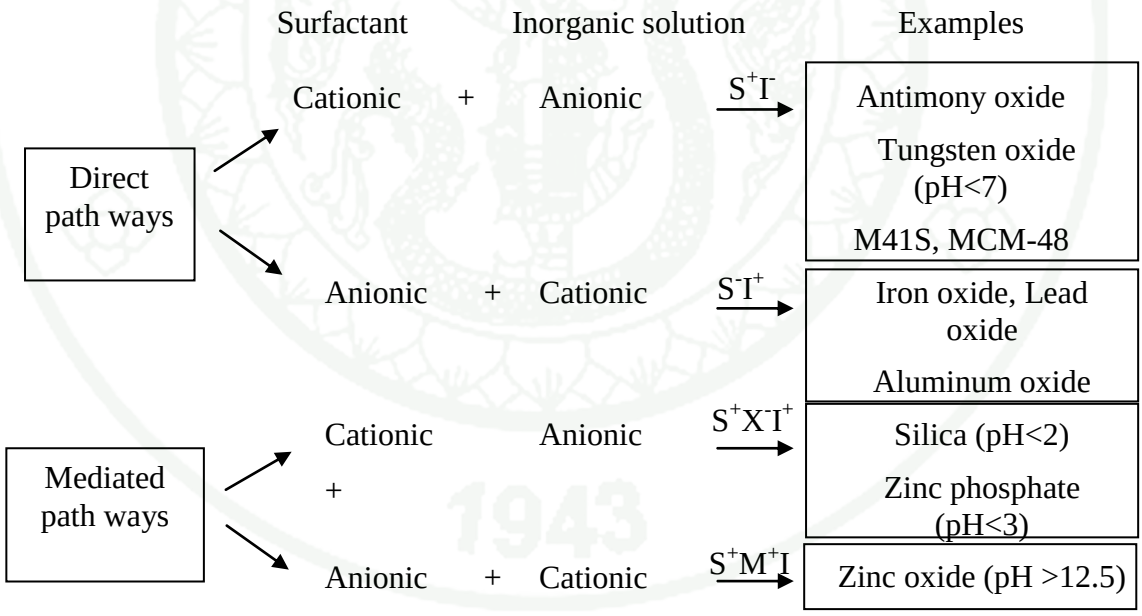

Figure 4 Synthesis of silica mesopores via combination of surfactant and inorganic solution

Source: Huo *et al.* (1994)

From the proposed mechanism, it was found that first two patterns showed the agglomeration between organic surfactants and inorganic silica precursors, having different charges. The other two patterns must have counter ions to act as intermediates to connect the organic surfactants and inorganic precursors which have the same charge together. The common used intermediates are alkaline metal and halide ion, which has cationic and anionic property, respectively. Cetyltrimethylammonium bromide (CTAB), which is the cationic surfactant having a hydrocarbon chain as the hydrophobic tail, a quarternary ammonium ion as the head group and bromide as counter ion, as shown in Figure 5., is often used for the synthesis of hexagonal mesoporous silica.

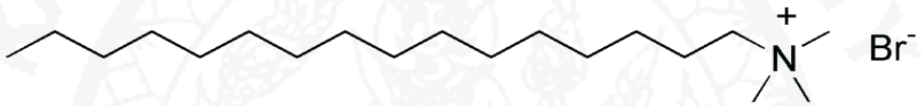

Figure 5 Chemical structure of Cetyltrimethyl ammonium bromide (CTAB)

Huo *et al.* (1994) proposed the path way embracing three steps to form mesoporous silica as shown in Figure 6. First, the molecules of organic surfactants and inorganic materials which is a silica precursor are interacted through the ion exchange process, which then the mesophase is formed. Lastly, the condensation process occurs resulting in the formation of rigid silica framework having the lamellar phase or hexagonal phase, both phases can be transformed to each other called “phase transformation”. As all mentioned above, it would be said that although the porous materials are formed from different path ways but the hierarchical structure of porous materials is controlled by the rearrangement of micelle in accordance with the concentration of surfactant, as schematically shown in Figure 7.

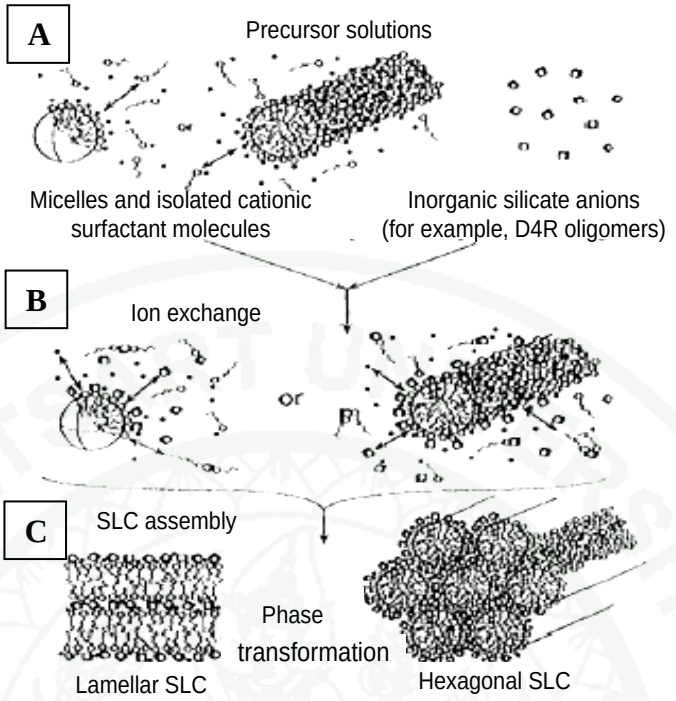

Figure 6 Schematic show formation mechanism of silica mesopore

Source: Huo *et al*. (1994)

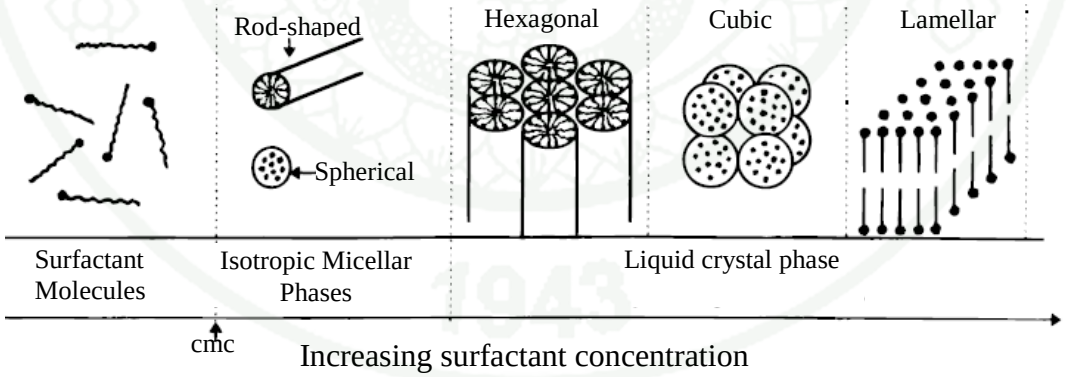

Figure 7 Phase sequence of surfactant-water binary system

Source: Myers (1992) and Lawrence (1995).

At low concentrations, the surfactant molecules exist as mono-molecules. As the concentration increased, the surfactant molecules will aggregate together to form

micelles in order to decrease the system entropy. The initial concentration threshold at which single atomic molecules aggregate to form isotropic micelles is called critical micellization concentration (CMC). As the concentration process still increases, hexagonal close packed arrays appear, producing the hexagonal phases (Lawrence, 1994). The next step in the process is the coalescence of the adjacent, mutually parallel cylinders to produce the lamellar phase. In some cases, the cubic phase also appears prior to the lamellar phase. The cubic phase is generally believed to consist of complex networks of rod-shaped aggregates (Fromherz, 1981).

According to Myers (1992), the particular phase present in a surfactant aqueous solution depends not only on the concentrations but also on the environmental parameters (pH, temperature, the ionic strength, and other additives) and the nature of surfactant itself (the length of the hydrophobic carbon chain, hydrophilic head group, and counter ion). Therefore, there was the developing of the use of bi-trinary template or dual surfactants in order to synthesize the porous silica having specialize structure such as bimodal porous materials. Sun *et al*. (2003) studied the synthesis of mesoporous silica contained two pore sizes by using two different types of surfactants including cetyltrimethylammonium bromide (CTAB) and pluronic P123. The synthesized processes could be divided into two steps comprising of the MCM-41 formation step using CTAB as a template, following by the addition of pluronic P123 to create the second pore sizes in the framework. These techniques were considered to be a model for many researched to prepare the bimodal porous materials which pore sizes could be varied from micropores to macropores.

Even though the silica mesopores possess a high surface area and thermal stability but when this kind of materials was applied for hydrocarbon cracking process, it was found that the catalytic activity of pure silica was lower than those of materials from aluminosilicate family. These could be explained that the acid sites of aluminosilicate, in particular the Brønsted ones (from the tetrahedral coordinated Al), are the active sites for most hydrocarbon reactions. As a result, many researchers have been proposed the procedures to induce the large amount of Al into the silica framework. The acidity of the mesoporous Al-containing MCM-41 catalysts was

increased with an increase Al incorporation into the framework of the materials. Jana *et al.* (2003) revealed four different techniques to prepare the mesoporous aluminosilicates including sol–gel technique, hydrothermal process, template cation exchange and grafting method. It was found that a different introduction of Al species into the silica framework greatly affected the amount of Al loaded and also physical-chemical properties of the prepared catalysts. The mesoporous Al-containing MCM-41 catalysts prepared by sol–gel, grafting and template cation exchange methods were effective for the incorporation of large amounts of Al into the framework of MCM-41, leading to different catalytic performances, as in these cases, the Al-containing MCM-41catalyst prepared by sol–gel method showed higher cracking activity, whereas that prepared by template cation exchange method showed higher dehydration activity. Also, the ordered mesoporous silica/aluminosilicate could be controlled via synthesis conditions (Wang, 2005; Yang, 2007).

Li (2006) synthesized the mesoporous aluminosilicates (Al-SBA-15) with low Si/Al ratios ranging from 1 to 10 using a single-source molecular precursor under acidic conditions. It was found that the pH values took the effect to the amount of Al incorporation. At pH lower than 1, the extremely low content of aluminum (Si/Al ratio of 79.47) in the materials was achieved, this caused from the dissociation of Si-O-Al bond in the single molecular precursor. However, when the pH was adjusted to 1.5, the Si/Al ratio of the sample was 9.50, implying that the dissociation of Al-O-Si bond was negligible. One thing should be concerned was the coordination environment of Al atoms. The ^{27}Al NMR spectra of samples were shown in Figure 8. Al-SBA-15 with Si/Al of 10 and 5 showed two resonance peaks at 0 and 50 ppm, which could be assigned to octahedral coordinated extra-framework aluminum and tetrahedral coordinated framework aluminum, respectively. In addition to the resonance at 0 and 50 ppm, the spectra of the samples with Si/Al ratios of 1 and 3 showed another resonance peak at 37 ppm, which can be assigned to distorted penta-coordinated aluminum species.

However, the mesoporous aluminosilicate can also be synthesized in a strong basic condition as reported by Yang (2007), who synthesized ordered 2D-hexagonal

(p6mm) mesoporous aluminosilicates with very low Si/Al ratio of 1.9 in strongly alkaline media (pH of 14) using aluminosilicate ester ($(Bu^sO)_2$-Al-O-Si-$(OEt)_3$) as single-source molecular precursor and CTMABr as surfactant.

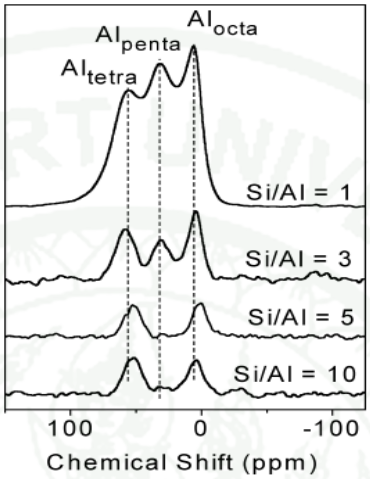

Figure 8 ^{27}Al MAS NMR spectra of the calcined Al-SBA-15 with Si/Al ratios of 1, 3, 5 and 10.

Source: Li *et al.* (2006)

^{27}Al NMR spectrum of as-synthesized mesoporous aluminosilicates showed a sharp and symmetrical signal centered at 53 ppm, indicating that aluminum atoms have been successfully incorporated into the mesoporous framework in tetra-coordinated position. There was very small resonance of Al atoms located in octahedral position at 0 ppm could be observed, indicative of the presence of a very small amount of extra framework Al species. These mean all the Al atoms are linked with Si atoms and there is no cleavage of Si–O–Al linkage present initially in single source molecular precursor, the homogeneity of Si–O–Al linkages and tetrahedral aluminum sites are essential and very important in catalysis for activity, selectivity and stability. From the previous researches, it would be said that the porous silica or aluminosilicate materials could be synthesized via a sol-gel process with the pore size, structure, morphology and inorganic contents of the materials were controlled by types of surfactants, concentration surfactants, temperature, pH values and so on.

2. Synthesis of silica/aluminosilicate composite materials

The synthesis of composite materials combining the advantages of two types of molecular sieves has been of great interest as they are of zeolite, with strong intrinsic acidities providing an important role in acid catalysis, and mesoporous silica, giving a better heat and mass transfer as well as high abrasive resistance. Moreover, it was found that these composite materials exhibited more advantageous and higher activity than mechanical mixtures (Huang *et al*., 2000; Li *et al.*, 2008; Zhang and Li, 2008). There are several techniques to prepare these composite materials, for example, a two-template system presenting the simultaneous synthesis of MFI/MCM-41 phases (Karlsson *et al.*, 1999; Hui *et al.*, 2008), a top-down and bottom-up synthesis of zeolite on a mesoporous silica wall (Ogura, 2008), impregnation-recrystallization method of zeolite-silica composites (Hui *et al.*, 2008) and a plasma-spray technique for synthesis of the silica–aluminosilicate composites (Cipri *et al.*, 2007). Karlsson *et al.* (1999), synthesized the composites of micro- and mesoporous materials: simultaneous synthesis of MFI/MCM-41 by using mixed templates of $C_6H_{13}(CH_3)_3NBr$ and $C_{14}H_{29}(CH_3)_3NBr$. The suitable concentration of templates and reaction temperatures were studied in order to obtain the fairly complex aggregates of MFI and MCM-41 type material. MFI-type crystals embedded partly in MCM-41 aggregates, as well as MFI type crystals partly covered with thin surfaces of MCM-41 like material occurred frequently. Hui *et al.* (2008) studied the crystallization periods which suitable for the synthesis of the composites of ZSM-5 on the silica gel microspheres by using n-butyl amine as the template. Silica gel microspheres were fully impregnated to incipient wetness by an aqueous $NaAlO_2$ solution, after drying process, the impregnated silica microspheres were mixed with an aqueous n-butyl amine solution, an aqueous sodium hydroxide solution and an aqueous sodium nitrate solution. This step the channels of the silica gel were filled with the aluminates source, alkaline source, and template, thus, the entire crystallization reaction occurred on the silica gel microspheres. Therefore, during the crystallization reaction, the silica gel played dual roles support and silica souses. Therefore, if the crystallization time was too short, the amount of synthesized zeolite would be insufficient to cover the silica gel microspheres but if the crystallization time was too long, the silica gel

would be consumed gradually as silicon source and finally completely transformed to ZSM -5 crystals as shown in Figure 9.

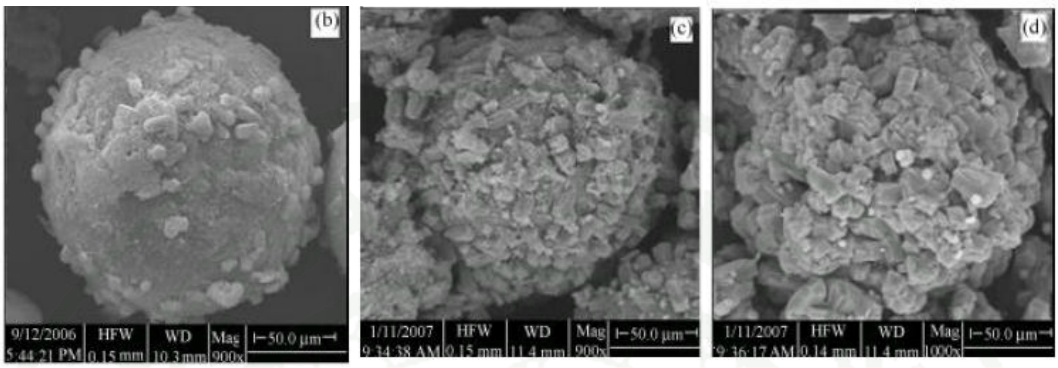

Figure 9 Scanning electron microscope (SEM) photographs of the composite materials with different crystallization times (b): 12 h; (c): 18 h; (d) 24 h

Source: Hui *et al.* (2008)

Huang *et al*. (2000) prepared the MCM-41/ZSM-5 composites by using dual templates, including cetyltrimethylammonium bromide and tetrapropylammonium bromide, through a process of two-step crystallization. During the pretreatment of inorganic species and TPA^+ cations, the amorphous framework of MCM-41 can be recrystallized, producing two kinds of MCM-41/ZSM-5 composites. Crystallized mesoporous MCM-41 containing only short-range ordered ZSM-5structure was first synthesized in the early stage of the recrystallization. With the increase of recrystallization time, some discrete micron-sized ZSM-5 crystals were produced and firmly attached to the loose aggregates of crystallized MCM-41, and another kind of MCM-41/ZSM-5 composite containing interconnected mesopores and micropore was therefore obtained. Hidrobo *et al.* (2003) also exhibited the formation of composites between commercial zeolite and a sol precursory of aluminosilicate in order to improve the diffusion of interested species towards active sites. The silica-alumina/zeolite composites were prepared at room temperature and basic pH by using the sol-gel method in combination with co-precipitation method.

However, most of these techniques were carried out by means of a two-step process, beginning with the preparation of a solution including a zeolite precursor and then followed by the use of surfactant micelles to assemble aluminosilicate species. By using this two-step process and controlling synthesis conditions such as hydrothermal temperature and crystallization period, the aggregation of zeolite/silica materials were achieved in each thermodynamically metastable region. (Huang *et al.*, 2000; Li *et al.*, 2008; Zhang and Li, 2008; Hui *et al.*, 2008; Prokesˇova´-Fojtı´kova´ *et al.*, 2006). In addition, it was also shown that the using two-step process, the core–shell structure of composite materials could be prepared e.g., the growth of silicalite shell on the surface of HZSM-5 core (Vu *et al.*, 2009), the composite of ordered mesoporous aluminosilicate core and wormhole structure of aluminosilicate shell (Zhai *et al.*, 2005).

Vu *et al*. (2009), synthesized silicalite/HZSM-5core-shell composite catalysts by optimizing the silicalite coating conditions, which was the changing of molar ratios of silica source and TPAOH structure directing agent (SDA) in the coating solutions. At low molar ratios of fumed silica SiO_2 and TPAOH in the coating solutions, a crystal growth of silicalite layer on the HZSM-5 surface was dominant instead of a homogeneous nucleation in the solution. Zhai *et al.* (2005) also prepared core-shell mesoporous materials comprised of aluminosilicate shell with wormhole framework structure and well-ordered hexagonal mesoporous aluminosilicate (MSU-S) core as shown in Figure 10. Obviously, it was demonstrated that the shells had a disordered wormhole-like pore structure, which was less ordered than that of the interior of the particles. The core/shell structure was created from the partly degraded of silicates from the parent MSU-S particles and led to the over growth of a thin aluminosilicate layer on the retained MSU-S particles.

Nevertheless, only a few studies focused on the synthesis of the core–shell structure by using one-pot synthesis, which exploited a combination of templating surfactant and the self-formation phenomenon of porous hierarchy. The formation of macroporous aluminosilicate with high Al content was mostly attributed to the fast hydrolysis and polymerization of the aluminosilicate ester, and the ordered

mesoporous shell with the lower Al content could only be formed via a surfactant-templating mechanism (Yang *et al.*, 2009).

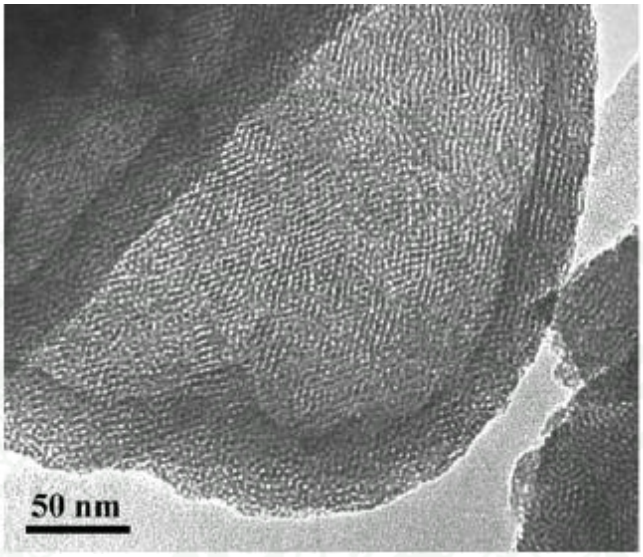

Figure 10 TEM images of the shell micro sectioned from the composite material

Source: Zhai *et al.* (2005)

3. The use of chitosan as a template

There are some catalysts require the large mesopores or macropores in order to control the reactants and products transfer. Therefore the addition of macromolecule polymers was used to modify the pore sizes as well as the domain sizes of these materials (Ishizuki *et al.*, 1991; Aramendía *et al.* 2004; Zhai et al., 2007; Li *et al.*, 2008). Chitosan is a low cost, nontoxic and biodegradable polymer. It is produced commercially by deacetylation of chitin, the molecular structure is formed from the amino and hydroxyl groups as shown in Figure 11, which make chitosan itself hydrophilic and poly-cationic property.

In 2000, chitosan biopolymer was first used as the template for the synthesis of monolithic silica with meso-macropore; the pre radius distribution was polymodal with maxima at 0.84, 1.0, 1.2 and 1.5 nm, and a broad band between 3 and 10nm. The

formation of these structures may be due to the aggregation of hydrated chitosan with different sizes and the gelation of the system (Pedroni *et al.*, 2000)

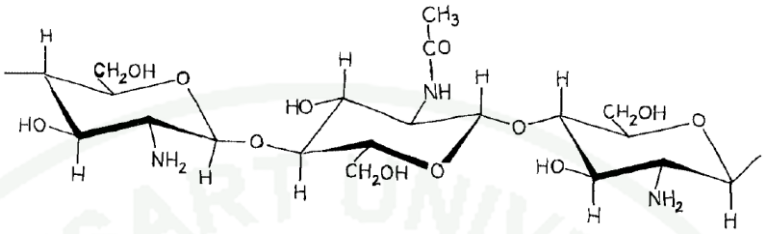

Figure 11 A schematic illustration of the structure of chitosan.

Source: Pedroni *et al.* (2000)

Hidrobo *et al.* (2003) synthesized bimodal micro-mesoporous silica-alumina/zeolite composites at room temperature using chitosan as a template. It was found that the present of chitosan leads to the narrower distribution of pore sizes since the chitosan can form a hybrid precursor with an inorganic network via hydrogen bond. Next year, Molvinger *et al.* (2004) also synthesized porous chitosan-silica hybrid microspheres with two step procedures. First, induce an auto assembling of the polymer chains as a gel and the second, concern the silica condensation. Depending on the experimental conditions, a core/shell structure could be formed with the core was constituted by a homogeneous hybrid, while the shell was pure silica.

Tsai and Li (2006) prepared a hollow silica sphere via chitosan-polyacrylic acid (CS-PAA) template. In an initial step, the colloidal silica was prepared from homogeneous nucleation and then was mixed with a solution of CS-PAA particles. The negatively charged colloidal silica was adsorbed on the positively charged surface of the CS-PAA particles resulting in the formation of a core-shell structure. The CS-PAA was removed from the core of the particles by adjusting with HCl to pH < 1 for obtaining the hollow silica structure as shown in a model in Figure 12.

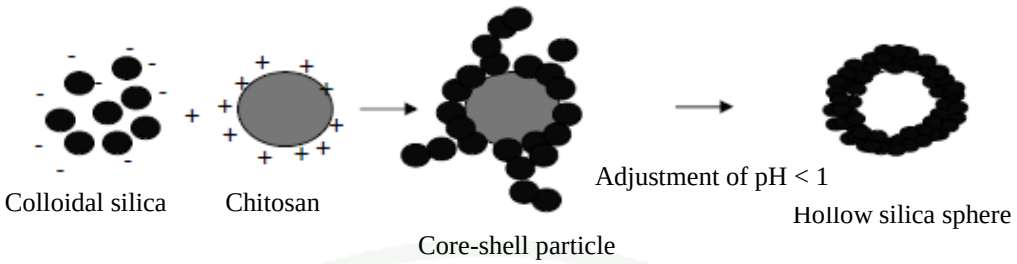

Figure 12 The model of formation hollow silica sphere

Source: Tsai and Li (2006)

Due to the chitosan is a natural material and there is a different polymerization and deacetylation degree of chitosan, these physical–chemical properties significantly influence the morphology of the synthesized materials. Braga *et al.* (2009) prepared hybrid mesoporous spheres of Al and Si oxides using the chitosan as template and it was observed that chitosan with larger polymerization degree, resulted in a larger mechanical resistance of the spheres. Since a greater molar mass of biopolymer requires a greater molar fraction of inorganic material in order to form spheres and the larger volume of inorganic material will increase the mechanical resistance of the spheres.

It is also known that the hydrodynamic and theological behavior of chitosan macromolecules in solution depends on factors such as polymer concentration, temperature, shear stress, surfactant concentration, hydrophobicity of the polymer and especially the pH of the solution. Due to the fact that the solubility of chitosan is depended on the pH value: the in acidic condition chitosan shows the highest solubility since the hydroxyl group is protonated and the solubility starts to be decreased as the increasing of pH. At pH value was higher than 6.4 the chitosan will be aggregated and precipitated, and the phase separation occurs (Kjoniksen *et al.*, 1997). As shown in Witoon *et al.* (2008)'s work which proposed that the pH values played the most important role on the directing of pore sizes in the range of mesoporous structure of the silica support. The bimodal meso-macroporous silica

was synthesized by using rice husk ash and chitosan as silica source and template, respectively. It was found that the formation of mesopores came from the aggregation of silica species while the formation of macropores was formed from the decomposition of chitosan template during the calcination process. At the pH value of 2, the dispersion of chitosan was high resulting in the formation of small pores in the region of micro-mesopores while at higher pH values there were the cross-linking between the chitosan and silica, leading the formation of meso-macropores inside the framework. In 2009, Witoon *et al.* (2009) investigated the effect of acidity on the formation of silica–chitosan hybrid materials turning the pH value of the mixture from 2 to 6, and it was found that in a strong acidic condition, the amino groups of chitosan were highly protonated while the zero charge of silica surface was simultaneously formed, resulting in the prevention of silica particles aggregation. On the other hand, at higher pH condition, the dense chitosan network was formed causing the silicate species can be condensed only in the void of chitosan network, therefore the growth of the silica framework was limited leading to the decreasing of silica clusters size and increasing the amount of macroporosity as shown in Figure 13.

Lixia Wang (2010) studied the interaction between chitosan and CTAB templates during the formation of porous silica, and it was found that the molecular orientations around the C=O groups and the NH_2 groups of chitosan were greatly affected by adding CTAB at lower pH, corresponding to a slow transition process of micelles. The work was indicated that micro–meso silica can be synthesized with the chitosan–CTAB hybrid which the meso-periodity of silica is formed from the inter-molecular interactions between chitosan and CTAB at proper pH value.

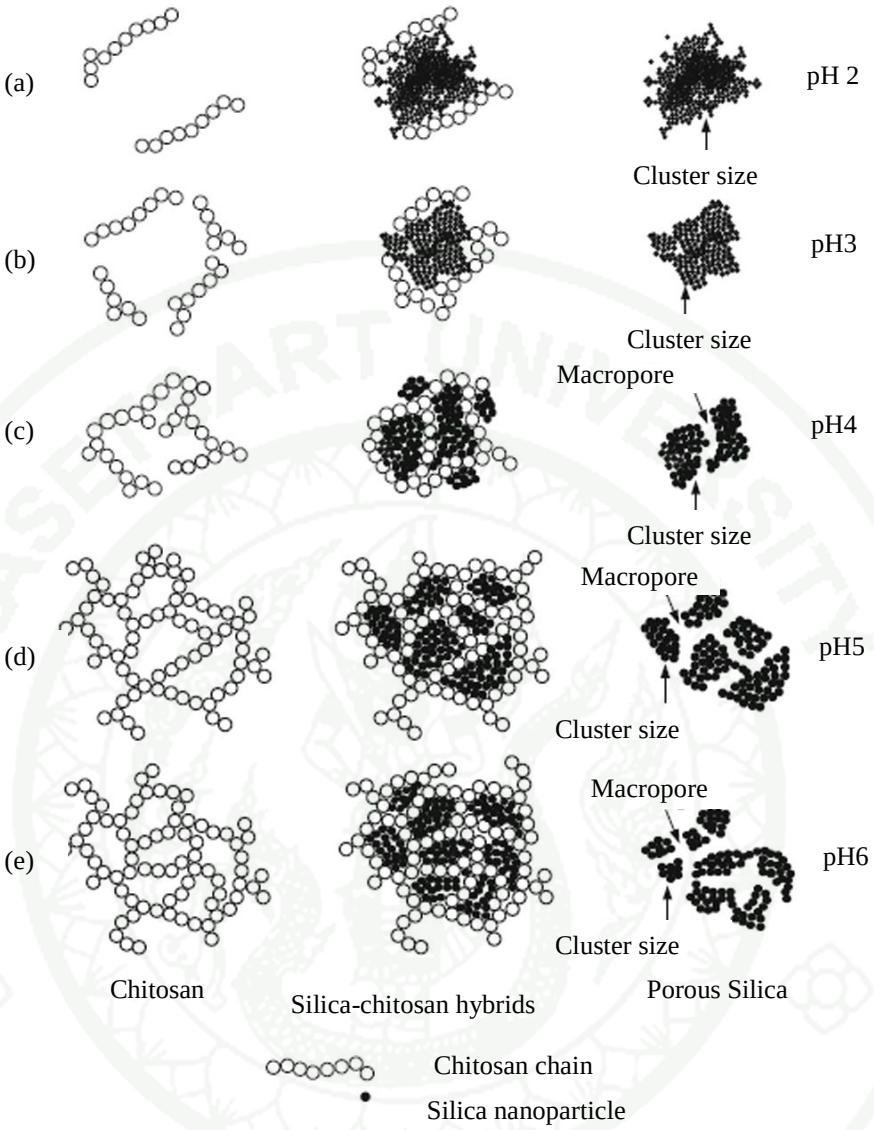

Figure 13 Schematic representation of silica–chitosan hybrids formation: structure of chitosan, as-synthesized silica–chitosan hybrids, and porous silica products synthesized at pH 2(a), pH 3 (b), pH 4 (c), pH 5 (d), and pH 6 (e)

Source: Witoon *et al.* (2009)

Removal of NO via reduction process

Selective catalytic reduction (SCR) is one of the main processes applied to remove NO from the automobile and stationary sources. By using this technique, the gaseous reactant is added to a stream and is adsorbed on the catalyst surface where the reduction reaction is taken place, and then NO_x will be converted into N_2 and H_2O. Since the catalysts play the most important role in this process therefore many types of high active and stable catalysts have been developed in order to apply for SCR process such as activated carbon-supported catalysts (Papageorgiou *et al.*, 2011), acidic catalysts (Kharas, 1995), bi-tri metallic catalysts (Hungr´ıa *et al.*, 2001; Pantazis and Pomonis, 2006), and structure-shape controlled porous catalyst (Liu *et al.*, 2010). Besides catalytic supporters, types and natures of metal, varieties of reducing agents and operating conditions also considerable affect the catalytic performance (Tseng *et al.*, 2010; Scholz *et al.*, 2008). In this work, the literatures of SCR process were studied, especially focusing on the using of silica/aluminosilicate as a supporter. Besides, the incorporation procedures of metal species into the support were also described. By using of different techniques were found to be affected the dispersion of metal and the position where metal particles were deposited, these related to the catalytic performances.

1. Selective catalytic reduction (SCR) for NOx removal process

In the past two decades, research in the field of NO_x abatement has grown significantly due to the noxious effect of nitrogen oxides (NO_x). The major source of NO_x is the combustion of fossil fuels such as petroleum in the engines of vehicles or coke in the electrical power plants as shown in Figure 14.

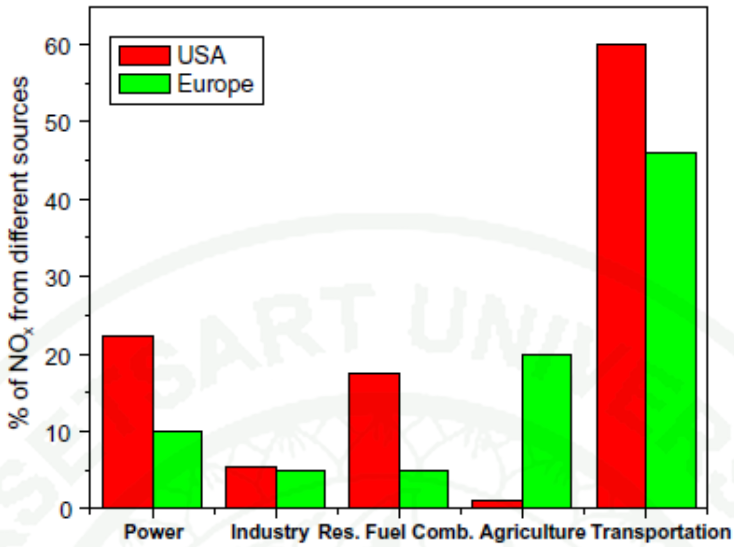

Figure 14 Emission of NO_x by source category in USA and European countries

Source: Roy *et al.* (2009)

It was found that the oxides of nitrogen acts as an essential messenger, which transmits the necessary information to the white blood cells within the bloodstream to destroy tumor cells and to the neurotransmitters to dilate the blood vessels (Fritz and Pitchon, 1997). In addition, NO_x also takes an effect on the photochemistry of the troposphere and stratosphere. NO_x catalyzed ozone destruction occurs via the following reactions:

$$NO + O_3 \rightarrow NO_2 + O_2 \quad (1)$$

$$NO_2 + O \rightarrow NO + O_2 \quad (2)$$

As a result, many researchers attempt to decrease the levels of nitrogen oxide emission by decompose this toxic gas in several methods. The main process can be divided into four major paths based on automobile and stationary sources involved:

(i) NO decomposition;

$$NO \rightarrow \frac{1}{2}N_2 + \frac{1}{2}O_2,\ \Delta H^o_{298} = -86.6\ kJ/mol \quad (3)$$

(ii) NO reduction by CO;

$$NO + CO \rightarrow \frac{1}{2}N_2 + CO_2,\ \Delta H^o_{298} = -328\ kJ/mol \quad (4)$$

(iii) NO reduction by H_2 and NH_3;

$$NO + H_2 \rightarrow \frac{1}{2}N_2 + H_2O,\ \Delta H^o_{298} = -287\ kJ/mol \quad (5)$$

$$6NO + 4NH_3 \rightarrow 5N_2 + 6H_2O \quad (6)$$

(iv) SCR (selective catalytic reduction) of NO by H_2, NH_3 or hydrocarbon.

$$4NO + 4NH_3 + O_2 \rightarrow 4N_2 + 6H_2O,\ \Delta H^o_{298} = -1{,}627\ kJ/mol \quad (7)$$

$$NO + CH_4 + \frac{3}{2}O_2 \rightarrow \frac{1}{2}N_2 + CO_2 + 2H_2O, \quad (8)$$

$$\Delta H^o_{298} = -847\ kJ/mol$$

The above four methods can be reclassified into two majors paths including the catalytic decomposition of NO_x occurs in absence of a reducing agent (i) and the catalytic reduction of NO_x occurs in the presence of a reducing agent (ii–iv) (Roy *et al.*, 2009). The common reducing agent which was used to remove NO is CO or H_2 which is sufficiently presented in the exhaust gas (which typically contains H_2, CO, HC and O_2) from the diesel or lean-burn engines (Wen, 2002).

However, in a diesel oxidation catalyst, a number of critical conditions were identified for which significant deactivation occurred, e.g.: (i) high temperature and presence of H_2O caused significant loss of hydrocarbon storage capacity; (ii) low temperature, generally in combination with H_2O, facilitated adsorption of sulfur species, which moreover proved to be stable at temperatures above normal operating

conditions of a typical converter; (iii) loss of catalyst performance at low temperature due to accumulation of catalyst poisons was equally pronounced as the degradation occurring from aging at high temperature (Andersson *et al.*, 2007). Therefore, in order to increase the catalytic activity and selectivity for the reduction of NO there are many developments and designs of catalyst such as the using of bimetallic catalyst, supported transition metals and supported noble metals, as well as controlling the activity and selectivity of such reactions by changing the architecture of nanoparticles. Moreover, in the last decade, many researchers proposed the architecture of nanoparticles and surface states of catalyst influence the catalytic properties, for instance, zeolite with different topologies showed the significantly differences in NO reduction activities (Sultana *et al.*, 2008), the metal oxide–support interaction affects both the redox properties and the dispersion of the active phase (Auroux *et al.*, 2000) and the co-precipitated could improve the sulfur resistance and the low-temperature activity (Spassova *et al.*, 1999; Si *et al.*, 2010).

2. Catalysts used for SCR process

2.1 The use of silica/aluminosilicate as a supporter

There are different types of materials which were reported as the candidates for the catalyst of the direct decomposition of NO such as TiO_2 (Jiang et al 2004), $A1_2O_3$ (Scholz *et al.*, 2008), MgO (Iwamoto *et al.*, 1990) and carbon (Papageorgiou *et al.*, 2011). However, ZSM-5 zeolite was found to be the most favorite support for NO removal process due to its own acidic property which enhances the NO decomposition step (Kharas *et al.*, 1995; Iwamoto *et al.*, 1990; Wen, 2002). Iwamoto *et al.* (1990) presented several works showing a high performance of copper containing zeolite support. Shibata *et al.* (2004) also reported that acidic supports, e.g. zeolites with Brønsted acid sites, are helpful to stabilize active metallic Pt, as a results, high SCR activity and high N_2 selectivity are achieved on Pt catalysts on acidic supports. On the other hand, the transition metal exchanged zeolites were found to be unstable under hydrothermal conditions hence they were unlikely to be practical catalysts for lean NO_x abatement Yahiro *et al.* (2001). Conversely, it has also

been reported that the use of silica materials as catalyst supports have remarkable effects on the activity of the resulting catalyst for NO reduction.

Actually, it was known for a long time that silica mesoporous material was the good choices to be used as catalytic supporters for many reactions as well as the selective catalytic reduction (SCR) of NO (Coma, 1997; Kresge *et al*. 1992). Shen and Kawi (2003) synthesized Pt supported on siliceous MCM-41, these catalysts showed better activity for NO reduction than Pt/SiO_2 and Pt/Al_2O_3 under the same reaction conditions, resulting from the larger surface area and pore volume of MCM-41. Moreover, it was also found that the adsorption amount of SO_2 over the Pt-MCM-41 catalyst was much less than those over Cu-ZSM-5 and Cu-MCM-41 (Shen and Kawi, 2003). As well as Pantazis 's work showed that Cu/Ce bimetallic loaded mesoporous silica could be used as catalyst for the simultaneous elimination of all three major air pollutants; SO_2 and NO with CO (Pantazis and Pomonis, 2006). Chmielarz *et al*. (2006) used the different types of mesoporous silicas (MCM-48, SBA-15, MCF), reflecting various porous structures, modified with transition metals for NO reduction. The catalytic performance of the studied samples depended on the type of silica support used and the method applied for the deposition of transition metal oxide. The surface acidity of pure mesoporous silica was characterized by ammonia chemisorptions and was found that MCM-48 support showed no ammonia chemisorption. Only a very small surface acidity was detected for the SBA-15 silica, while significantly larger surface concentration of acid sites was measured for MCF support. Strongly chemisorbed ammonia partially reduced transition oxide species with the evolution of N_2 and N_2O.

In 1999, Long and Yang (1999) showed the conversion of NO_x with C_2H_4 on copper and/or cerium ion-exchanged Al-MCM-41 compared with Cu-ZSM-5, the results are showed in Figure 15.

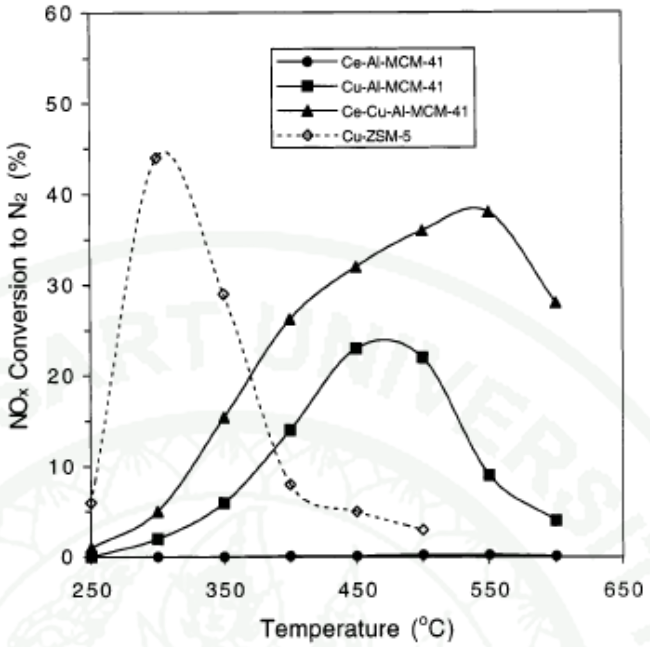

Figure 15 Conversions of NO_x for the SCR reaction on Ce-Al-MCM-41, Cu-Al-MCM-41, Ce-Cu-Al-MCM-41, and Cu-ZSM-5

Source: Long and Yang (1999)

It was found that the maximum activity of Ce-Cu-Al-MCM-41 was close to that of Cu-ZSM-5, but the former had a wider temperature window. Moreover, the using of Al-MCM-41 as the support also showed a high hydrothermal stability after heating at 800 ˚C in the presence of H_2O. Karthik *et al*. (2009) also compared the catalytic activity of Cu-Al-MCM-41 materials synthesized by hydrothermal treatment method with those of copper ion-exchanged H-ZSM-5 (Cu-ZSM-5) for the SCR of NO with hydrocarbon. The result was found that the Cu–Al–MCM-41 catalyst exhibited a long-term-stability than that of copper ion-exchanged H–ZSM-5 (Cu–ZSM-5) zeolite based on the deactivation of Cu-ZSM-5 by coke deposition in the vapor phase. In addition, the presence of aluminum (Al^{3+} ions) within the framework of Cu–Al–MCM-41 stabilized the isolated Cu^{2+} ions thus it led to higher and stabilized activity in terms of NO_x reduction.

Therefore the incorporation of Al species into the MCM-41 such as AlSBA-15 and aluminosilicate (Al-MCM-41) supports was considered to be a new material having the strong acid site and enhancing the NO conversion (Brandhorst *et al*., 2005; Wu *et al.*, 2010). Oh and Woo (2006) prepared Pt-supported on mesoporous Al/SBA-15 and Pt-supported on mesoporous SBA-15, the results were found that the incorporation of aluminum into SBA-15 created acidic sites. With the presence of acid sites, the performance of NO removal will be enhanced. Also, Wu *et al*. (2010) introduced Al species into the framework of Si-MCM-41 support by isomorphous substitution (Al-M-xs) and wet impregnation (Al-M-xi), and where x indicated the Si/Al ratio, and Brønsted acid sites can be created in Al-MCM-41. Pt catalysts supported on Si-MCM-41 and Al-MCM-41 were studied for the selective catalytic reduction of NO by hydrogen in excess oxygen, the results were showed in **Figure 16**. It was found that the N_2 selectivity over Pt/Al_2O_3 was the lowest one at the whole temperature range whereas the N_2 selectivity of 50–80% can be obtained on Pt/Si-MCM-41 in the temperature range of 60–160 ˚C. The introduction of Al species to MCM-41 results in the enhancement of N_2 selectivity at high temperatures.

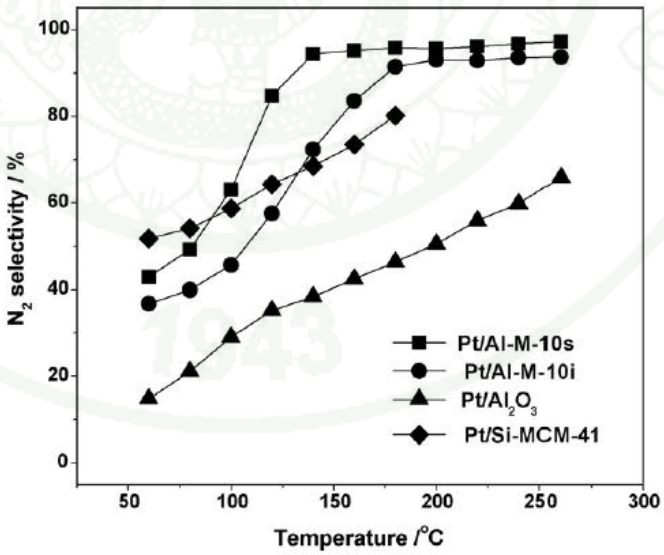

Figure 16 N_2 selectivity during H_2-SCR on different Pt catalysts

Source: Wu *et al*. (2010)

However, there are different H_2-SCR reaction part ways between the use of Si-MCM-41 and Al-MCM-41 as supports. Based on in situ DRIFT spectra observation, Burch and Coleman (2002) proposed the H_2-SCR pathway on Pt/Si-MCM-41 as shown below:

At an initial step, gaseous NO adsorbs on the surface of Pt species as

$$NO(g) + * \rightarrow NO* \quad (*: \text{active sites})$$

Adsorbed NO may dissociate and recombine to produceN_2 and by-product N_2O

$$NO* + * \rightarrow N* + O*$$
$$N* + N* \rightarrow N_2 + 2*$$
$$N* + NO* \rightarrow N_2O + 2*$$

The adsorbed NO species are oxidized to adsorbed nitrites or nitrates

$$NO* + O_2 \rightarrow NO_2*/NO_3*$$
$$NO_2*/NO_3* + N* \rightarrow N_2 + N_2O$$

In addition, with the introduction of Al species to Si-MCM-41, the introduction of Brønsted acid sites, the adsorbed species on catalysts change greatly and a different H_2-SCR reaction pathway is proposed for Pt/Al-MCM-41 with Brønsted acid sites by Richter *et al.* (1998) as shown below:

In the initial step, gaseous NO adsorbs as linear NO species on the sites of Pt. The adsorbed NO species easily dissociate to produced adsorbed N and adsorbed O

$$NO + {}^{*} \rightarrow - NO$$
$$-NO + {}^{*} \rightarrow -N + -O$$

The adsorbed N may react with active hydrogen to produce $–NH_3$ on Pt sites. This may be possible pathway for the formation of N_2 and N_2O at low temperature, similar to that on Pt/Si-MCM-41.

$$N^* + N^* \rightarrow N_2 + 2^*$$
$$N^* + NO^* \rightarrow N_2O + 2^*$$

Alternatively, the adsorbed N may react with active hydrogen to produce $–NH_3$ on Pt sites

$$N^* + 3H^* \rightarrow –NH_3 + 3^*$$

The NH^{4+} species react with gaseous NO and O_2 to produce N_2 and H_2O with high reactivity and selectivity which then migrate and store on the Brønsted acid sites

$$4NH^{4+*} + 4NO + O_2 \rightarrow 4N_2 + 6H_2O + 4H^{+*}$$

These could be concluded that the acidic sites on the support enhanced the catalytic activity, therefore, in the last decades many reports have been proposed the use of silica/aluminosilicate as a catalytic supporter for NO removal process as aforementioned.

2.2 Types and natures of metal species

Several types of metal have been loaded into the supports in order to use as catalyst for the selective catalytic reduction (SCR). The three-way catalyst (Pt, Pd, and Rh) has been used commercially in gasoline engines for reduction of NO to N_2 by carbon monoxide and hydrocarbons. However, the using of these kinds metals

becomes ineffective in the presence of excess oxygen (Long and Yang, 1999). Since reported by Iwamoto *et al.* (1990); Held *et al.* (1990) that copper metal could selectively reduce NO_x by hydrocarbons (e.g., C_2H_4,C_3H_6, C_3H_8, etc.) in the presence of excess oxygen, this topic has been extensively studied all over the world in recent years (Long and Yang, 1999). It have been found that copper catalysts could be applied in a wide range of this reactions such as; photocatalytic NO (Anpo *et al.*, 1997) and selective catalytic reduction of NO with ammonia (Chmielarz *et al.*, 2005).

Brandhorst *et al.* (2005) compared the activity of cobalt-, copper-, and iron-supported on Aluminium-doped mesoporous monolithic silica in the selective catalytic reduction (SCR) of NO with ammonia in the presence of oxygen at low temperatures in the range of 373–723 K. It was found that the SCR activity decreased in the order: Cu > Fe > Co as shown in **Figure 17** these results caused from the highly dispersed of Cu (II) ions.

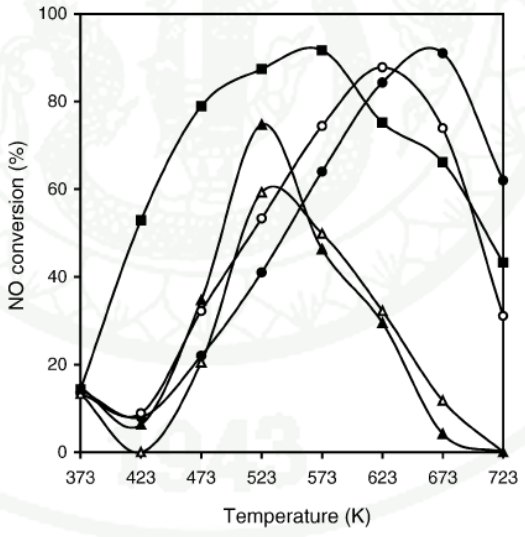

Figure 17 Catalytic activities for SCR of NO by ammonia on transition-metal impregnated aluminosilicate monolith-supported catalytic preparations: MO-SiAl10Cu10$_{IM}$ (■), MO-SiAl10Fe24$_{IM}$ (○), MO-SiAl10Fe35$_{IM}$ (●), MO-SiAl10Co10$_{IM}$ ( ), MO-SiAl10Co15$_{IM}$ (▲)

Source: Brandhorst *et al.* (2005)

Yahiro *et al.* (1981) introduced copper metal into the FAU-zeolite by ion-exchange technique and applied to decompose NO. Later in 1995, Centi *et al.* proposed the reaction mechanisms of NO decomposition as shown in Figure 18.

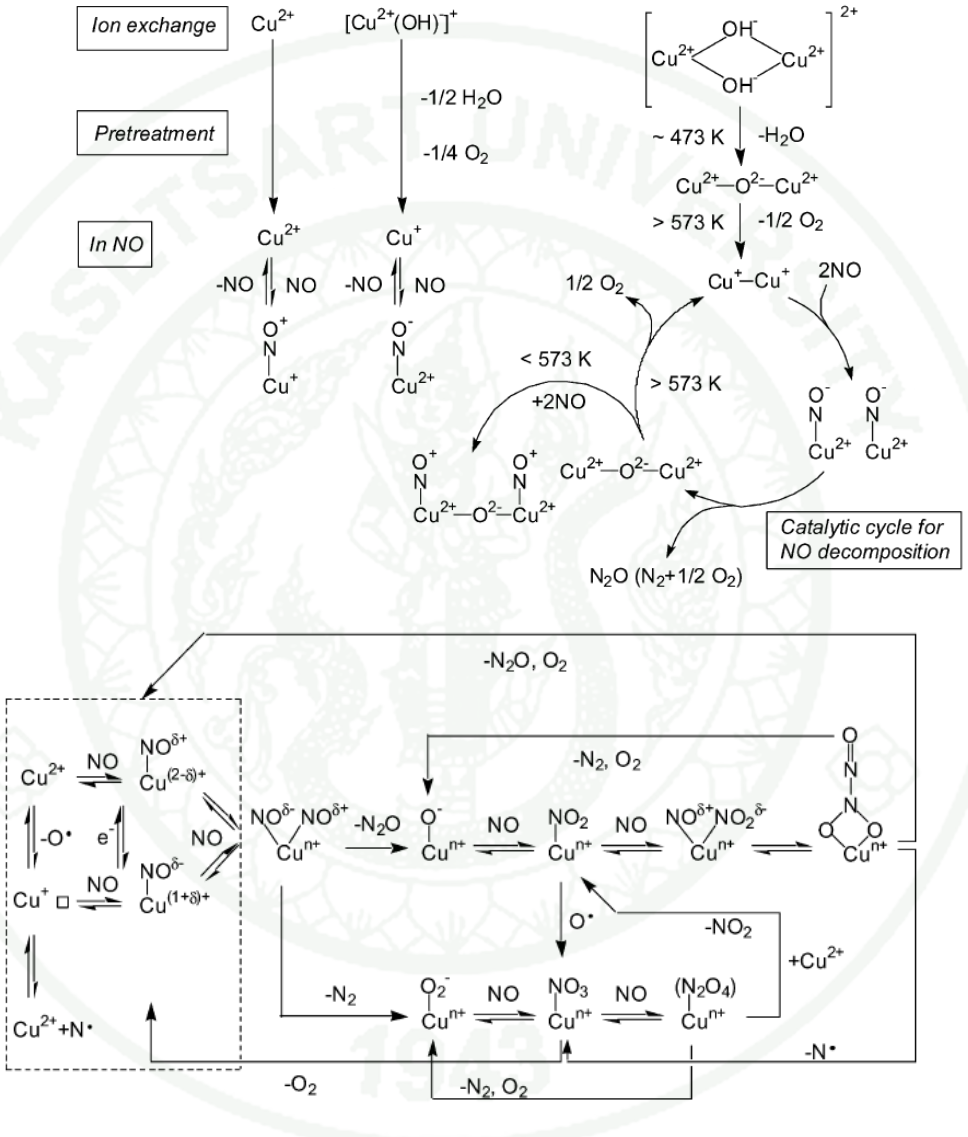

Figure 18 The mechanism for NO decomposition

Source: Centi *et al.* (1995) in Yahiro *et al.* (2001)

The preparation techniques involved the incorporation of copper metals loaded on the supports take an effect on the nature of active metals which affected the

decomposition of NO. Generally, main processes which were used to prepare or introduce active metal into the support comprise of ion-exchange (Iwamoto et al., 1991; Long and Yang, 1999; Scholz *et al*., 2008), wet impregnation (Janas *et al.*, 2009), substitution technique (Janas *et al.*, 2009) and mechanical mixing (Miha´lyi *et al.*, 2009). Additionally, the nature and role of copper have been widely discussed (Janas *et al.*, 2009; Wu *et al.*, 2010).

The Cu-MFI-116 zeolite prepared by ion-exchange technique, copper atoms were existed as Cu(II) (50%), Cu(I) (40%), and unknown species (10%) (Iwamoto *et al.*, 1991). Mostly, the symmetrical coordination of Cu (II) ions to four framework oxygen atoms is the most stable site is hard to be reduced (Wan *et al*, 2004), however, the selectivity toward N_2 can also be controlled by types of Cu (II) species (Wu *et al.*, 2010) while Cu(I) ions can be assigned as the sites where N_2 is generated from two adsorbed NO molecules (Dˇedeˇcek *et al*., 2011). It was also shown that under reaction conditions the copper exhibits dynamic inter conversion between +1 and +2 oxidation states (Schay *et al.*, 2000], and the active form of Cu^{2+} on catalyst surface was an intermediate in the decomposition of NO (Liu and Robota, 1994). Chmielarz *et al*. (2006) used mesoporous silica (MCM-48, SBA-15, MCF) modified with copper by two different methods; the molecular designed dispersion (MDD) method and the incipient wetness impregnation method. The samples obtained by the MDD method have been found to be more active and selective compared to the analogous samples prepared by the impregnation technique. This effect related to the nature of metal species which identified on the support surface; copper in the form of isolated Cu^{2+}cations dominated in the Cu(IMP)-MCM- 48 sample, while for the Cu(MDD)-MCM-48 catalyst, the metals were presented mainly in the form of clustered species ([Cu–O–Cu]n and bulky CuO clusters).

Cu-Al-MCM-41 could be prepared by a modified hydrothermal method (Wan *et al.*, 2004). The catalytic activity for NO selective catalytic reduction was based on the copper exchanged level, and the copper was mainly in the form of isolated Cu^{2+} ions in Cu-Al-MCM-41 catalysts with copper-exchange level ≤100%, whereas at higher copper-exchange CuO species were also present. Janas *et al*.

(2009), proposed a two-step post-synthesis method which allows to control the introduction of copper into SiBEA zeolite and thus to obtain catalysts with isolated tetrahedral Cu (II) species (see Figure 19). First, AlBEA zeolite was treated with aqueous HNO_3 solution involves the elimination of Al atoms from the framework (1), followed by the incorporation of copper leading to Cu_xSiBEA (2). The reaction was showed in scheme 1. By using this technique, the copper incorporated in SiBEA zeolite was present mainly as isolated tetra coordinated Cu(II) and was very active in SCR of NO by ethanol with the maximum NO conversion at 573 K of 50% and selectivity towards N_2 of 75%.

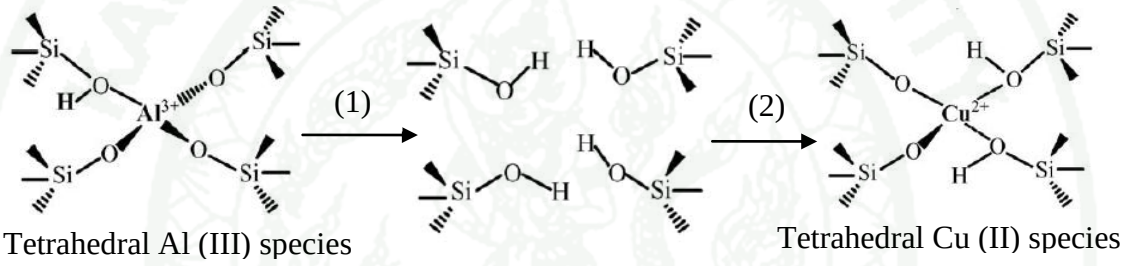

Figure 19 The scheme for the formation of Cu_xSiBEA by two-step post-synthesis

Source: Janas *et al*. (2009)

3. Structure of support affecting catalytic performance

Not only the support types that researchers have been tried to investigate but also they made an effort to develop and search for special characteristics of supports, Sultana *et al*. (2008) studied the role of zeolite structure;Pt-ZSM-5, Pt-FER, Pt-MOR and Pt-BEA, on NO reduction. Pt-MOR was found to be the most active catalyst, 90% NO conversion at 300 ˚C whereas the ZSM-5, BEA and Y with three dimensional pore structures extensive carbonaceous deposits were observed. Pt-FER zeolite having one dimensional pore structure did not allow extensive coke formation resulting in a highly desired low temperature NO conversion. Palomares *et al*. (2002) synthesized zeolite "ITQ7" with 12-member rings and loaded with copper or cobalt metal. The catalysts showed a high conversion of NO at low oxygen concentration

and in the absence of water and SO_2, similarly performance in as other active catalysts (Palomares *et al*., 2002). Spassova *et al*. (1999) co-precipitated unsupported CuO–MnO_x mixed oxide with a spinel-like structure in order to study the activity of amorphous catalyst via NO_x reduction at low temperature (Spassova *et al*., 1999). Li *et al*. (2005), synthesized Cu-ZSM-5 on the surface of honeycomb cordierite substrate to enhance the thermal and hydrothermal stability of ZSM-5/cordierite for the conversion of NO_x.

Pranit S. Metkar (2012) synthesized dual layer SCR catalyst comprising a thin Fe-zeolite layer on top of a thick Cu-zeolite layer as shown in Figure 20, and it was found that the dual layer Fe/Cu catalyst expanded temperature window of high NO_x conversion for SCR process. Based on the fact that Cu-zeolite was very active at lower temperatures (≤350 °C) while Fe-zeolite was more active at higher temperatures (≥400 °C).Therefore sequential brick design with Fe-zeolite brick followed by a Cu-zeolite brick gave a high catalytic performance over a wide range of temperatures.

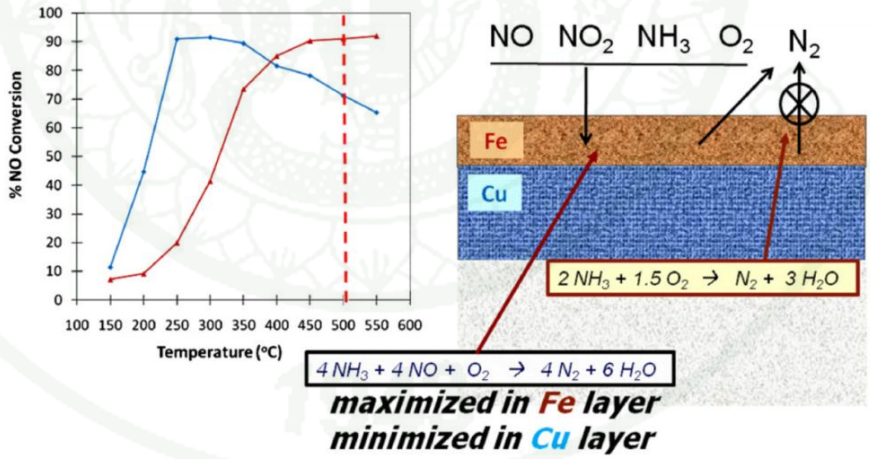

Figure 20 Schematic of the working principle of the dual-layer SCR catalyst of Fe-zeolite layer on top of a thick Cu-zeolite layer at various temperatures

Source: Pranit S. Metkar (2012)

In addition, there were also some research studying on the synthesis of catalyst with core-shell structure which can be enhanced performance of the catalyst for heterogeneous NO_x reduction.

Core-Shell nanoparticles have been interested in the last few years, especially the heterogeneous catalysts that contain composite materials. Zhou *et al*. (2005) compared the catalytic activity and thermal stability between Pt–Cu Core–Shell and PtCu alloy nanoparticles in the removal of NO. It was found that the Cu-core with Pt-shell (Cu@Pt) showed the conversion and selectivity higher than Pt-core with Cu-shell (Pt@Cu) and PtCu. These results may due to the fact that the increasing of crystallinity of the PtCu alloy catalyst changed surface structure, leading to the loss of activity during the first three hours. Tao *et al.* (2008) synthesized the core-shell Rh0.5Pd0.5 and Pt0.5Pd0.5 bimetallic nanoparticles by using colloidal chemistry methods and study in situ the structure and composition of catalysts during oxidizing, reducing, and catalytic reactions involving NO, O_2, CO, and H_2. The results revealed that the shell region with Pd substantial was more active than Pt-shell, these caused from the Pd has a lower surface energy than Pt.

However, the use of core-shell mesoporous silica/aluminosilicate as the catalyst for NO reduction has not been proposed before. Thus, in this work, the mesoporous silica-aluminosilicate composite materials composed of mild acidic aluminosilicate and high abrasive resistant silica were considered to be used as a catalytic supporter. The copper species were introduced into the composite materials by substitution technique and incipient wetness impregnation method and then the nature of the active metal, and the interaction between active metals and their supports were investigated. Moreover, the formation of core-shell structure under acidic condition (pH6.5) and the addition of chitosan in order to control the cluster size and create macro pores in the catalyst as well as the catalytic performances via NO removal process at moderate temperature (280°C) were also discussed.

MATERIALS AND METHODS

Materials and Equipments

In this section, the methods for the synthesis of mesoporous silica–aluminosilicate composites using CTAB and chitosan as binary templates, and the incorporation techniques of copper metal into the synthesized materials were described in detail in the first part. While the activity and selectivity of the synthesized materials which were used as the catalysts for NO reduction process were expressed in the second part. The materials and equipments used for silica–aluminosilicate composites preparation and analysis are listed as follows:

1. Equipments for silica–aluminosilicate composites preparation

1.1 Digital hot plate and stirrer (Schott, SLR)
1.2 Magnetic hot plate and stirrer (Schott, SLR)
1.3 Furnace (Carbolite, ELF10/6), (see Figure 21)
1.4 Digital weighing machine (Metler Toledo, AT 400)
1.5 Hot air oven (Binder, GmbH Model FP240)
1.6 Autoclave (made by order), (see Figure 21)

Figure 21 390 ml Teflon-lined home-made design stainless steel autoclave with circulating air drying oven

2. Equipmentsand condition for sample analysis

2.1 Surface area and pore size distribution of porous silica products were analyzed by using N_2 sorption equipment of Quantachrome Corporation, Autosorb1 as shown in Figure 22. Nitrogen isotherms of the products were measured at -196 $^{\circ}$C using a Quantachrome Autosorb-1C instrument. Prior to N_2-physisorption measurements, the products were degassed at 200 $^{\circ}$C for 12 h. The adsorption isotherms were run at 10^{-5}< P/P0 < 1.0. Using the nitrogen adsorption data, the specific BET (S_{BET}) was estimated for P/P_0 values between 0.05-0.30. The micropore volume and the micropore surface area of the products were calculated using relative pressure range of 10^{-4}< P/P0 < 10^{-2} of the Dubinin-Radushkevich (DR) plots. The pore size distribution was calculated using desorption branch of the Barrett-Joyner-Halenda (BJH) method. The total pore volume was obtained from adsorption data at P/P_0 of 0.99.

Figure 22 Autosorb1, (Quantachrome Corporation)

2.2 The morphology of the products was examined by using a Transmitting Electron Microscope (TEM, JEOL JEM-2100 LaB6) with an acceleration of 200 kV as shown in Figure 23. Samples preparation entailed suspension of the samples in

ethanol and, following this, thermal evaporation of ethanol on a copper grid coated with a carbon film. The Si/Al ratios of the obtained products were determined by using TEM-EDS (NORAN).

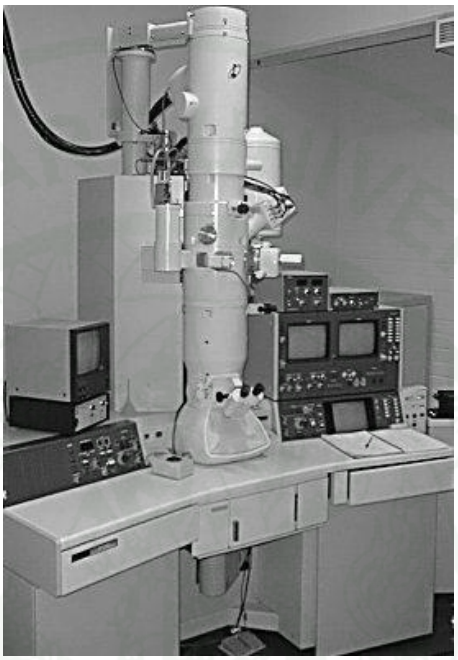

Figure 23 Transmitting Electron Microscope (TEM, JEOL JEM-2100 LaB6)

2.3 The hexagonal orientation of the mesopore structure was observed by using a Small Angle X-ray Diffraction Spectroscopy (SAXS, JEOL JDX-3530) with Cu Kα radiation, 50 kV/300 mA. The diffraction pattern was recorded in the range of 0.8˚ to 7˚ (2θ) with a step scan of 0.01˚ and a rate of 0.6˚ min^{-1}.

2.4 The FT-IR spectra of the synthesized products were recorded in the range of 4,000–400 cm^{-1} at room temperature using GX FT-IR (Perkin Elmer), equipped with the Deuterated Triglycine Sulfate (DTGS) detector as shown in Figure 24. Each sample was coated on the KBr crystal, then ground, and pressed into a tablet form before analysis.

Figure 24 GX FT-IR (Perkin Elmer) which was equipped with the Deuterated Triglycine Sulfate (DTGS) detector

2.5 Diffuse reflectance UV–vis–NIR (DR UV–vis–NIR) spectra were recorded on a Lambda 650 PerkinElmer UV/VIS spectrometer equipped with an integrator and a double monochromator at room temperature and ambient atmosphere.

2.6 The infrared spectroscopy was studied with a Bruker IFS 28 spectrometer equipped with an MCT detector at a resolution of 4 cm^{-1}. In order to study reduced samples, the catalyst was pretreated with flowing H_2 at 320 $^{\circ}$C for 1 h. After that each sample was then cooled to the room temperature at 30 $^{\circ}$C to collect an interferogram which was used as the background reference. Subsequently, after purging the catalyst with 5 mbar of CO at room temperature another interferogram was kept. Following this, the catalyst was then cooled down again until -100 $^{\circ}$C with liquid nitrogen, and the last interferogram was collected after the sample was exposed again to 5 mbar of CO.

3. Materials for the synthesis of silica–aluminosilicate composites and Cu-containing silica–aluminosilicate composites

The materials used for the synthesis of silica–aluminosilicate compositesand copper-containing silica–aluminosilicate compositesare listed as follows:

3.1 Tetraethyl orthosilicate (TEOS: 98%, Fluka)

3.2 Aluminum nitrate ($Al(NO_3)3{\cdot}9H_2O$: 98%, APS Ajax Finechem)

3.3 Chitosan (CS: 90% deacetylation, Biolife ELAND)

3.4 Cethyltrimethyl ammonium bromide, ($C_{16}H_{33}N$ $(CH_3)_3$-Br, CTAB (AJAX, No. A147))

3.5 Copper nitrate, $Cu(NO_3)_2{\cdot}2.5H_2O$ (Ajax Finechem)

3.5 Sodium hydroxide, NaOH (Merck; Purity, 99 %)

3.6 Hydrochloric acid, HCl (J.T. Baker; Purity, 36.5 -38.0 wt. %)

3.7 Distilled water

Experimental procedures

1. Synthesis of silica-aluminosilicate composites

The mesoporous silica-aluminosilicate composites were prepared by using sol-gel process, in this work the effect of alternated pH value on the formation of core-shell structure and the effect of chitosan addition on the development of macrospores were mainly focused. A mesoporous silica-aluminosilicate composite was prepared via a sol-gel process by using the material components based on MCM-41 gel composition (in molar unit) of SiO_2:0.2CTAB:100H_2O (Liu *et al.*, 2001), whereas Al_2O_3/SiO_2 and chitosan/SiO_2 molar ratios were fixed at 0.1 and 2.4×10^{-5}, respectively. Both ratios were found in the earlier work to yield the highest and most uniform macroporosity (Witoon *et al*. 2009; Chareonpanich *et al.* 2004). At first, an aluminum nitrate solution was slowly added into CTAB solution that was being stirred at 40 °C. The TEOS solution was subsequently added into the mixture; at this stage the pH value of mixture was approximately 1.97–1.98 measured by a pH meter model CG842, Schott (see Figure 25) and the hydrolysis–condensation reaction was expected to start. After stirring for 1 h, the pH value of the mixture was then immediately adjusted to 11.5 or 6.5 using 1M sodium hydroxide (referred to as pH-x) and the mixture was kept stirring at 40 °C for an additional 5 h.

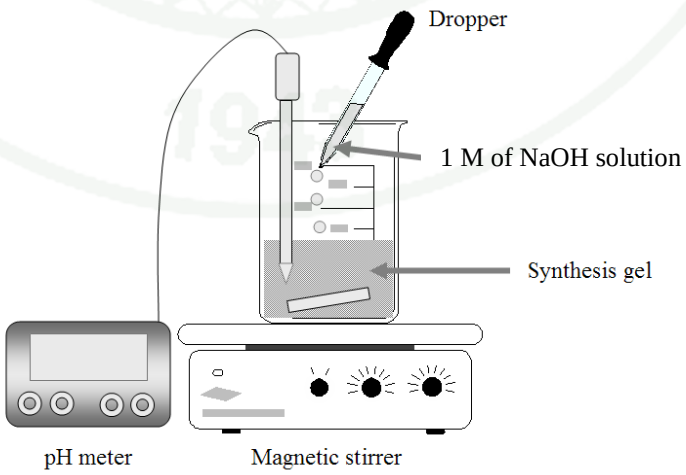

Figure 25 The equipment setup of "pH adjusting" process

Chitosan solution was prepared by dissolving 0.1 g of chitosan in 30 ml of 2% acetic acid was slowly poured into the mixture that was maintained the pH at 11.5 or 6.5 (referred to as pH-y). The pH of another sample was adjusted from 11.5 to 6.5 using 1M hydrochloric acid. The obtained mixture was then transferred to a Teflon-lined autoclave for hydrothermal treatment at 100 °C for 24 h. During this stage, the hydrolysis–condensation reactions were expected to be formed, the picture of obtained white creamy gel solution is shown in Figure 26.

Figure 26 White creamy gel solution of silica-aluminosilicate composites after hydrothermal treatment

Next, the solid product was filtered, washed with distillated water and dried at 80 °C overnight. After that obtained solid powder was grinded into fine particle before it was calcined in air at 600 °C for 5 h. The achieved white fine powder is shown in Figure 27.

Figure 27 Fine powder of silica-aluminosilicate composites after calcinations at 600 °C for 5 hours

In order to investigate the effect of pH of the mixture on the hydrolysis–condensation stage and the hydrothermal stage, a pH value at each stage was varied as shown in detail in Table 1. The effect of chitosan was also clarified by repeating the experiment with a similar procedure but excluding chitosan.

Table 1 The pH value of the mixture at each stage

Sample [a]	Chitosan addition(g)	pH-x	pH-y
ASC11.5-11.5	-	11.5	11.5
ASC11.5-6.5	-	11.5	6.5
ASC6.5-6.5	-	6.5	6.5
ASP11.5-11.5	0.1	11.5	11.5
ASP11.5-6.5	0.1	11.5	6.5
ASP6.5-6.5	0.1	6.5	6.5

[a] Products prepared without (P) and with (C) chitosan template, designated as ASP*x-y* and ASC*x-y* where *x* and *y* are the pH values during hydrolysis-condensation stage and hydrothermal treatment stage, respectively.

2. The synthesis of copper containing silica-aluminosilicate composites

There were two different methods used to incorporate copper metals into the synthesized silica-aluminosilicate composites, including substitution technique and incipient wetness impregnation method.

2.1 Substitution technique

The substitution technique was similar to the synthesis of silica-aluminosilicate composites but before TEOS solution was added, 10 ml of the copper nitrate solution at different concentration was added instead. In this work, the amount of copper nitrate was varied between 0.5, 1.0, 1.5 and 2.0 wt.%. Then the whole process was repeated again in the same way of silica-aluminosilicate composites was produced. In this case, the final product was defined as SASC*x* or SASP*x* which S referred to the substitution technique, and *x* referred to the pH values of the synthesis conditions.

2.2 Incipient wetness impregnation method

By using this method, the silica-aluminosilicate composites which were synthesized in the first part were used as supports. 1 g of silica-aluminosilicate composites was impregnated with 5ml $Cu(NO_3)_2 \cdot 2.5H_2O$ (Ajax Finechem) solution at various concentration in order to obtain 0.5, 1.0 and 1.5 wt.% of Cu in final step. After stirring for 1 hr the slurry was evaporated under stirring at 80 $^{\circ}$C until the all the water was completely vaporized and then it was ground into fine particle before calcination in air at 600 $^{\circ}$C for 5h. The light blue fine powder products were defined as IASC*x* or IASP*x* which I referred to the incipient wetness impregnation method, and *x* referred to the pH values of the synthesis conditions.

3. Catalytic test

All synthesized catalysts were tested their activities for NO reduction to N_2 by using H_2 as reducing agent, the reaction was carried out in a fixed bed reactor at atmospheric pressure. The schematic set up for the NO_x reduction is shown in Figure 28.

Prior to reaction, the catalyst was activated for one hour under H_2 flow at 350 $^{\circ}$C and then it was cooled to 280 $^{\circ}$C. The feed composition was 250 ppm NO, 20000 ppm H_2 and balance He with a catalyst volume of 0.15 g and 12,000 h^{-1} gas hour space velocity.

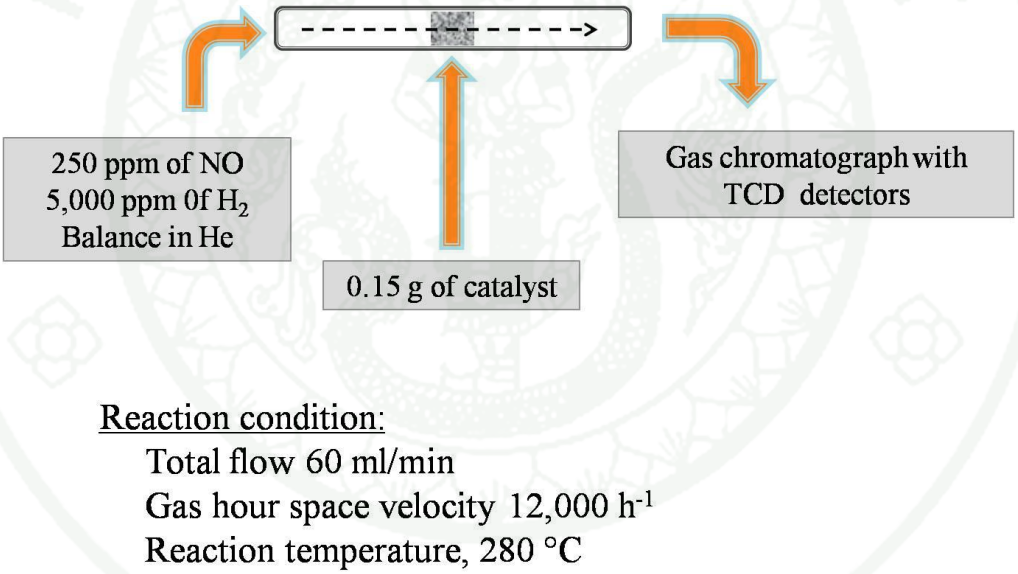

Figure 28 Schematic setup for the NO_x reduction.

The reactant gases were regulated by a mass flow controller [Aalborg GFC 17] and the outlet gases were analyzed using a gas chromatograph consisting of Shimadzu gas chromatograph and a chromatopac data processor (GC-2014) equipped with a thermal conductivity detector (TCD) (Figure 29). The gaseous products consisted of N_2, NO and H_2 were analyzed using a Unibead-C packed column at 40°C and using helium (99.5 % purity) as a carrier gas.

Figure 29 Shimadzu gas chromatograph (GC-2014) equipped with thermal conductivity detector (TCD) and chromatopac data processor.

The performance of the catalysts was expressed in term of NO conversion (XNO) and N_2 selectivity (SN_2), which were calculated from following equations

$$xNO = \frac{[NO]_{inlet} - [NO]_{outlet}}{[NO]_{outlet}}$$

The details of qualitative and quantitative analysis results from gas chromatographs are reported in Appendix A.

RESULTS AND DISCUSSION

Results and discussion can be divided into two parts; the synthesis of mesoporous silica-aluminosilicate composites by using chitosan and CTAB as binary templates. In this part, the formation of silica-aluminosilicate composites via a sol-gel process at different pH conditions was described in details, also the addition of chitosan in order to control particle size and create the macropores, and the effect of alternated pH on phase arrangements to form homogeneous infiltration and core-shell structure are also illustrated in this part.

For the second part, the synthesized materials were used as supports and were tested for their performance via NO reduction reaction under a moderate temperature (280 $^{\circ}$C). Based on the literatures aforementioned above it was revealed that the position of loaded metal species on the support was one of the factors affecting the performances of the catalysts. The use of various incorporated procedures makes the great impact on a nature of active metals. Therefore in this work, copper was considered to be an active metal and was incorporated into the supports by using two different techniques; substitution technique and incipient wetness impregnation method. The effect of support structure including homogeneous infiltration and core-shell structure of silica-aluminosilicate, the amount and nature of copper were examined also.

Synthesis of mesoporous silica–aluminosilicate composite

1. One pot synthesis of silica-aluminosilicate

In the first step of this experiment, all the reagents including aluminum nitrate and TEOS were mixed together with CTAB micelle solution under acidic condition (the initial pH ≈ 2.0). Under this strong acidic condition, TEOS solution was rapidly hydrolyzed and formed silicate species $(SiO_4)^{4-}$surrounding the hexagonal arrays of CTAB micelles. This phenomenon could promote the formation of Si-O-Si bonding, whereas the formation of Al-O-Si bonding hardly occurred because it was easily dissociated under this condition (Li *et al*. 2004; Brinker *et al*. 1990; Mehner *et al*. 2010). Consequently, only the mesoporous silica framework was formed through the hydrolysis-condensation of the silicate species via a surfactant-templating mechanism.

After the solution was cured in a strong acidic condition for 1 h., the pH of solution was slowly adjusted to 6.5 and 11.5 by using 1 M NaOH. At higher pH, ΔG°_{rxn} of cross-condensation between $Si(OH)_4$ and $Al(OH)_4^-$ was found to be highly negative (Tagirov *et al*. 2004; Fedeyko *et al.* 2007) resulting in the spontaneous formation of the silica-alumina composite. Therefore, the formation of composite materials between silica and aluminosilicate was possible to be prepared by using one-pot synthesis. The self-organized formation of silica-alumina was confirmed by the FT-IR and NMR.

Basically, the IR vibrational bands are characterized by their frequency (energy), intensity (polar character or polarizability), and band shape (environment of bonds). Since the vibrational energy levels are unique to each molecule, the IR spectrum provides a "fingerprint" of a particular molecule and is able to indicate the functional groups in a molecule. The FT-IR spectra of samples are shown in Figure 30 which confirms the formation of silica-aluminosilicate composites prepared with CTAB and chitosan. Similar to the results reported by Wang *et al.* (2005), the bands in the region of 400-600 cm^{-1} and close to 550 cm^{-1} represent the existence of silica Si-O-Si and M-O-Si (where M is metal), respectively. The existence of

aluminosilicate having different numbers of ring members was confirmed by the absorption bands in the range of 400-800 cm^{-1} (Lei *et al*. 2008). Moreover, the corner linkage of $(AlO_4)^{5-}$ and $(SiO_4)^{4-}$ forming aluminosilicate was confirmed by the vibration band of Al-O-Si stretching at 570 cm^{-1}, while the most intense band in the range of 950-1,200 cm^{-1} reveals asymmetric Si-O and Al-O stretching (Mozgawa and Sitarz 2002; Blackwell 1979).

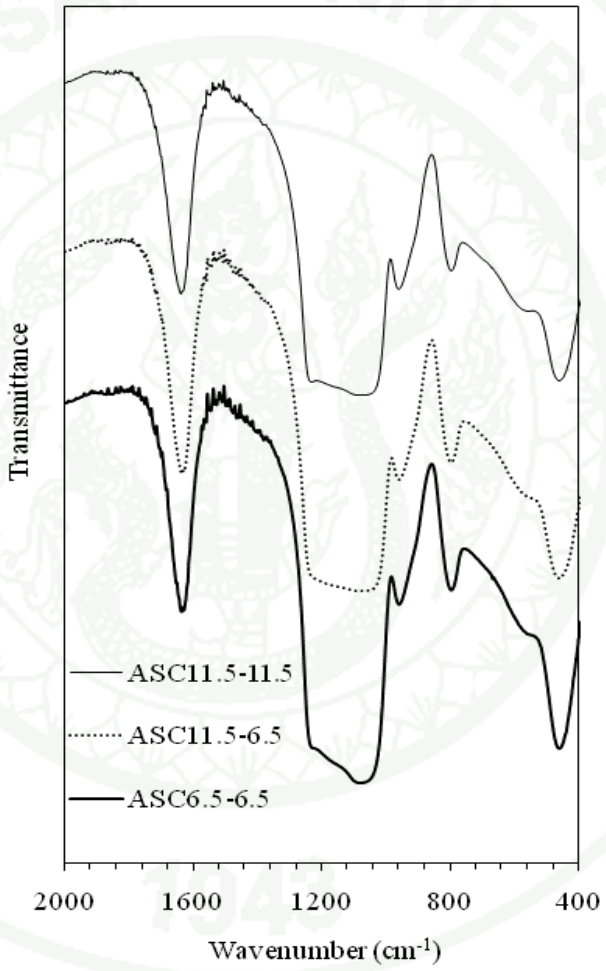

Figure 30 FTIR spectra of the mesoporous silica-aluminosilicates synthesized by using CTAB-chitosan template

In order to prove that the Al species were introduced and formed bond with the silica framework, the local Al environment and molecular structure of synthesized materials were determined by a solid state NMR spectroscopy. As reported in many

works (Yang *et al.* 2007; Wu *et al.* 2010) that the isotropic chemical shifts of Al species are specific to their coordinated environment atoms. The tetrahedrally coordinated Al in the framework always shows the resonance peak at around 50 ppm while the resonance at around 0 ppm corresponded to the Al atoms in octahedral position. The aluminum species of silica-aluminosilicate composites prepared without chitosan addition (ASP) at different pH conditions including constant pH 11.5 (ASP11.5-11.5), alternated pH11.5-6.5 (ASP11.5-6.5) and constant pH6.5 (ASP11.5-6.5) were clarified by an ^{27}Al MAS NMR spectroscopy as shown in Figure 31.

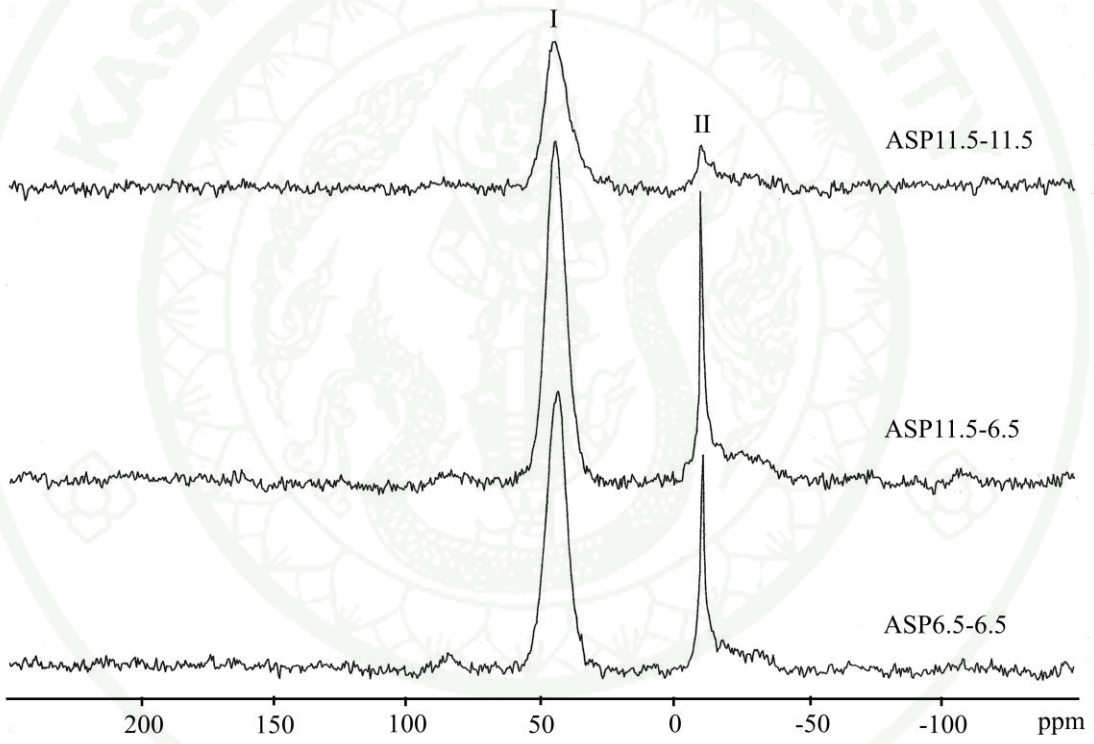

Figure 31 ^{27}Al MAS NMR spectra of porous silica-aluminosilicate prepared without chitosan

It is clearly observed that all the samples exhibited two signals peaks with similar chemical shift at about 44 (I) and -10 ppm (II). The first peak corresponds to tetrahedral (AlO_4) and the second peak relates to octahedral (AlO_6) aluminate (Phillips *et al*. 1995; Lippmaa *et al*. 1986). However, the ratio of peak intensity between 4- and 6- coordinated aluminum of ASP11.5-11.5 is above 4, while they are

close to 1 for ASP11.5-6.5 and ASP6.5-6.5. This comparison reveals that most of the aluminum of the ASP11.5-11.5 sample favorably incorporated into the silica framework in the tetrahedral coordinated position as $(AlO_4)^{5-}$, and only a small number of octahedral Al_2O_3 was formed. On the other hand, for ASP11.5-6.5 and ASP6.5-6.5 there was a significant amount of Al_2O_3 formed. This Al_2O_3 might come from the unbound tetrahedral aluminate and the unreacted $Al(NO_3)_3$ that was trapped inside the pores and subsequently converted to Al_2O_3 after calcination. It should be noted that even rinsing with water for several times the trapped $Al(NO_3)_3$ was hardly leached out due to the capillary force inside the pores. Since the cethyl trimethylammonium bromide (CTAB) was used as a pore structure-directing agent, therefore in the suitable conditions, the CTAB micelles will aggregate and hexagonal close packed arrays will be appeared, producing the hexagonal phases as mentioned above in literatures. Figure 32 shows the ordered hexagonal structure of ASC6.5-6.5.

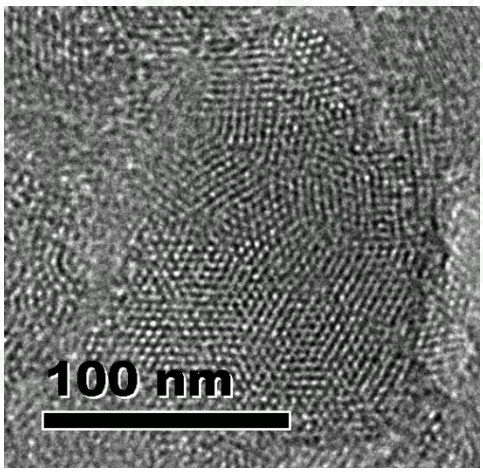

Figure 32 TEM image of ordered hexagonal structure of ASC6.5-6.5.

Theoretically, the main characteristic planes representing the hexagonal pore structure of porous materials are observed by the small angle X-ray diffraction (SXAS) at (100), (110) and (200). Figure 33 shows the SXAS of materials synthesized with chitosan addition at different pH values; ASC11.5-11.5, ASC11.5-6.5 and ASC6.5-6.5.

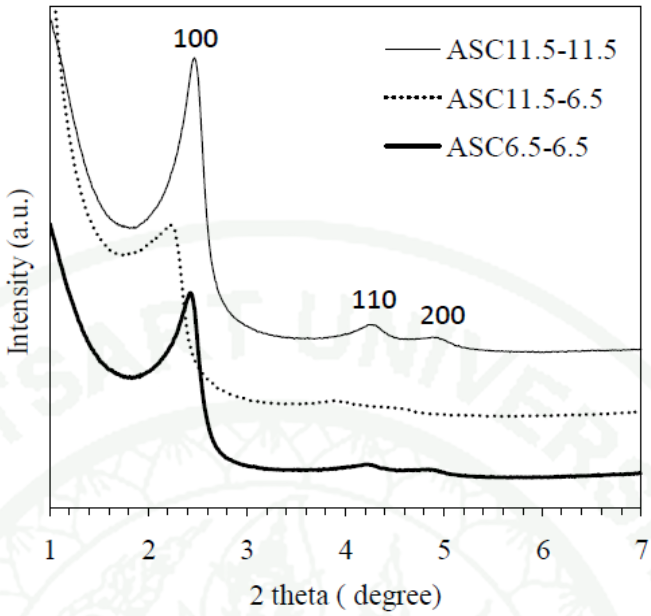

Figure 33 Small angle X-ray scattering (SAXS) patterns of silica-aluminosilicate synthesized with CTAB-chitosan template at various pH values

It is clearly seen that the corresponding peaks of ASC11.5-6.5 have the lowest intensities implied the least order of the hexagonal pores. This could be attributed to the effect of pH value alternation (pH change from 11.5 to 6.5) on the deformation of the hexagonal framework of ASC11.5-6.5. While under a strongly basic condition at pH 11.5, the size of the mesopores corresponded to the size of micelle of a cationic surfactant CTA^+, therefore the fundamental hexagonal mesostructure was constructed by self-assembly of anionic species and cationic CTA^+ micelles through an electrostatic interaction. Conversely, a decrease in pH increased the amount of the suppressant or spacer micelles and also resulted in a decreasing of negative charge of silica species, and then the ordered array of the template micelles in the particles was degraded. Therefore both products synthesized at fixed pH 6.5 and alternated pH from 11.5 to 6.5 were shown the same results that was a lower peak intensity compared to that of products synthesized at 11.5. In addition, ASC11.5-6.5 showed a lower order of the hexagonal pores, which resulted from a more disturbed of a system.

2. pH affecting the formation of core-shell structure

In this work, the alternated pH values were the most important factor which affected not only the formation silica and aluminosilicate but also the formation of the special structure that was a core-shell structure. These may cause from the solubility of silica framework changes with the pH, leading to the changing of hierarchical morphology. In the series of experiments, since the solubility of silica framework was significantly increased at pH higher than 10 (Rimer *et al*. 2005) and in a strong basic condition the Si-O-Si bonds were hydrolyzed to form $Si(OH)_4$. Therefore when the pH was raised up to 11.5, the primary mesoporous silica matrix was then partially dissolved back into the solution. Simultaneously, under the same basic condition, the tetrahedral aluminates $Al(OH)_4^-$ were favorably created and could subsequently penetrate into the matrix and finally incorporated with the available silicate to form an aluminosilicate framework. Thus, the composite of mesoporous aluminosilicate uniformly infiltrated in mesoporous silica was then established as shown in Figure 34 (a, b), which shows the TEM images of the products synthesized without and with chitosan, respectively.

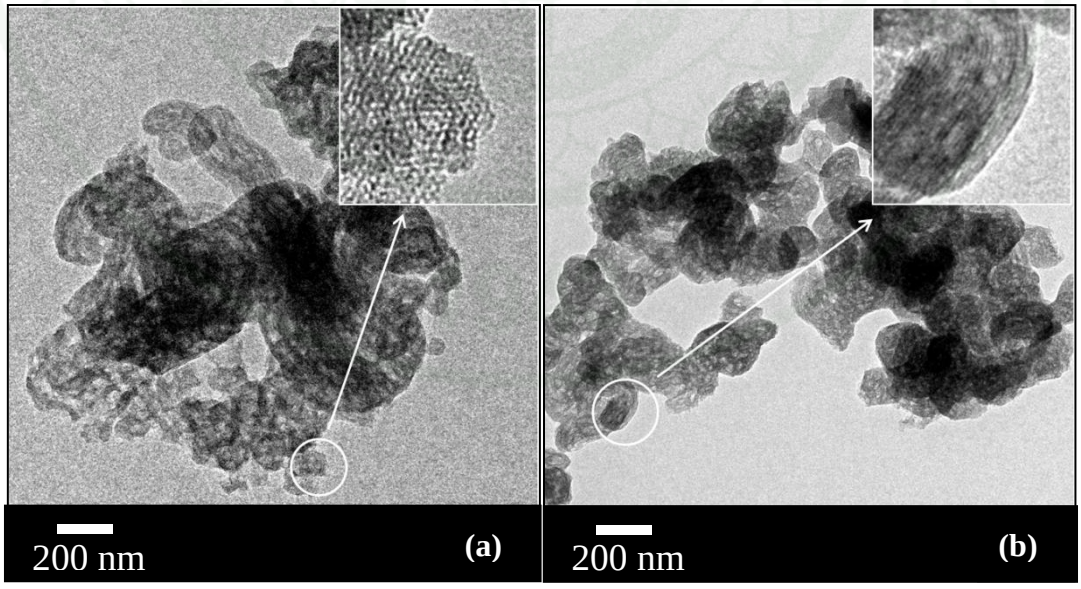

Figure 34 TEM images of porous silica-aluminosilicate prepared without chitosan (a) ASP11.5-11.5 and with chitosan (b) ASC11.5-11.5

Conversely, when the pH of the mixture was raised up from 2.0 to 6.5, the dissolution of the silica framework hardly occurred. Therefore, the primary mesoporous silica still remained as the dense matrix. At this condition, the aluminate tetrahedra could be formed and subsequently corner-linked with the unbound silicate tetrahedra starting from the outer layer of the dense silica matrix. As a result, the self-assembled core-shell mesoporous silica-aluminosilicate composites were then fabricated. The TEM images of these composites synthesized without and with chitosan at pH 6.5 are shown in Figure 35.

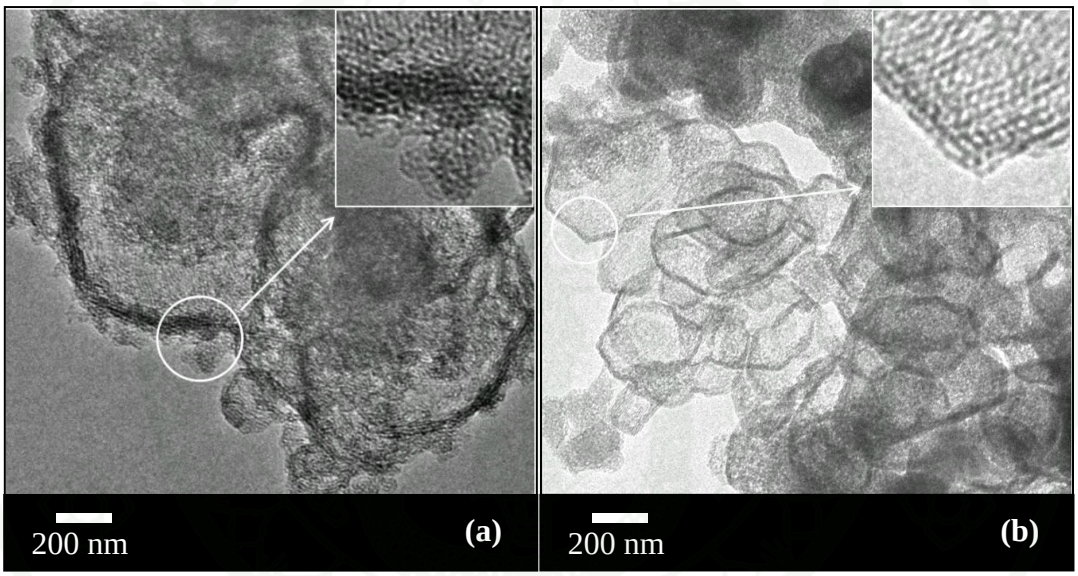

Figure 35 TEM images of porous silica-aluminosilicate prepared without chitosan (a) ASP 6.5-6.5, and with chitosan (b) ASC6.5-6.5

However, the unbound aluminate tetrahedra that still remained in the form of $Al(OH)_4^-$ were connected together, creating the octahedral Al_2O_3. This phenomenon was confirmed by the NMR results presented in Figure 31 as discussed earlier.

On the other hand, when the pH was alternated from the raising to 11.5 and then dropping to 6.5 (ASP11.5-6.5 and ASC11.5-6.5), the mixed phases between core-shell and uniformly infiltrated mesoporous silica-aluminosilicate composites were accordingly formed (Figure 36 (a), (b)).

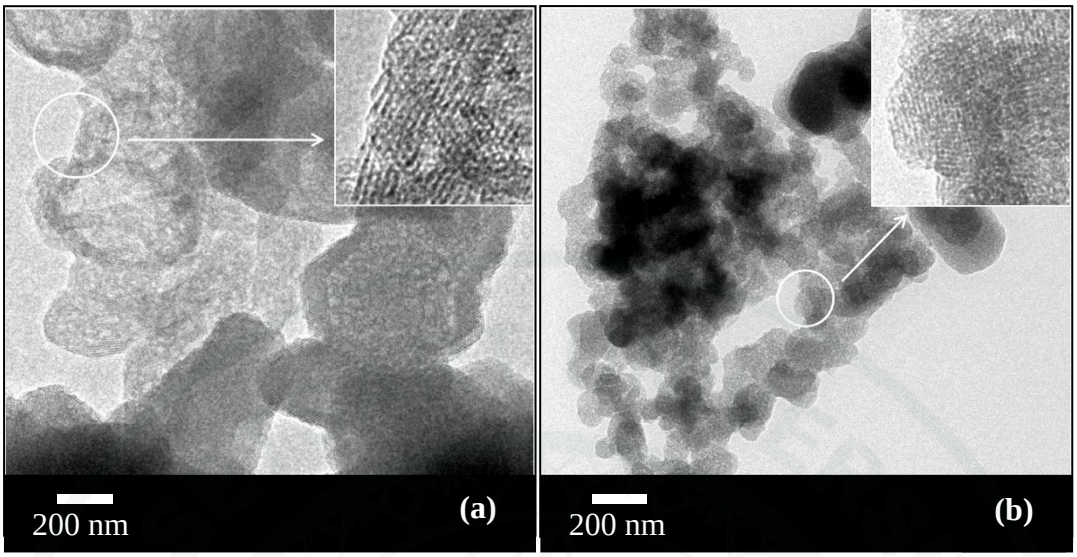

Figure 36 TEM images of porous silica-aluminosilicate prepared without chitosan (a) ASP11.5-6.5 and with chitosan (b) ASC11.5-6.5

The formation mechanism of a uniform infiltrated silica-aluminosilicate and a silica-core aluminosilicate-shell structure is simplified and shown in Figure 37.

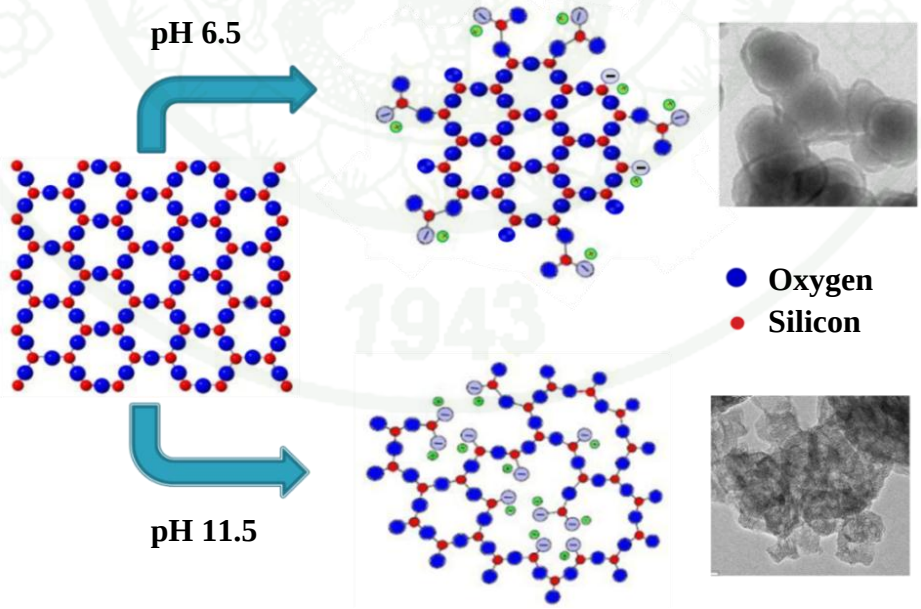

Figure 37 Diagram showed the formation mechanism of mesoporous silica-aluminosilicate materials synthesized at pH 6.5 and 11.5.

Figure 38 shows the STEM and TEM images of the cross-sectional view of the ASC6.5-6.5 sample. The core-shell structures of mesoporous silica-aluminosilicate composites are clearly observed. In the core area, the well-ordered hexagonal pores of a MCM-41-like structure were exhibited, while, in the shell having 15–20 nm thickness, the less-ordered hexagonal orientation of aluminosilicate was observed.

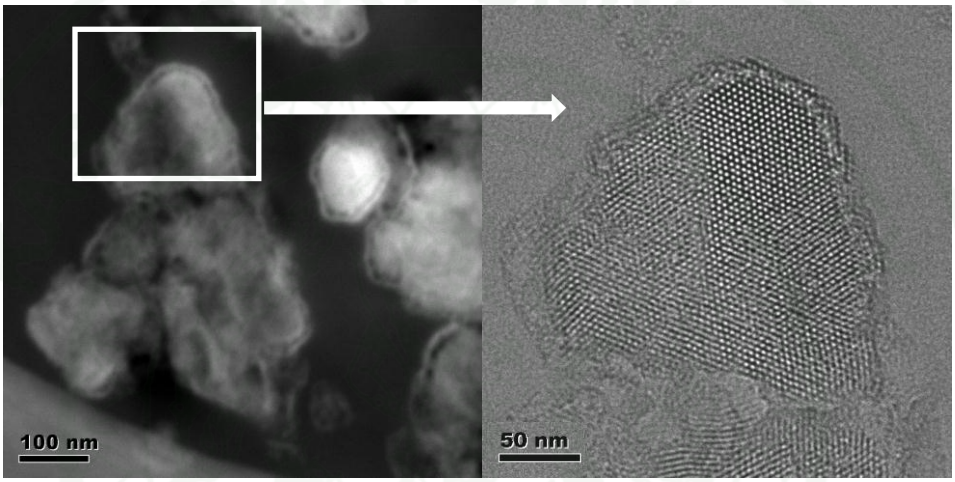

Figure 38 STEM and TEM images of the cross-sectional view of silica-aluminosilicate prepared with CTAB-chitosan at pH 6.5 (ASC6.5-6.5)

The EDS analysis was also used to determine the average Si/Al molar ratio of the clusters formed with different conditions. The result is summarized in Table 2. The details of sample preparation for TEM, EDS and raw data are reported in Appendix D.

Table 2 Silica-alumina ratios of synthesized materials detected by EDS

Sample	Si/Al [a]
ASC11.5-11.5	23.39
ASC11.5-6.5	27.75
ASC6.5-6.5	29.38
ASP11.5-11.5	24.38
ASP11.5-6.5	29.02
ASP6.5-6.5	33.84

[a] Calculation of Si/Al from EDS X-ray point analysis.

It was found that the Si/Al ratio decreased in sequence with the increase of pH during the hydrolysis-condensation stage. This was due to the core-shell mesoporous silica-aluminosilicate formed at pH 6.5 (both without (ASP) and with chitosan template (ASC)) composed of mainly dense cores, in which aluminate species hardly penetrated to react and form aluminosilicate. Additionally, the solubility of alumina was found to increase with increasing pH value (Fedeyko *et al*. 2007). Aluminum hydroxide has low solubility in water at the intermediate pH values. However, further increasing the pH value could shift the equilibrium. The soluble aluminate ions ($Al(OH)_4^-$) were finally formed through following steps (Gregory and Duan 2001):

$$Al^{3+} \rightarrow Al(OH)^{2+} \rightarrow Al(OH)_2^{+} \rightarrow Al(OH)_3 \rightarrow Al(OH)_4^-$$

Therefore, when the pH value was raised to 6.5, only small amounts of aluminate species were generated and reacted with the dense mesoporous silica core to form aluminosilicate shell. On the other hand, at the strong basic condition (pH 11.5) a large number of soluble aluminate tetrahedra were favorably formed together with the loosening of the silica matrices as mentioned earlier. Thus, the infiltration of aluminosilicate into the silica matrices was formed. As a result, the highest aluminum contents (lowest Si/Al) were detected. However, when the pH was raised to 11.5 and

then dropped to 6.5 (ASP11.5-6.5 and ASC11.5-6.5), the Si/Al ratios were found to be in between those of ASC11.5-11.5 and ASC6.5-6.5.

It should be noted that Si/Al ratios of the composites synthesized without chitosan template (ASP) were slightly higher than that of the products synthesized with chitosan in all pH conditions. This should be attributed to the electrostatic adhesion between aluminum species and chitosan, retarding the aluminum species leached during the washing step (Falco 2009).

In order to prove that the core section of an ASC6.5-6.5 sample comprises only silica, the aluminosilicate shell was removed before examining by an EDS. The solution containing 12 wt% HCl and 3 wt% HF was used to leach a core–shell sample (ASC6.5-6.5) following a method previously reported by Bertaux and Dowell (1989), and only shell part was expected to be leached out. Then, the sample was analyzed by a TEM with an EDS mode. It was clearly observed that after leaching process, the domain size became smaller and a core–shell structure was not observed as shown in Figure 39 (a)-(b). Moreover, when an EDS mode was applied for identifying all elements in the sample, it was found that only silicon (Si) and oxygen (O) atoms are detected without any aluminum (Al) atoms existed (Figure 39 (b)). Therefore, it could be concluded that the core of the ASC6.5-6.5 sample comprises only silica.

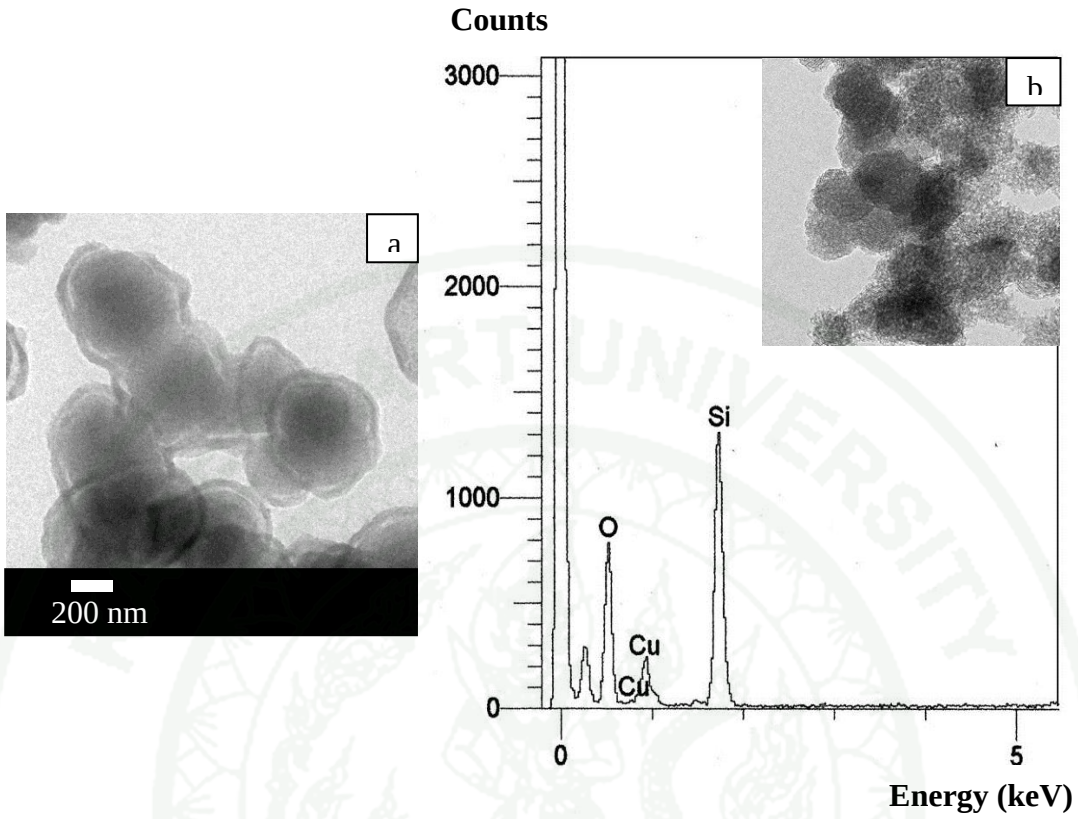

Figure 39 TEM image of core-shell ASC6.5-6.5 before shell leaching (a) and EDS element of ASC6.5-6.5 after a leaching of shell (b)

3. Effect of chitosan addition on the formation of macropores

Chitosan, a natural biodegradable polymer, has been reported to exhibit the potential function in controlling the cluster size of the mesoporous silica products. These may due to the fact that there is an electrostatic interaction between positively charged NH^{3+} along chitosan molecules and negatively charged silicate species, promoting the formation of silica-chitosan composite. However, pH values below 4, the crystallinity of chitosan decreases due to the electrostatic repulsion between protonated amine groups. Conversely, NH_3^+ groups on chitosan are mostly deprotonated by OH^- under the alkaline condition and the positive charges of chitosan are neutralized, leading to coagulation of chitosan macromolecule (Mi *et al*. 2003).

Figure 40 shows TEM images of silica-aluminosilicate composites synthesized at pH 11.5 without chitosan ASP11.5-11.5 (a) and with chitosan ASC 11.5-11.5 (b). It was clearly observed that the domain sizes of silica-aluminosilicate composites synthesized without chitosan ASP11.5-11.5 did not significantly change compared to that with chitosan ASC 11.5-11.5.

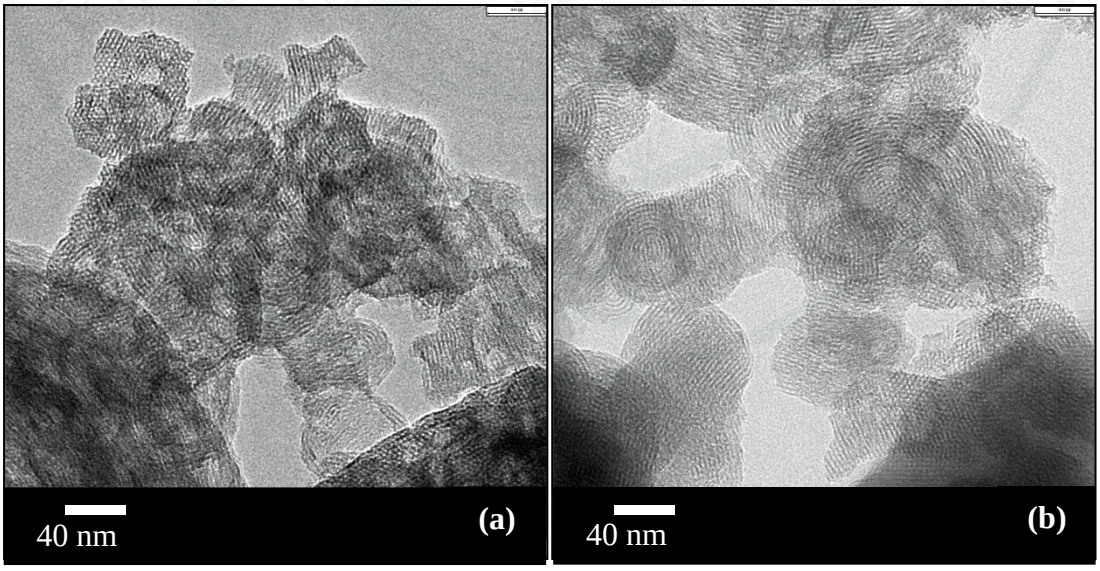

Figure 40 TEM images of silica-aluminosilicate composites prepared without chitosan (a) ASP 11.5-11.5, and with chitosan (b) ASC11.5-11.5

It could be explained that the formation of these nanoparticles was controlled by the rate of hydrolysis and condensation. Under strong basic condition the rate of the condensation reaction was faster than that of the hydrolysis reaction, leading to the formation of isolated clusters (Mozgawa and Sitarz 2002). Moreover, due to chitosan coagulation under strong alkaline condition, it rarely affected the domain size of silica-aluminosilicate composites. On the other hand, under weak acidic condition (pH 6.5), the condensation polymerization of silica and aluminosilicate networks constantly occurred. However, under the presence of chitosan that was much better dissolved than under alkaline condition, the growth of the domains was consequently limited compared to similar experiments without chitosan. This evidence can be seen in Figure 41.

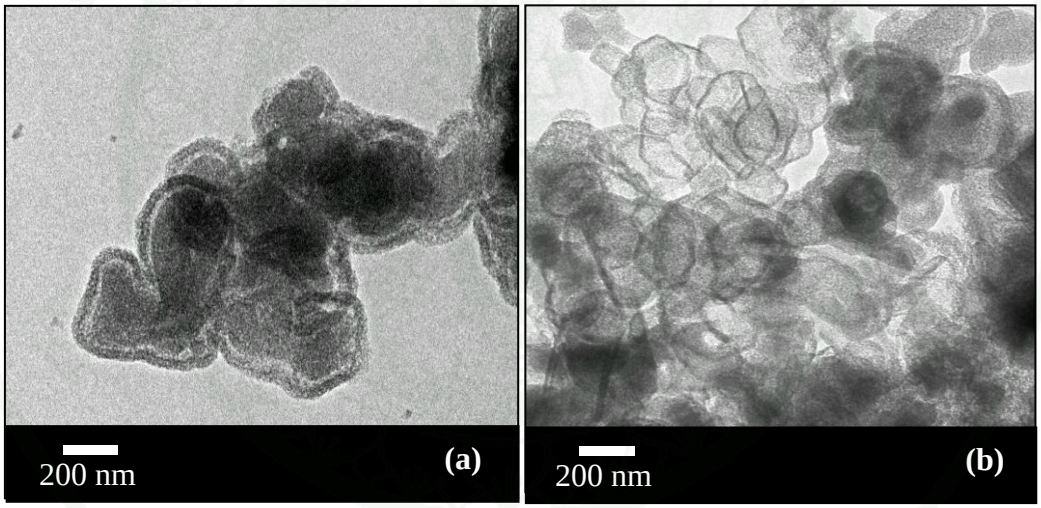

Figure 41 TEM images of silica-aluminosilicate composites prepared without chitosan (a) ASP 6.5-6.5, and with chitosan (b) ASC6.5-6.5

In addition, the products synthesized with chitosan template revealed a relatively high macroporosity. This can be attributed to the encapsulation of coagulated chitosan and after calcination it was removed leaving macropores within the matrices. The schematic in Figure 42 shows the function of chitosan addition on the formation of macroporosity in the structure.

Figure 42 The schematic formation of macropores by chitosan addition
Source: Witoon *et al*. (2009)

The BET surface areas, micropore surface area and pore volumes of porous silica-aluminosilicate products are summarized in Table 3 With chitosan, the macropores (>100 nm) were formed in significant numbers for all conditions due to the chitosan encapsulation as described earlier.

Table 3 Physical properties of mesoporous silica-aluminosilicates composites

Sample [a]	S_{BET} (m^2/g)	V_t (cc/g)	$V_{macro.}$ (cc/g)	V_{micro} [b] (cc/g)	S_{micro} [c] (m^2/g)
ASC11.5-11.5	1610	2.05	0.95	0.41	1167
ASC11.5-6.5	1595	2.53	1.26	0.36	1011
ASC6.5-6.5	1428	1.85	0.79	0.35	1079
ASP11.5-11.5	1484	1.15	0.25	0.40	1148
ASP11.5-6.5	1359	1.68	0.69	0.36	1006
ASP6.5-6.5	1288	1.21	0.30	0.33	943

[a] Products prepared without (P) and with (C) chitosan template, designated as ASP*x-y* and ASC*x-y* where *x* and *y* are the pH values during hydrolysis-condensation stage and hydrothermal treatment stage, respectively.

[b,c] Calculation of micropore volume and surface area from DR equation.

The N_2 adsorption-desorption isotherms and corresponding pore size distributions (PSD) are shown in Figure 43 and Figure 44, respectively. It was clearly observed that all the samples are classical of type IV, characteristic of mesoporous materials. The adsorption isotherms of samples prepared with chitosan all exhibited a steep inflection point at P/P_0 = 0.95, thus indicating the large macropores

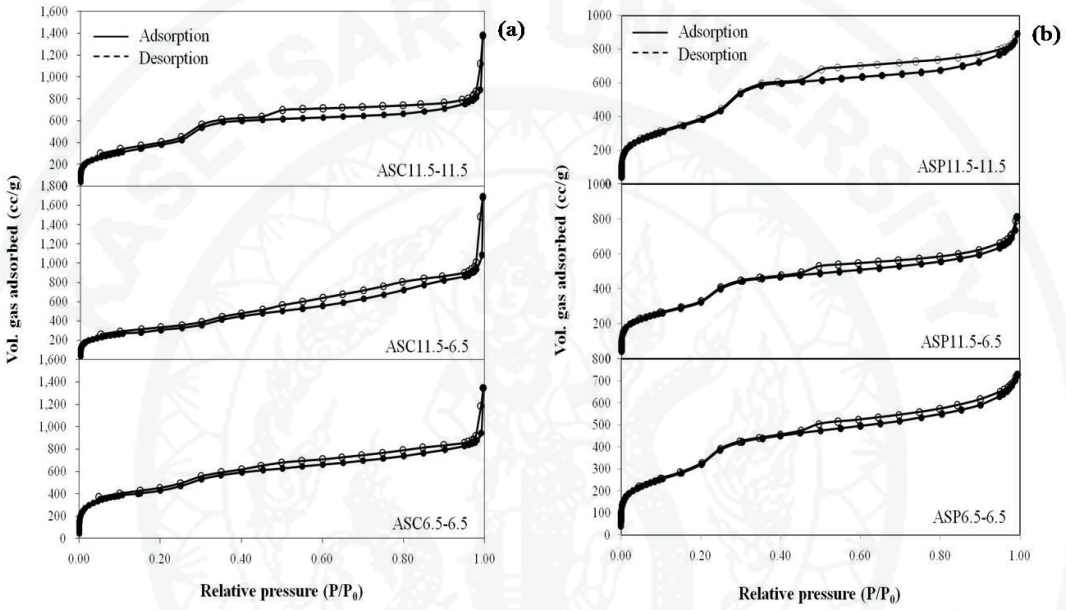

Figure 43 N_2 adsorption-desorption isotherms of ordered mesoporous silica-aluminosilicate prepared (a) with chitosan template and (b) without chitosan template

Bimodal mesopores with narrow PSDs in the diameter range of 2.5-4.0 nm were observed from both without and with chitosan samples. The existences of bimodal mesopore structures were the result of the formation of the core-shell and the uniformly infiltrated mesoporous silica-aluminosilicate composites at relatively low and high pH values. The first peak at ≈ 2.5 nm, which has a larger peak area, should be belonged to mesoporous silica that was the main matrix controlled by CTAB, whereas the smaller peak at ≈ 3.5 nm should be belonged to the aluminosilicate shell and the infiltrated aluminosilicate inside the silica matrix. It was found that the

infiltrated aluminosilicate inside the silica matrix showed the highest microporosity and the addition of chitosan molecules did not significantly alter the microporosity.

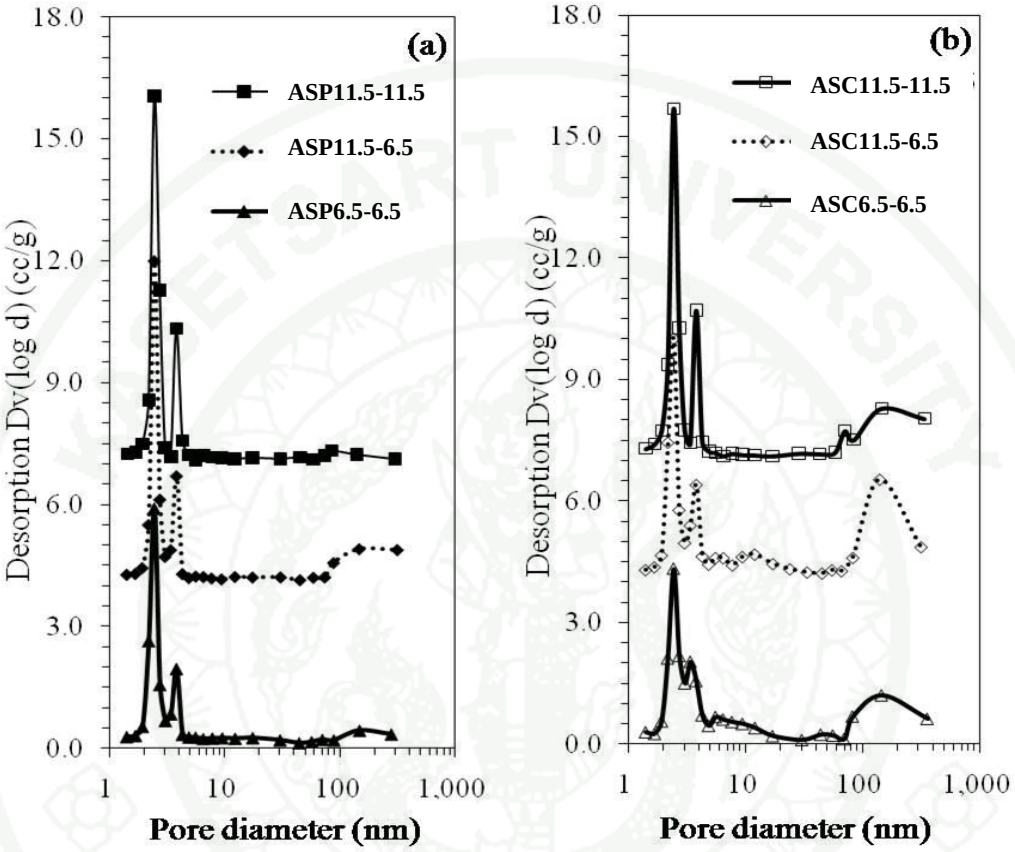

Figure 44 Pore size distribution of ordered mesoporous silica-aluminosilicate prepared (a) without chitosan template and (b) with chitosan template

$DeNO_x$ reaction by H_2

1. Synthesis of Cu-containing silica/aluminosilicate composites

In this work, two different procedures were used to introduce copper metal into silica-aluminosilicate supports including substitution technique and incipient wetness impregnation method. However, only the products having unique physical properties including core-shell structure (products synthesized at pH 6.5-6.5) and the uniformed infiltration (products synthesized at pH 11.5-11.5) were tested for NO reduction in order to investigate the effect of specific active area on the catalytic performance.

Based on the substitution technique, the level of copper species which were substituted instead of aluminum position were limited. Therefore, it was necessary to determine the maximum amount of aluminum which could be incorporated without leaving the unbound species. The amount of copper loaded on uniformed infiltration structure of silica-aluminosilicate (ASC11.5) was varied from 0.5, 1.0, 1.5 and 2.0 wt%, following the substitution procedure as mentioned in the experimental part. The excess copper species would be formed a crystalline structure of CuO which could be detected via X-ray diffraction spectroscopy. The spectra of all synthesized materials are shown in Figure 45. The results were found that only the sample containing the highest amount of copper of 2.0 wt% exhibiting two diffraction peaks at 2θ = 35.7 and 39.0°, these two peaks corresponding to CuO phase (Lin *at al.,* 2010). While, both of them were not presented in other samples which contained a lower percentage of copper metal. It could be implied that copper species were totally incorporated inside the framework. Therefore, the amount of copper used in this work was studied in the range between 0.5-1.5 wt%.

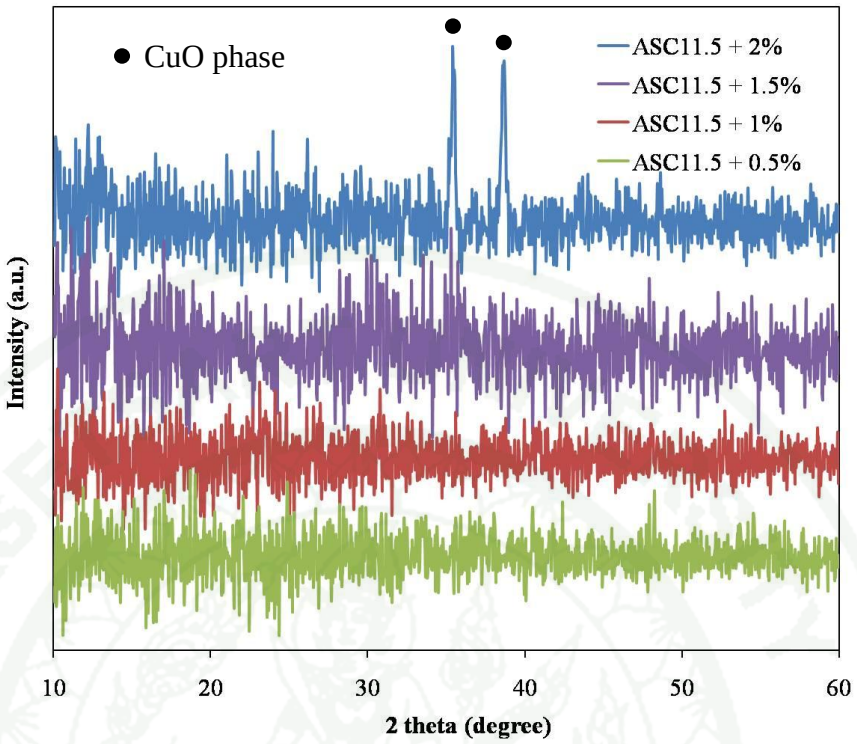

Figure 45 XRD spectra of mesoporous silica-aluminosilicate composites with various amount of copper loading from 0.5-2.0 wt%

Table 4 presents the physical properties of Cu-containing silica–aluminosilicates composite materials. It was found that by using substitution technique, the total pore volume and average pore diameter were increased while the total surface areas of all any supports were decreased reasonably after 1.5 wt% of copper species were introduced into the silica-aluminosilicate composite. These results could be implied that the hexagonal pore structure might be distorted due to the substitution of aluminum species by copper species which having a smaller atomic radius, therefore the hexagonal structure was partially deformed resulting in the increasing of pore sizes.

Table 4 Physical properties of Cu-containing mesoporous silica–aluminosilicates composite Materials

Samples	Surface area (m^2/g)	Total pore volume	Avg. pore diameter	Copper content (%)
ASC11.5-11.5	1783	1.83	40.86	-
SASC11.5 + 1.5%	1387	2.51	47.63	1.61
ASC6.5-6.5	1350	2.13	40.27	-
SASC6.5 + 1.5%	1234	2.48	47.65	1.12
ASP11.5-11.5	1813	1.38	30.44	-
SASP11.5 + 1.5%	1767	1.68	38.10	1.23
ASP6.5-6.5	1468	1.12	30.69	-
SASP6.5 + 1.5%	1381	1.26	34.15	0.95

All samples exhibited the characteristic plane at (100) whereas the diffractions peaks that can be indexed as (110) and (200) were not present obviously comparing to the mesoporous silica-aluminosilicate those synthesized without copper loading shown inset.

The data was confirmed by small angle X-ray diffraction (SAXS) patterns (Figure 46) of both mesoporous silica-aluminosilicate synthesized with and without chitosan template at 1.5 wt% copper.

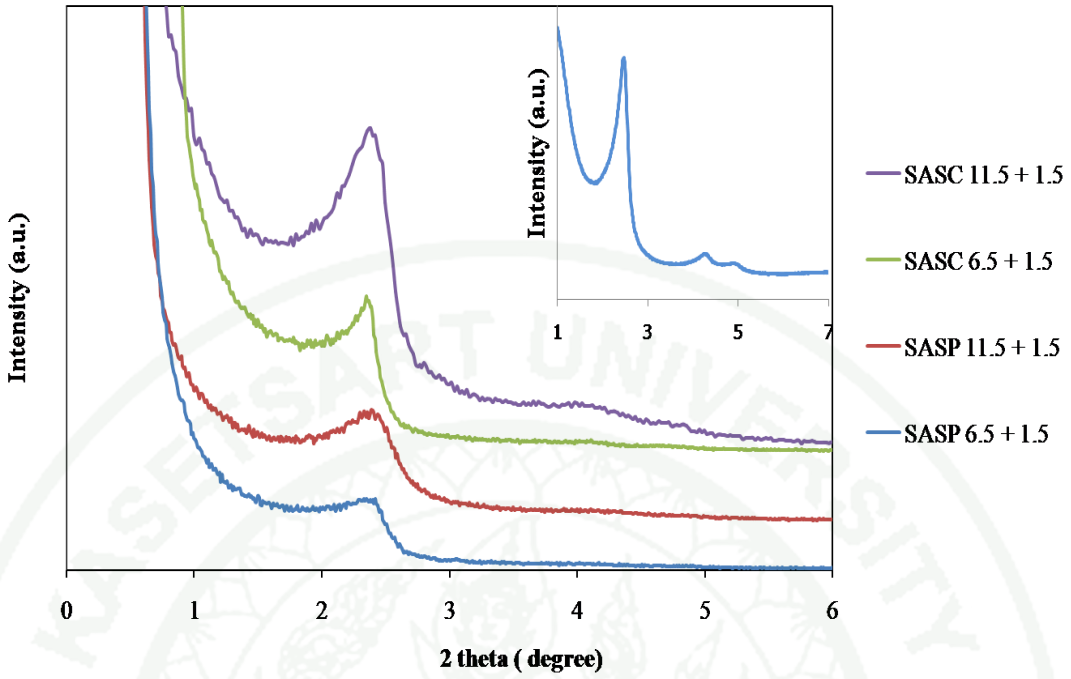

Figure 46 SAXS of mesoporous silica-aluminosilicate composites with 1.5 wt% copper loading, prepared by substitution technique.

TEM images in Figure 47 (a) and (c) show the silica-aluminosilicate composites of ASP11.5 and ASP6.5. Images clearly demonstrated that the products synthesized in a strong basic condition (pH 11.5) showed the uniformly infiltrated aluminosilicate in the silica matrix (Figure 47 (a)) while the materials prepared under slightly acidic condition (pH 6.5) visibly revealed the silica-core and aluminosilicate-shell composites (Figure 47 (c)), the formation of core-shell structure was clearly described in the synthesis part. Figure 47 (b) and (d) show the images of samples with the incorporation of 1.5 wt% of copper by substitution technique which was SASP11.5+1.5 and SASP6.5+1.5. It was found that the core-shell structure of SASP6.5+1.5% was still preserved after the copper was substituted into the framework as shown in Figure 47 (d).

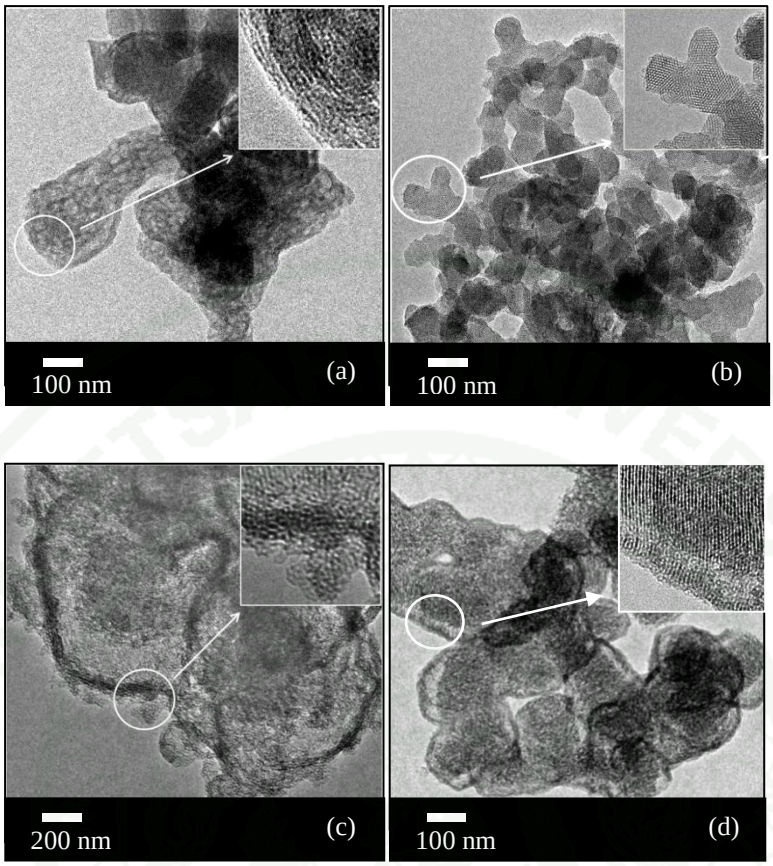

Figure 47 TEM images of mesoporous silica-aluminosilicate composites without copper loading ASP11.5 (a) and ASP6.5 (c), and with copper loading SASP11.5 + 1.5 (b) and SASP6.5+1.5

2. Nature of copper species

The existence of Cu-O was confirmed by FTIR (GX FTIR, Perkin Elmer) (Figure 48), a Cu^{2+}-O^{2-} stretch mode peak exhibiting at around 1400 cm^{-1}(Li 2008). The comparison between samples synthesized via substitution technique with and without chitosan addition was clearly seen that the peak intensity of the sample synthesized with chitosan (SASC11.5 + 1.5%) showed a higher peak intensity than those prepared without chitosan addition (SASP11.5 + 1.5%), suggesting that there were a small amount of CuO presented in the sample prepared without chitosan. In other words, the addition of chitosan helped trapping the copper metals during the washing process, leaving the copper species in the form of CuO.

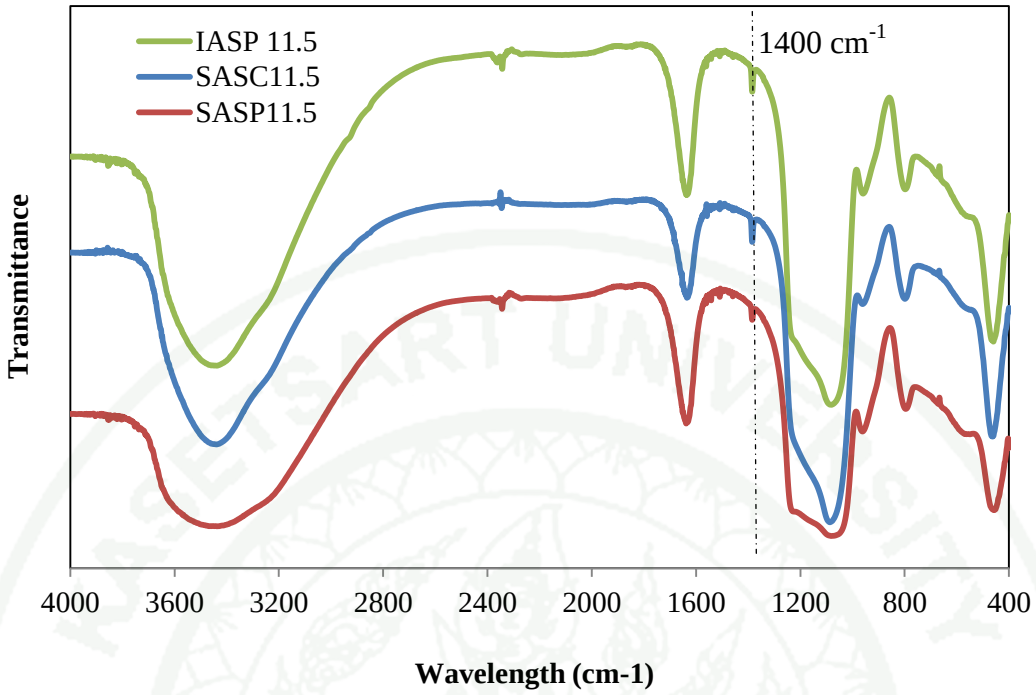

Figure 48 FTIR spectra of mesoporous silica-aluminosilicate composites with 1.5 wt% copper loading, which were prepared by substitution technique with and without chitosan addition

On the other hand, in case of sample prepared by impregnation method (IASP11.5+1.5), all added copper was assumed to be constant for the whole process. After the sample was determined by FTIR, it was found that the peak intensity of Cu-O stretching was as much as in case of SASC11.5 + 1.5%. It could be indicated that by using the impregnation method, copper species were mainly existed in a form of CuO. Even though the copper species were introduced via a substitution technique but not all of them were incorporated in the tetrahedral position and there were some of CuO left in the sample. The results related with the amount of copper contents which were determined by XRF and were shown in Table 4. In order to study the oxidation state of metal, the diffuse reflectance UV-vis-NIR spectroscopy was applied. The catalysts synthesized by substituting technique with 1.5wt% copper were characterized by UV-vis-NIR spectroscopy in the wavelength between 220-850 nm (Figure 49) and it was found that all of them exhibited the sharp peak at around 240

nm and broad peak 820 nm which could be attributed to charge transfer between lattice oxygen and Cu^{2+}, and d-d electron transition of isolated Cu (II) in tetrahedral coordination (Janas *et al* 2009; Dzwigaj *et al*. 2008).

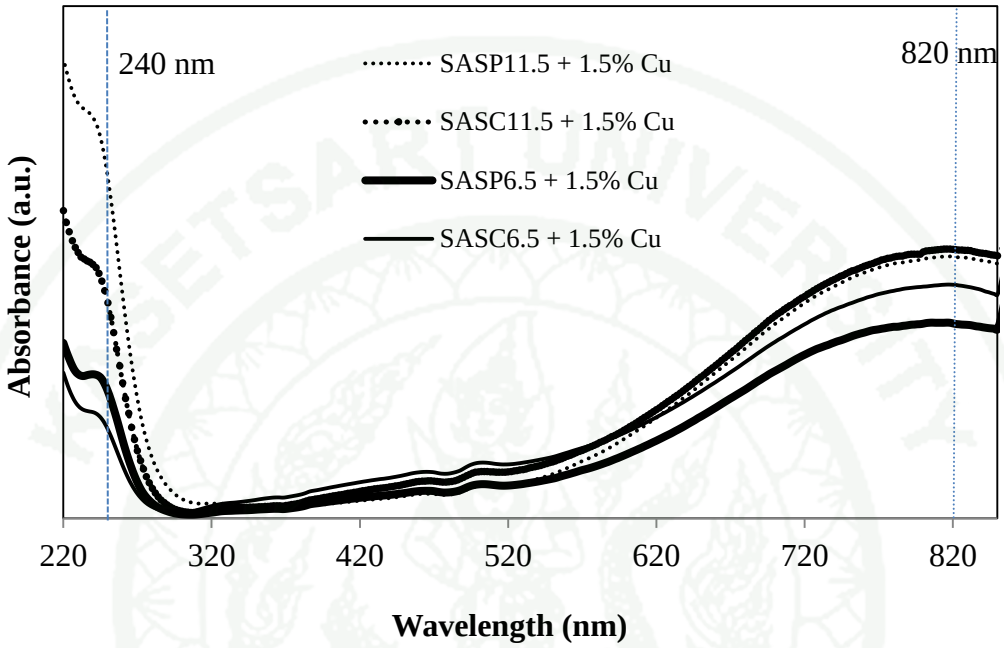

Figure 49 UV-vis-NIR spectra of products synthesized with and without chitosan at various amount of copper contents

The data was clearly seen that both samples synthesized with and without chitosan in a strong basic condition possessing the uniformed infiltration structure (SASP11.5+1.5 and SASC11.5+1.5) showed higher peak intensity than samples having core-shell structure (SASP6.5+1.5 and SASC6.5+1.5). These results indicated that with the uniformed infiltration structure the large amount of copper could be incorporated and positioned in the tetrahedral coordination instead of aluminum species. Whereas in case of samples with core-shell structure, there were less amount of Cu (II) in tetrahedral coordination detected, resulting from the fact that there was only the shell area where aluminum species existed while the core area were mainly belonged to silica framework. Therefore, the replacement of copper and aluminum atoms were limited. When the effect of chitosan addition was considered, the samples with chitosan (SASC11.5+1.5 and SASC6.5+1.5) showed a lower peak intensity than

sample prepared without chitosan (SASP11.5+1.5 and SASP6.5+1.5). These could be suggested that there were a few amounts of copper species that could be incorporated into tetra-coordinated position of aluminosilicate framework and they were mainly existed in a form of CuO although the products prepared with chitosan occupied higher total amount of copper than the products prepared without chitosan as data shown in Table 4 and FTIR spectra. In addition, the present of Cu (II) in tetrahedral coordination in the framework of samples prepared by substitution technique and incipient wetness impregnation method is also shown in Figure 50. Clearly, there were only few copper species which could replace the aluminum positioned in the framework by using the impregnation method.

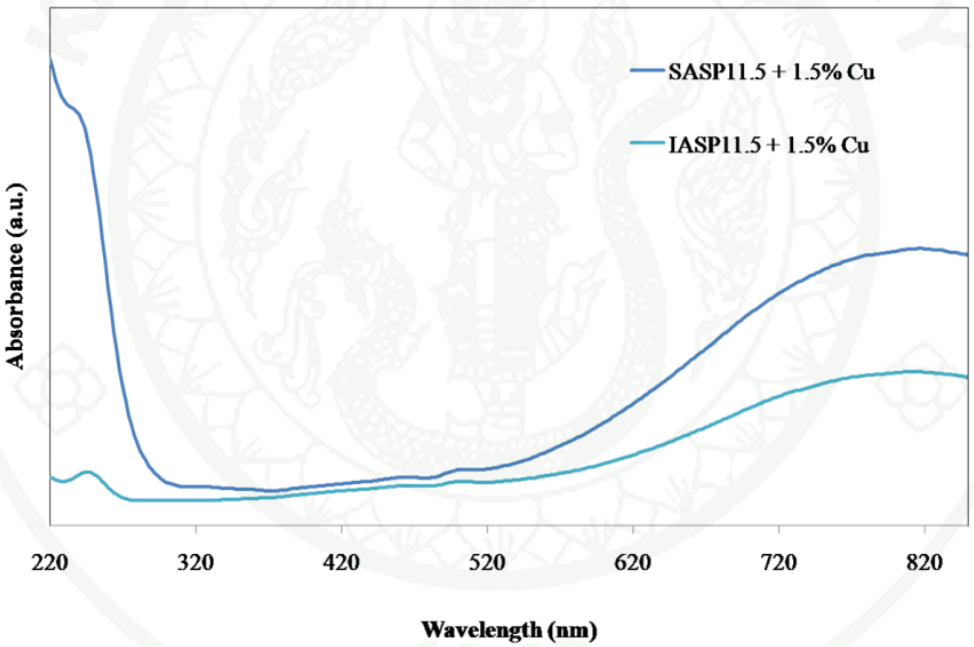

Figure 50 UV-vis-NIR spectra of products synthesized via substitution technique and incipient wetness impregnation method

The nature of Cu species was also observed from the IR spectra, there are reported that Cu supported on MCM-41 with low copper content shows CO adsorption bands similar to those observed on all zeolite types in which the band in the region of 2135–2151 cm $^{-1}$ represented the existence of Cu^{+}-CO (Nachtigallova *et al.* 2001). Figure 51 shows the IR spectrum of adsorbed CO at low temperature (-

100°C) of SASP6.5+1.5% and IASP6.5+1.5% after they were reduced at 320 °C, the IR spectra of both samples exhibited the two sharp peaks at 2150 and 2169 cm^{-1}. The former peak could be attributed to the stretching frequencies of dicarbonyls bands of isolated Cu^{+} site while later could be defined as the Cu^{2+} ions embedded in the silica matrix. However there were no peaks presented at the frequencies below 2110 cm^{-1}, this band can be assigned to Cu^{0}–CO species, indicating that there were no Cu^{0} but mainly Cu^{+} existed on the catalyst surface after the reduction process (Joyner and Shpiro 1994).

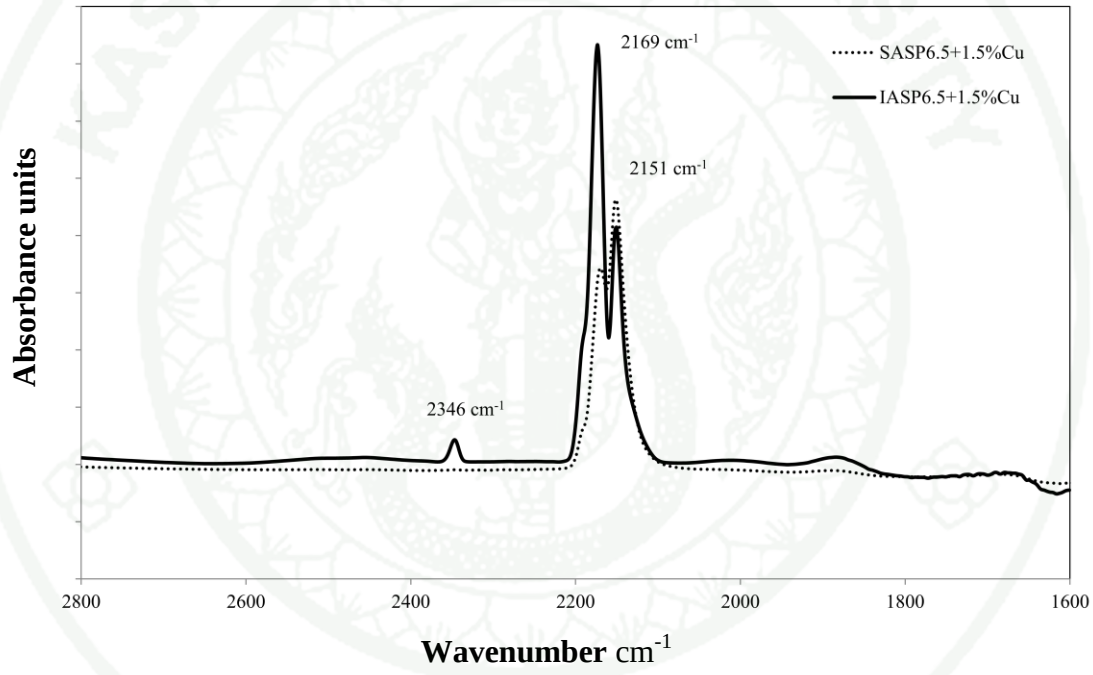

Figure 51 IR spectrum of CO adsorbed at -100 °C on SASP6.5+1.5% and IASP6.5+1.5% after reduction at 320 °C

3. Catalytic performance

Due to the pH values play an important role in hydrolysis and polymerization of silicate species, the formation of the core–shell structure of silica–aluminosilicate composites were obtained under mild acidic condition (pH 6.5), whereas the uniformly infiltrated aluminosilicate in silica matrix was formed at high basic

condition (pH11.5) (Chamnankid *et al*. 2011). By using the incipient wetness impregnation method, the samples having core-shell structure exhibited a higher catalytic performance for NO reduction process than those having a uniformed infiltration structure as shown in Figure 52. These could be described that the aluminosilicate-shell creating the specific active sites surrounding the outer surface of the cluster therefore it was more easily for Cu^{2+} to be reduced into Cu^{1+}. Moreover, it was clearly observed that NO conversion was increased with the increasing of Cu contents. After running the reaction for 3 h., IASP6.5 + 1.5% sample showed the highest NO conversion at 59%, the results could be described that the higher amount of loaded Cu providing the higher Cu^{+} active sites (after reduction process), which NO could be adsorbed and decomposed into N_2 easily.

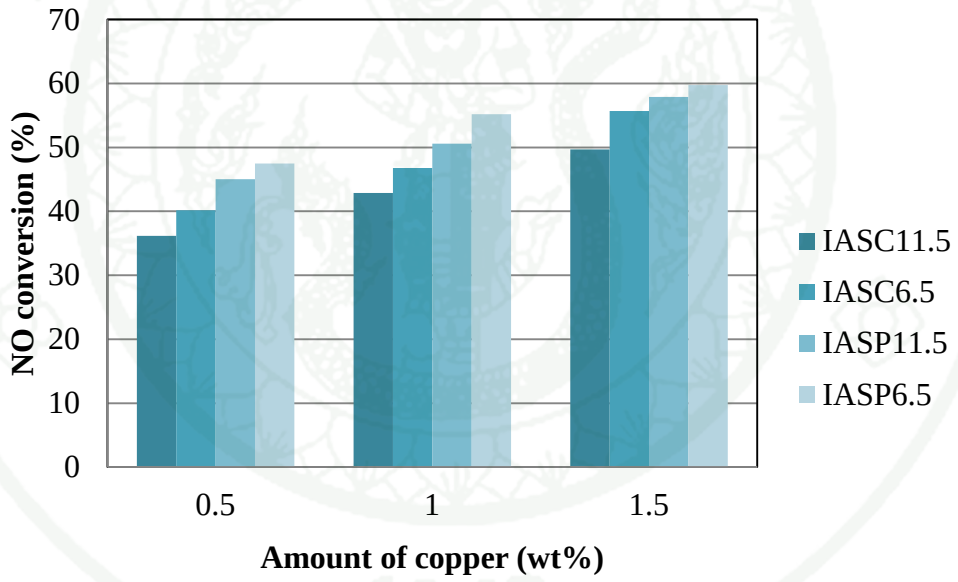

Figure 52 NO conversion of IASC and IASP samples at various copper contents (0.5-1.5 wt%)

On the other hand, the activity of all catalysts prepared by substitution technique increased when the amount of Cu was increased from 0.5% to 1% but at the highest amount of Cu loading (1.5 wt%), the conversion of NO increased only with the products possessed the uniformly infiltrated aluminosilicate in silica matrix (SASC11.5 and SASP11.5) as data shown in Figure 53. In other words, the catalytic

activities of catalysts possessed core-shell structure were found to be dropped significantly.

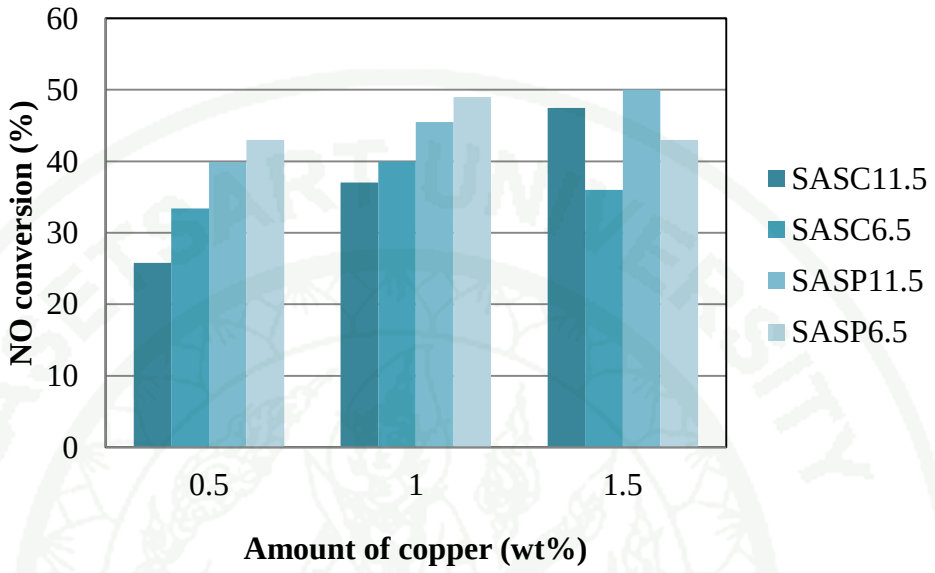

Figure 53 NO conversion of SASC and SASP samples at various copper contents (0.5-1.5 wt%)

These results could be explained that the composite materials synthesized at pH 6.5 providing the core-shell structure of silica-core and aluminosilicate-shell had a limitation of Cu incorporation because only the tetrahedral coordinated Al species located in the outer layer of the cluster domain that could be replaced by the Cu species. Therefore at too high of Cu loading, the hexagonal structure was deformed easily, the results was clearly seen from SAXS pattern in Figure 46, in addition the excess amount of Cu atoms that could not introduce into the framework was leached out during the washing process leading to the smaller remaining of copper contents than that of products synthesized at pH 11.5.

By using this technique, SASP11.5+1.5 exhibited the best catalytic activity of 50% NO conversion. The performance of this sample was compared to that of copper containing silica-BEA zeolite catalysts of Janas *et al*. (2009) which were synthesized by using the same technique. The catalytic activity of Janas's catalysts was shown in

Fig. 54. It was found that at the same copper content of 1.5 wt%, SASP11.5+1.5 showed a higher NO conversion for the whole temperature range.

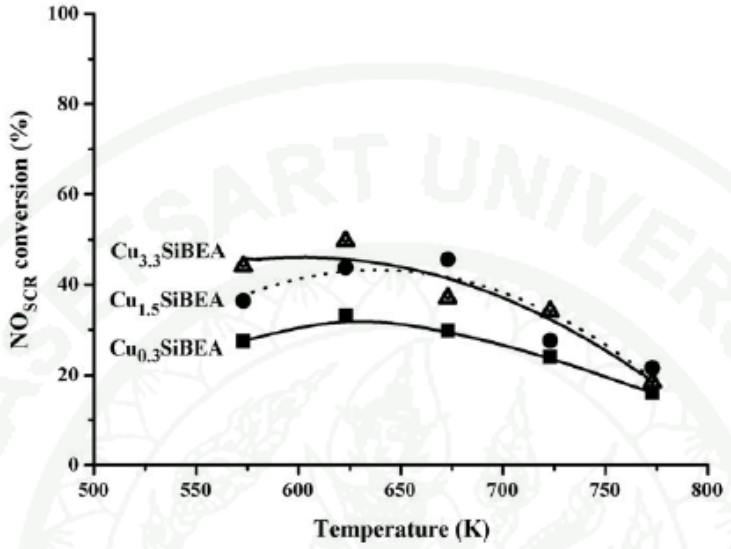

Figure 54 Temperature-dependence of NO conversion in SCR of NO by ethanol on $Cu_{0.3}$SiBEA $Cu_{1.5}$SiBEA and $Cu_{3.3}$SiBEA

Source: Janas *et al*. (2009)

In this work, the catalytic performances of samples prepared by using different techniques including the incipient wetness impregnation method and the substitution technique were compared. With 1.5 wt% of Cu loaded, all catalysts synthesized by substitution technique exhibited lower NO removal activity than those synthesized by incipient wetness impregnation method as shown in Figure 55.

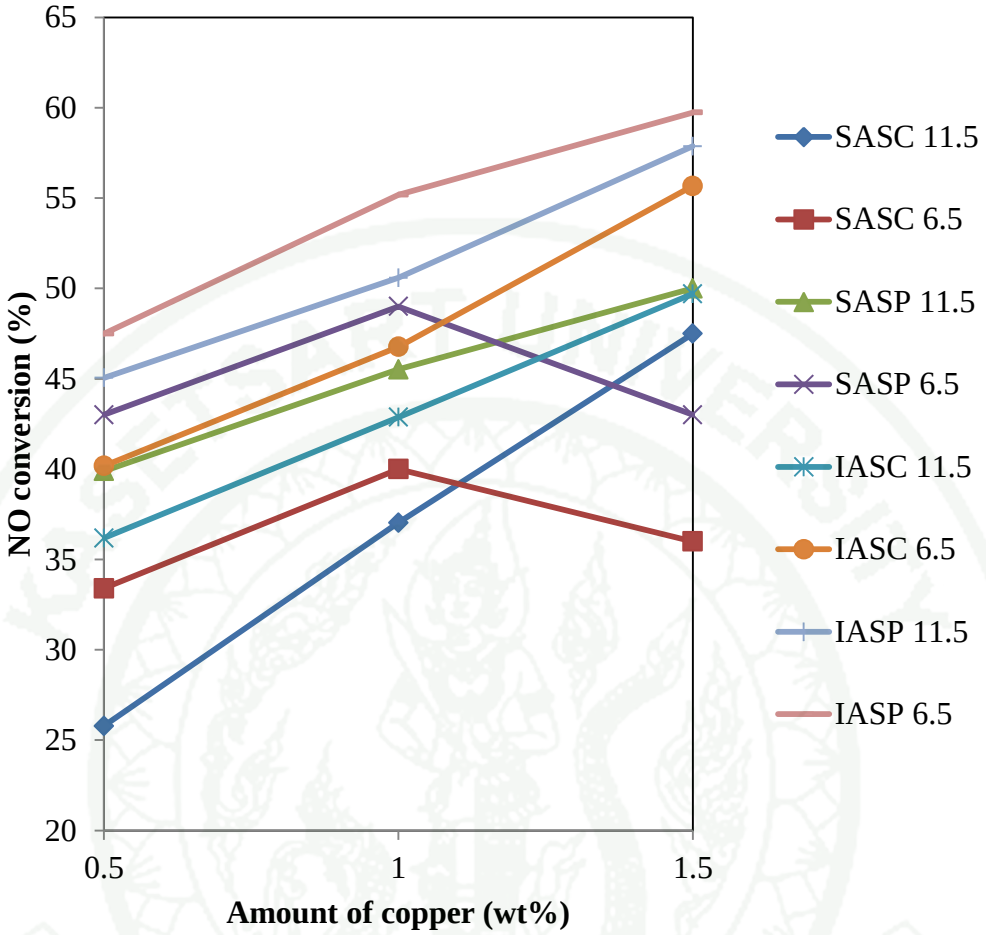

Figure 55 NO conversion of silica-aluminosilicate composites prepared in various conditions; pH values, chitosan addition and Cu loading methods

These results suggesting that the by using substation technique, the tetrahedral coordination of Cu^{2+} atoms were surrounded with four framework oxygen atoms, at this position the Cu^{2+} atoms was being in the most stable site then it was hard to be reduced. On the contrary, the products synthesized with impregnation method the copper metals were located on the outer surface and were easily reduced into Cu^{+1}, which was the active form to convert NO to N_2. As data shown in IR spectra, it was clearly seen that the catalysts synthesized by impregnation method revealed higher amount of Cu^{+1} than the catalysts prepared by substitution technique, and it could be concluded that the different synthesized techniques resulted in dissimilar Cu oxidation

states. It could be clarified that IASP6.5+1.5 showed the best performance of 59% NO conversion. The result was compared to other works which the catalysts were prepared by the impregnation method. It was found that 10 wt% of copper loaded on monolithic aluminosilicate-supported materials prepared by impregnation method showed the maximum NO conversion of 90% (Brandhorst *et al*. 2005). However, the different types of reducing agent, amount of copper content and reaction temperature may be the factors that affected the results.

Figure 56 shows the catalytic activity of two samples with 1.0 wt% of Cu loaded; IASC6.5+1.0 and SASC6.5+1.0. NO conversion data were collected every 15 minutes in order to study the stability of the catalysts. It was found that the catalytic activity of SASC6.5+1.0 showed the highest conversion at the earliest time and then the performance dropped continuously and maintained constant at around 40% conversion of NO. Conversely, the activity of IASC6.5+1.0 catalyst was not steady on time. This may cause from the copper metals which deposit on the outer surface were rapidly reacted and deactivated, in other words, they were reduced easily also therefore the performance of this catalyst were reversible.

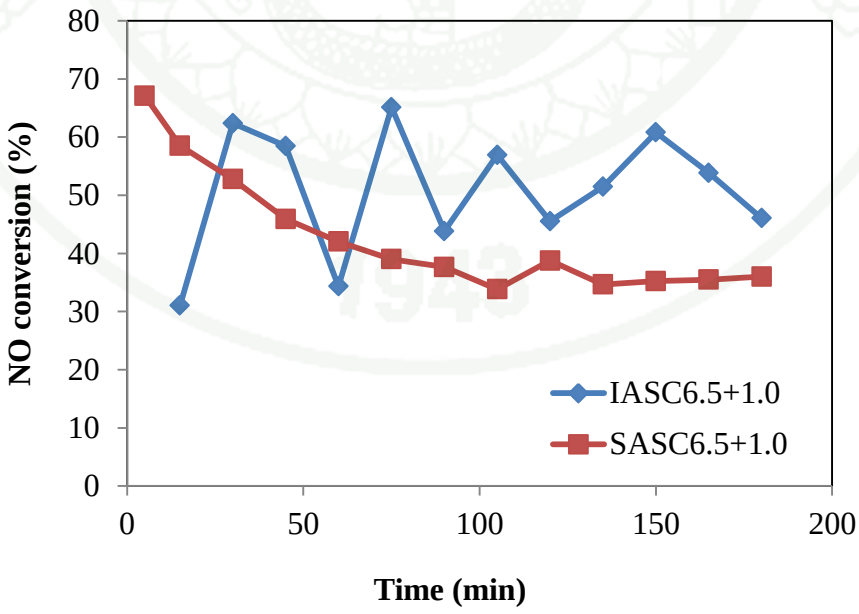

Figure 56 NO conversion of Cu-containing silica-aluminosilicate composites prepared with different methods; IASC6.5+1.0 and SASC6.5+1.0

When the effect of added chitosan on the was considered, it was found that the mesoporous silica–aluminosilicate composites prepared with chitosan addition showed a uniform and smaller domain size compared with those synthesized without chitosan addition. Bimodal mesopores with narrow pore size distributions (PSDs) in the diameter range of 2.5–4.0 nm were observed in all products synthesized with and without chitosan. The first peak at ≈ 2.5 nm should belong to mesoporous silica core and main matrix that was controlled by CTAB, whereas the smaller peak at ≈ 3.5 nm should belong to the aluminosilicate shell and the infiltrated aluminosilicate, the results could be described in the previous work (Chamnankid *et al*. 2011). Moreover, all products synthesized with chitosan addition revealed a relatively high macroporosity this can be attributed to the encapsulation of coagulated chitosan and after calcination process it was removed leaving large pores within the matrices, resulting in the increasing of average pore sizes and pore volumes of products synthesized with chitosan addition as given data in table 4. Figure 57 exhibits the pore size distribution (PSD) of ordered mesoporous silica-aluminosilicate prepared without Cu incorporation (a) and with 1.5 wt% Cu incorporation (b). The results showed that the macroporosity was still preserved after the introduction of 1.5 wt% copper by using substitution technique. However, all the products synthesized with chitosan addition showed a lower NO conversion than that of synthesized without chitosan in any copper contents. These may cause from a larger pore a higher chance for the copper to be overlapped. The formed multi-layer particle caused a lower metal distribution, less surface area and active site, resulted in the catalytic performances.

However, the intensity of the first peak was decreased in both products prepared with chitosan addition suggesting that there are less numbers of small pores around 2.5 nm, although the total pore volume and average pore diameter increased after the incorporation of 1.5 wt% of Cu but the small pores might be blogged by aggregated Cu cluster. Moreover, the addition of chitosan created a small domain providing a higher capillary force between cluster of silica-aluminosilicate composites leading to a higher amount of Cu atoms which were trapped inside the pores and were not leached out during the washing process thus the Cu atoms in SASC6.5 and

SASC11.5 materials were slightly higher than that of the products synthesized with chitosan SASP6.5 and SASP11.5, the data are shown in table 4.

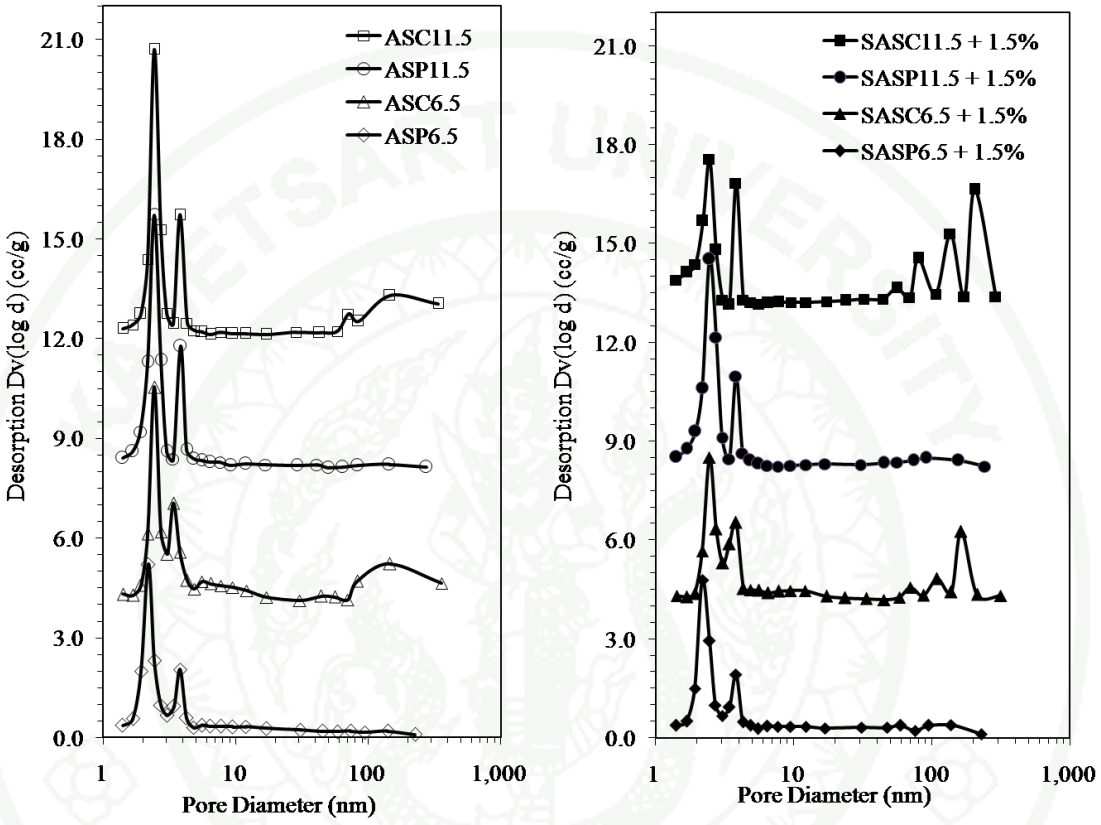

Figure 57 Pore size distribution of ordered mesoporous silica-aluminosilicate prepared without Cu loading (a) and with 1.5 wt% Cu loading (b)

CONCLUSIONS AND RECOMMENDATIONS

Conclusions

The mesoporous silica/aluminosilicate composite materials are successfully synthesized via a one-pot synthesizing process by using TEOS and aluminum nitrate as silica and alumina source, respectively. With the use of CTAB-chitosan as binary templates, it is found that the hexagonal pore structure is resulted from the effect of CTAB surfactant while the addition of chitosan brings about the controlling of cluster sizes and also the developing of macropores. In addition, the alternation of pH value affects the solubility of silica and the rate of hydrolysis-condensation process, resulting in the formation of unique morphology including the silica-core aluminosilicate-shell structure and uniformly infiltration of silica-aluminosilicate.

The performances of the synthesized materials are tested for the NO reduction process with the copper as an active metal. By studying the effect of copper metal incorporation methods, it is found that the samples prepared with the impregnation method show the higher activities than those prepared with substitution technique. These results may cause from the fact that the copper metals are mainly located on the outer surface and are easily reduced into Cu^{+1}, which is the active form to convert NO to N_2. On the other hand, by using the substation technique, the tetrahedral coordination of Cu^{2+} atoms is surrounded with four framework oxygen atoms. At this position the Cu^{2+} atoms are being in the most stable sites then they are difficult to be reduced. Moreover, it is found that the samples possessed core-shell structure show the catalytic activities better than that of acquired an infiltration phases, these may cause from an aluminosilicate shell is an active site where the reaction occurred. In addition, the added chitosan creates the macropores and also helps controlling the particles. The smaller particles the higher capillary force which traps the metals inside the pores though the excess metals may agglomerate and sintering during the calcination process, and may not enhance the catalytic performance at all.

Recommendations

Even though the results from this research indicated new findings for novel technique of nanostructured materials synthesis and their applications, the other issues related to this study should be further studied in detail. The recommendations regarding the further studies are given as follows.

1. As a result of this work, it was found that the catalytic activity for NO conversion greatly affected by the position of copper metals and copper oxidation state. Therefore it would be interested to study an ion-exchange technique in order to incorporate the copper species into the framework. By using this technique, the amount of copper loaded and located in the framework should be investigated by varying the concentration of copper and timing for ion exchanging. It is expected that catalysts prepared by should have two kinds of possibilities for copper active sites, including the $Cu^{2+} - O^{-}$ or $Cu^{2+} - O_2^{-}$ species which may form on the exchanged Cu-support and act as the active sites for NO reduction.

2. Copper-containing silica-aluminosilicate catalysts which were synthesized by using the substitution technique at various copper contents should be clarified the existence of hexagonal structure. By using this technique, it is expected that the incorporation of copper may affects the deformation of catalyst framework. Therefore the peaks intensity obtained from a small angle X-ray scattering spectroscopy of synthesized materials should be decreased as the copper content is increased.

3. The catalytic stability of the synthesized materials should be systematically investigated in a long term effect. In this work, the catalytic performances were recorded only for 3 hours and it was found that the catalysts synthesized by substitution technique showed a higher stability than those prepared by impregnation method. However, inconsistence data were obtained from the catalysts prepared by impregnation method. It could be described that free copper species deposited on the catalyst surface were easily to be reduced in the presence of H_2 as it was used as a

reducing agent during the reaction occurred. Conversely, the result and discussion of this phenomenon should be proved.

4. The synthesized catalysts should be determined the catalytic activity and stability for the NO reduction process in the presence of H_2O and O_2.

LITERATURE CITED

Andersson, J., M. Antonsson, L. Eurenius, E. Olsson and M. Skoglundh. 2007. Deactivation of diesel oxidation catalysts: vehicle- and synthetic aging correlations. **Appl. Catal., B-Environ.** 72(1-2): 71-81.

Anpo, M., M. Matsuoka, H. Mishima and H. Yamashita. 1997. The design of photocatalysts for the removal of NO_x at normal temperatures – copper (I) and silver (I) ion catalysts anchored within zeolite cavities**. Res. Chem. Intermed.** 23(3): 197-217**.**

Auroux, A., D. Sprinceana and A. Gervasini. 2000. Support effects on de-NOx Catalytic Properties of Supported Tin Oxides. **J. Catal.** 198: 140-150.

Aramendía, M.A., V. Borau, C. Jiménez, J.M. Marinas and F.J. Romero. 2004. Poly(ethylene oxide)-based surfactants as templates for the synthesis of mesoporous silica materials. **J. Colloid Interface Sci.** 269: 394–402.

Barrer R.M. 1982. **Hydrothermal Chemistry of Zeolites.** Academic Press. London.

Beck, J.S., J.C. Vartuli, W.J. Roth, M.E. Leonowicz, C.T. Kresge, K.D. Schmitt, C.T-W. Chu, D.H. Olson, E.W. Sheppard, S.B. Mccullen, J.B. Higgins and J.L. Schlenker. 1992. A new family of mesoporousmolecular sieves prepared with liquid crystal templates. **J. Am. Chem. Soc.** 114: 10834-10843.

Bertaux, J. and S. Dowell. 1989. Treatment-fluid selection for sandstone acidizing: permeability impairment in potassic mineral sandstones. **SPE Prod. Eng.** 4: 41–48.

Blackwell, C.S. 1979. Investigation of zeolite frameworks by vibrational properties. 1. The double-four-ring in group 3 zeolites. **J. Phys. Chem.** 83: 3251–3257.

Braga, T.P., E.C.C. Gomes, A.F. de Sousa, N.L.V. Carreño, E. Longhinotti and A. Valentini. 2009. Synthesis of hybrid mesoporous spheres using the chitosan as template. **J. Non-Cryst. Solids.** 355: 860–866.

Brandhorst, M., J. Zajac, D.J. Jones, J. Rozie`re, M. Womes, A. Jimenez-Lo´pez and E. Rodrı´guez-Castello´n. 2005. Cobalt-, copper- and iron-containing monolithic aluminosilicate-supported preparations for selective catalytic reduction of NO with NH_3 at low temperatures. **Appl. Catal., B-Environ.** 55: 267–276.

Brinker, C.J. and G.W. Scherer. 1990. **Sol–Gel Sci. The Physics and Chemistry of Sol–Gel Processing.** Academic Press Inc., New York.

Burch, R. and M.D. Coleman. 2002. An investigation of promoter effects in the reduction of NO by H_2 under lean-burn conditions. **J. Catal.** 208: 435–447.

Centi, G. and S. Perathoner. 1995. Role and importance of oxidized nitrogen oxide adspecies on the mechanism and dynamics of reaction over copper-based catalysts. **Appl. Catal., A-Gen.** 132: 179.

Chakarova, K., G. Petrova, M. Dimitrov, L. Dimitrov, G. Vayssilov, T. Tsoncheva and K.Hadjiivanov. 2011. Coordination state of Cu^+ ions in Cu-[Al]MCM-41. **Appl. Catal., B-Environ.** 106: 186– 194.

Chamnankid, B., T. Witoon, P. Kongkachuichay and M. Chareonpanich. 2011. One-pot synthesis of core–shell silica–aluminosilicate composites: effect of pH and chitosan addition. **Colloid. Surface. Physicochem. Eng. Aspect.** 380: 319–326.

Chao, M.C., H.P. Lin, C.Y. Mou, B.W. Cheng and C.F. Cheng. 2004. Synthesis of nano-sized mesoporous silicas with metal incorporation. **Catal. Today.** 97: 81-87.

Chareonpanich, M., T. Namto, P. Kongkachuichay and J. Limtrakul. 2004. Synthesis of ZSM-5 zeolite from lignite fly ash and rice husk ash. **Fuel Process. Technol.** 85: 1623–1634.

Chmielarz, L., P. Kus´trowski, M. Kruszec and R. Dziembaj. 2005. Nitrous oxide reduction with ammonia and methane over mesoporous silica materials modified with transition metal oxides. **J. Porous Mater.** 12: 183–191.

Chmielarz, L., P. Kus´trowski, R. Dziembaj, P. Cool and E.F. Vansant. 2006. Catalytic performance of various mesoporous silicas modified with copper or iron oxides introduced by different ways in the selective reduction of NO by ammonia. **Appl. Catal., B-Environ.** 62: 369–380.

Cipri, F., C. Bartuli, T. Valente and F. Casadei. 2007. Electromagnetic and mechanical properties of silica-aluminosilicatesplasma sprayed composite coatings. **J. Therm. Spray Technol.** 16(5-6): 831-838.

Corma, A. 1997. Frommicroporous to mesoporousmolecular sieve materials and their use in catalysis. **Chem. Rev.** 97: 2373.

Dˇedeˇcek, J., L. ˇCapek, P. Sazama, Z. Sobalík and B. Wichterlová. 2011. Control of metal ion species in zeolites by distribution of aluminium in the framework: From structural analysis to performance under real conditions of SCR-NOx and NO, N2O decomposition. **Appl. Catal., A-Gen.** 391: 244–253.

Dzwigaj, S., J.Janas, J.Mizera, J.Gurgul, R. P. Socha and M.Che. 2008. Incorporation of copper in SiBEA zeolite as isolated lattice mononuclear Cu(II) species and its role in selective catalytic reduction of NO by ethanol. **Catal. Lett.** 126: 36–42.

Falco, M., J. Retuert, A. Hidrobo, C. Covarrubias, P. Araya and U. Sedran. 2009. Catalytic performance of silica–aluminas synthesised with the help of chitosan biopolymer. **Appl. Catal., A-Gen.** 366: 269–274.

Fedeyko, J.M., H. Egolf-Fox, D.W. Fickel, D.G. Vlachos and R.F. Lobo. 2007. Initial stages of self-organization of silica–alumina gels in zeolite synthesis. **Langmuir.** 23: 4532–4540.

Fritz, A. and V. Pitchon. 1997. The current state of research on automotive lean NOx catalysis. **Appl. Catal., B: Environ.** 13: 1–25.

Fromherz, P. 1981. Micelle Structure: A surfactant-block model. **Chem. Phys. Lett.** 77: 460-465.

Gregory, J. and J. Duan. 2001. Hydrolyzing metal salts as coagulants. **Pure Appl. Chem.** 73: 2016–2017.

Held, W., A. Konig, T. Richter and L. Puppe. 1990. Catalytic NO_x reduction in net oxidizing exhaust gas. **SAE Paper** 900496.

Hidrobo, A., J. Retuert. P. Araya and E. Wolf. 2003. Aluminosilicates of bimodal porosity prepared by hydrothermal treatment starting from hybrid composites. **Emerging fields in sol-gel science and technology**. 123 – 131

Huang, L., W. Guo, P. Deng, Z. Xue and Q. Li. 2000. Investigation of synthesizing MCM-41/ZSM-5 composites. **J. Phys. Chem. B.** 104: 2817-2823.

Hui, F., C. Yan-hong, L. Chun-yi and S. Hong-hong. 2008. In-situ synthesis of ZSM-5 on silica gel and studies on its catalytic activity. **J. Fuel. Chem. Technol.** 36(2): 144-150.

Hungr´ıa, A. B., A. Iglesias-Juez, A. Mart´ınez-Arias, M. Fern´andez-Garc´ıa, J. A. Anderson, J. C. Conesa and J. Soria. 2002. Effects of copper on the catalytic properties of bimetallic Pd–Cu/(Ce,Zr)Ox/Al2O3 and Pd–Cu/(Ce,Zr)Ox catalysts for CO and NO elimination. **J. Catal.** 206: 281–294.

Huo, Q., D.I. Margolese, U. Ciesla, D.G. Demuth, P. Feng, T.E. Gier, P. Sieger, A. Firouzi, B.F. Chmelka, F. Schuth and G.D. Stucky. 1994. Organization of organic molecules with inorganic molecular species into nanocompositebiphasearrays. **Chem. Mater.** 6: 1176-1191.

Huo, Q., D.I. Margolese, U. Ciesla, P. Feng, T.E. Gier, P. Sieger, R. Leon, P. Petroff, F. Schuth and G.D. Stucky. 1994. Generalized synthesis of periodic surfactant inorganic composite material. **Nature.** 368: 317.

Ishizuki, N., K. Torigoe, K. Esumi and K. Meguro. 1991. Characterization of precious metal particles prepared using chitosan as a protective agent. **Colloids Surf.** 55: 15-21.

Iwamoto, M., H. Yahiro, K. Tanda, N. Mizuno, Y. Mine and S. Kagawa. 1990. Removal of nitrogen monoxide through a novel catalytic process. 1. Decomposition on excessively copper ion exchanged ZSM-5 zeolites. **J. Phys. Chem.** 95(9): 3727-3730.

Jana, S.K., H. Takahashi, M. Nakamura, M. Kaneko, R. Nishida, H. Shimizu, T. Kugita and S. Namba. 2003. Aluminum incorporation in mesoporous MCM-41 molecular sieves and their catalytic performance in acid-catalyzed reactions. **Appl. Catal., A-Gen.** 245: 33–41.

Janas, J., J. Gurgul, R.P. Socha and S. Dzwigaj. 2009. Effect of Cu content on the catalytic activity of CuSiBEA zeolite in the SCR of NO by ethanol: Nature of the copper species. **Appl. Catal., B-Environ.** 91: 217–224.

Jiang, X., G. Ding, L. Lou, Y. Chen and X.Zheng. 2004. Effect of ZrO_2 addition on CuO/TiO_2 activity in the NO + CO reaction. **Catal. Today.** 93–95: 811–818.

Joyner, R.W. and E.S. Shpiro. 1994. Handbook of American Chemical Society. *In* **Proceedings of the Symposia on Distillate Fuel Auto-Oxidation Chemistry 39**. Division of Petroleum Chemistry. San Diego. 103.

Karlsson, A., M. Stocker and R. Schmidt. 1999. Composites of micro- and mesoporousmaterials: Simultaneous syntheses of MFI/MCM-41 like phases by a mixed template approach. **Micropor. Mesopor. Mater.** 27: 181–192.

Karthik, M., L.Y. Lin and H. Bai. 2009. Bifunctionalmesoporous Cu–Al–MCM-41 materials for the simultaneous catalytic abatement of NOx and VOCs. **Micropor. Mesopor. Mater.** 117: 153–160.

Kharas, K.C.C., D.J. Liu and H.J. Robota. 1995. Structure-function properties in Cu-ZSM-5 NO decomposition and NO SCR catalysts. **Catal. Today.** 26: 129-145.

Kjoniksen, A.L., B. Nystrom, T. Nakken, O. Palmgren and T. Tande. 1997. Effect of surfactant concentration, pH, and shear rate on the rheological properties of aqueous systems of a hydrophobically modified chitosan and its unmodified analogue. **Polym. Bull.** 38: 71-79.

Kresge, C.T., M.E. Leonowicz, W.J. Roth, J.C. Vartuli and J.S. Beck.1992. Ordered mesoporous molecular sieves synthesized by a liquid-crystal template mechanism. **Nature.** 359: 710-712.

Lawrence, M. J. 1994. Surfactant systems: their use in drug delivery. **Chem. Soc. Rev.** 23: 417-424.

Lei, Q., T. Zhao, F. Li, Y.F. Wang and L. Hou. 2008. Zeolite beta monoliths with hierarchical porosity by the transformation of bimodal pore silica gel. **J. Por. Mater.** 15: 643–646.

Li, D., Y. Huang, K.R. Ratinac, S.P. Ringer and H. Wang. 2008. Zeolite crystallization in crosslinked chitosan hydrogels: Crystal size control and chitosan removal. **Micropor. Mesopor. Mater.** 116: 416–423.

LI, L., J.X. Chen, S.J. Zhang and N.J. Guan. 2005. In-situ Synthesis of Binderless ZSM-5 Zeolitic Coatings on Aluminum. **Chinese Chemical Letters.** 16: 253-256.

Li, L., P. Wu, Q. Yu, G. Wu and N. Guan. 2010. Low temperature H_2-SCR over platinum catalysts supported on Ti-containing MCM-41. **Appl. Catal., B-Environ.** 94: 254–262.

Li, Y. 2008 Synthesis of copper (II) oxide particle and detection of photoelectrochemically generated hydrogen. **NNIN REU Research Accomplishments.** 46-47.

Li, Y., Q. Yang, J. Yang and C. Li. 2006. Synthesis of mesoporous aluminosilicates with low Si/Al ratios using a single-source molecular precursor under acidic conditions. **J. Porous Mater.** 13: 187–193.

Li, Y., W. Zhang, L. Zhang, Q. Yang, Z. Wei, Z. Feng and C. Li. 2004. Direct synthesis of Al-SBA-15 mesoporous materials via hydrolysis-controlled approach. **J. Phys. Chem. B.** 108: 9739–9744.

Li, Y., W. Zhang, X. Wang, Y. Zhang, T. Dou and K. Xie. 2008. Synthesis, characterization, and catalytic properties of a hydrothermally stable beta/MCM-41 composite from well-crystallized zeolite beta. **J. Porous Mater.** 15: 133–138.

Lippmaa, E., A. Samoson and M. Magi. 1986. High-resolution aluminum-27 NMR of aluminosilicates**. J. Amer. Chem. Soc.**, 108: 1730-1735.

Liu, D.J., H.J. Robota. 1994. In situ characterization of Cu-ZSM-5 by X-ray absorption spectroscopy: XANES study of the copper oxidation state during selective catalytic reduction of nitric oxide by hydrocarbons. **Appl. Catal., B-Environ.** 4(2-3): 155-165.

Liu, L., J. Cai, L. Qi, Q. Yu, K. Sun, B. Liu, F. Gao, L. Dong and Y. Chen. 2010. Influence of supports structure on the activity and adsorption behavior of copper-based catalysts for NO reduction. **J. Mol. Catal. A: Chem.** 327: 1–11.

Long, R.Q. and R.T. Yang. 1999. Selective catalytic reduction of nitric oxide with ethylene on copper ion-exchanged Al-MCM-41 catalyst. **Ind. Eng. Chem. Res.** 38: 873-878.

Mehner, A., J. Dong, T. Prenzel,W.Datchary and D.A. Lucca. 2010. Mechanical and chemical properties of thick hybrid sol–gel silica coatings from acid and base catalyzed sols. **J. Sol–Gel Sci. Technol.** 54: 355.

Mi, F.L., H.W. Sung, S.S. Shyu, C.C. Su and C.K. Peng. 2003. Synthesis and characterization of biodegradable TPP/genipin co-crosslinked chitosan gel beads. **Polymer.** 44: 6521–6530.

Miha´lyi, R.M., Z. Schay and A´.Szegedi. 2009. Preparation of In,H-ZSM-5 for DeNOx reactions by solid-state ion exchange. **Catal. Today.** 143: 253–260.

Molvinger, K., F. Quignard, D. Brunel, M. Boissie`re and J.M. Devoisselle. 2004. Porous chitosan-silica hybrid microspheres as a potential catalyst. **Chem. Mater.** 16: 3367-3372.

Mozgawa, W. and M. Sitarz. 2002. Vibrational spectra of aluminosilicate ring structures. **J. Mol. Struct.** 614: 273–279.

Myers, D. 1992. **Surfactant Science and Technology.** VCH. New York.

Nachtigallova, D., P.Nachtigall and J. Sauer. 2001. Coordination of Cu^{+}'and Cu^{2+} ions in ZSM-5 in the vicinity of two framework Al atoms. **Phys. Chem. Chem. Phys.** 3: 1552-1559.

Ogura, M. 2008. Towardsrealization of a micro- and mesoporous composite silicate catalyst. **Catal. Surv. Asia.** 12: 16–27.

Oh, K.S. and S.I. Woo. 2006. Catalytic property of Pt/AlSBA-15 in selective catalytic reduction of NO. **Catal. Lett.** 110(3–4): 247-254.

Palomares, A.E., J.G. Prato and A. Corma. 2002. A new active zeolite structure for the selective catalytic reduction (SCR) of nitrogen oxides: ITQ7 zeolite the influence of NO_2 on this reaction. **Catal. Today.** 75: 367–371.

Pantazis, C.C. and P.J. Pomonis. 2006. Synthesis of highly loaded Cu/Ce mesoporous silica active catalyst for the simultaneous reduction of SO_2 and NO with CO. **Chem. Commun.** 28(12): 1268–1270.

Papageorgiou, S.K., E.P. Favvas, A. A. Sapalidis, G.E. Romanos and F.K. Katsaros. 2011. Facile synthesis of carbon supported copper nanoparticles from alginate precursor with controlled metal content and catalytic NO reduction properties. **J. Hazard. Mater.**189: 384 – 390.

Pedroni, V., P.C. Schulz, M.E. Gschaider de Ferreira and M.A. Morini. 2000. A chitosan-templated monolithic siliceous mesoporous-macroporous material. **Colloid. Polym. Sci.** 278: 964-971.

Phillips, R.L., E.M. Allen and R.I. Kirkpatrick. 1995. High-resolution 27Al-NMR ofaluminosilicates, pp. 39-45. *In* P.J. Dirken, A.P.M. Kentgens and G.H. Nachtegaal, eds. Solid-state MAS NMR study of pentamericaluminosilicate groups with 180° intertetrahedral AI–Q–Si angles in zunyite and harkerite**. Am. Miner.** 80: 39-45.

Prokesˇova´-Fojtı´kova´, P., S. Mintova, J. Cˇejka, N. Zˇilkova´ and A. Zukal. 2006. Porosity of micro/mesoporous composites. **Micropor. Mesopor. Mater.** 92: 154–160.

Metkar, P.S., M.P. Harold and V.Balakotaiah. 2012. Selective catalytic reduction of NOx on combined Fe- and Cu-zeolite monolithic catalysts: Sequential and dual layer configurations. **Appl. Catal., B-Environ.**111–112: 67–80.

Richter, M., R. Eckelt, B. Parlitz and R. Fricke. 1998. Low-temperature conversion of NO_x to N2 by zeolite-fixed ammonium ions. **Appl. Catal., B-Environ.** 15: 129–146.

Rimer, J.D., R.F. Lobo and D.G. Vlachos, 2005. Physical Basis for the Formation and Stability of Silica Nanoparticles in Basic Solutions of Monovalent Cations. **Langmuir**. 21; 8960-8971.

Roy, S., M.S. Hegde and G. Madras. 2009. Catalysis for NOx abatement. **Appl. Energy.** 86: 2283–2297.

Ryoo, R. and J. M. Kim. 1995. Structural order in MCM-41 controlled by shifting silicate polymerization equilibrium. **J. Chem. Soc. Chem. Commun.** 711-712.

Schay, Z., V.S. James, G. Pa´l-Borbe´ly, A. Beck, A.V. Ramaswamy and L. Guczi. 2000. Decomposition and selective catalytic reduction of NO by propane on CuZSM-5 zeolites: a mechanistic study. **J. Mol. Catal. A: Chem.** 162: 191–198.

Scholz, C.M.L., K.M. Nauta, M.H.J.M. de Croon and J.C. Schouten. 2008. Kinetic modeling of NO_x storage and reduction with different reducing agents (CO, H_2, and C_2H_4) on a Pt–Ba/γ-Al2O3 catalyst in the presence of CO_2 and H_2O. **Chem. Eng. Sci.** 63: 2843 – 2855.

Shen, S.C. and S. Kawi. 2003. Selective catalytic reduction of NO by hydrocarbons in the presence of excess oxygen using Pt/MCM-41 catalysts. **Appl. Catal., B-Environ.** 45: 63–76.

Shibata, J., M. Hashimoto, K. Shimizu, H. Yoshida, T. Hattori and A Satsuma. 2004. Factors controlling activity and selectivity for SCR of NO by Hydrogen over supported platinum catalysts. **J. Phys. Chem. B.** 108: 18327-18335.

Si, Z., D. Weng, X. Wu, J. Li and G. Li.2010. Structure, acidity and activity of $CuO_x/WO_x–ZrO_2$ catalyst for selective catalytic reduction of NO by NH_3. **J. Catal.**271: 43-51.

Spassova, I., M. Khristova, D. Panayotov and D. Mehandjiev. 1999. Coprecipitated $CuO–MnO_x$ catalysts for low-temperature CO–NO and CO–NO–O_2reactions. **J. Catal.** 185: 43–57.

Sultana, A., M. Haneda, T. Fujitani and H. Hamada. 2008. Role of zeolite structure on NO reduction with diesel fuel over Pt supported zeolite catalysts. **Micropor. Mesopor. Mater.** 111: 488–492.

Sun, J.H., Z. Shan, T. Maschmeyer and M.O. Coppens. 2003. Synthesis of bimodal nanostructured silicas with independently controlled small and large mesopore sizes. **Langmuir.** 19: 8395-8402.

Tao, F., M.E. Grass, Y. Zhang, D. R. Butcher, J.R. Renzas, Z. Liu, J.Y. Chung, B.S. Mun, M. Salmeron and G.A. Somorjai. 2008. Reaction-driven restructuring of Rh-Pd and Pt-Pd core-shell nanoparticles. **Sci.** 322: 932-934.

Tagirov, B., J. Schott, J.C. Harrichoury and J. Escalier. 2004. Experimental study of the stability of aluminate–borate complexes in hydrothermal solutions. **Geochim. Cosmochim. Acta.** 68: 1333–1345.

Tsai, M.S. and M.J. Li. 2006. A novel process to prepare a hollow silica sphere via chitosan-polyacrylic acid (CS-PAA) template. **J. Non-Cryst. Solids**. 352: 2829–2833.

Tseng, H.H., H.Y. Lin, Y.F. Kuo and Y.T. Su. 2010. Synthesis, characterization, and promoter effect of Cu-Zn/-Al2O3 catalysts on NO reduction with CO. **J. Chem. Eng.** 160: 13–19.

Vu, D.V., M. Miyamoto, N. Nishiyama, Y. Egashira and K. Ueyama. 2009. Morphology control of Silicalite/HZSM-5 composite catalysts for the formation of para-xylene. **Catal. Lett.** 127: 233–238.

Wan, Y., J. Ma, Z. Wang, W. Zhou and S. Kaliaguine. 2004. Selective catalytic reduction of NO over Cu-Al-MCM-41. **J. Catal.** 227: 242–252.

Wang, C., G. Zhu, T. Shang, X. Cai, C. Liu, N. Li, Y. Wei, J. Li, W. Zhang and S. Qiu. 2005. Ordered hexagonal mesoporous aluminosilicates synthesized using zeolite as precursor and the wall-thickness tuned by pH control. **Solid State Commun.** 135: 257–259.

Wen, B. 2002. NO reduction with H_2 in the presence of excess O_2 over Pd/MFI catalyst. **Fuel**. 81: 1841–1846.

Witoon, T., M. Chareonpanich and J. Limtrakul. 2008. Synthesis of bimodal porous silica from rice husk ash via sol–gel process using chitosan as template. **Mater. Lett.** 62: 1476–1479.

Witoon, T., M. Chareonpanich and J. Limtrakul. 2009. Effect of acidity on the formation of silica–chitosan hybrid materials and thermal conductive property. **J. Sol-Gel Sci. Technol.** 51(2): 146-152.

Wu, P., L. Li, Q. Yu, G. Wu and N. Guan. 2010. Study on Pt/Al-MCM-41 for NO selective reduction by hydrogen. **Catal. Today.** 158: 228-234.

Yahiro, H. and M. Iwamoto.2001. Copper ion-exchanged zeolite catalysts in deNO_x reaction. **Appl. Catal., A-Gen.** 222: 163–181.

Yang, X.Y., A. Vantomme, F.S. Xiao and B.L. Su. 2007. Ordered mesoporous aluminosilicates with very low Si/Al ratio and stable tetrahedral aluminum sites for catalysis. **Catal. Today.** 128: 123–128.

Yang, X.Y., Y. Li, G. V. Tendeloo, F.S. Xiao and B.L. Su. 2009. One-pot synthesis of catalytically stable and active nano-reactors: encapsulation of size-controlled nanoparticles within a hierarchically macroporous core ordered mesoporous shell system. **Adv. Mater.** 21: 1–5.

Zhai, S.R., C.S. He, D. Wu and Y.H. Sun. 2007. Hydrothermal synthesis of mesostructured aluminosilicate nanoparticles assisted by binary surfactants and finely controlled assembly process. **J. Non-Cryst. Solids.** 353: 1606–1611.

Zhai, S.R., J.L. Zheng, D. Wu, Y.H. Sun and F. Deng. 2005. CTAB-assisted fabrication of mesoporous composite consisting of wormlike aluminosilicate shell and ordered MSU-S Core. **J. Solid State Chem.** 178: 85–92.

Zhang, H. and Y. Li. 2008. Preparation and characterization of beta/MCM-41 composite zeolite with a stepwise-distributed pore structure. **Powder Technol.** 183: 73–78.

Zhou, S., B. Varughese, B. Eichhorn, G. Jackson and K. McIlwrath. 2005. Pt–Cu core–shell and alloy nanoparticles for heterogeneous NOxreduction: anomalous stability and reactivity of a core–shell nanostructure. **Angew. Chem. Int. Ed.** 44: 4539 –4543.

APPENDICES

Appendix A

Qualitative and Quantitative Results from Gas Chromatography

Quantitative and Qualitative Results from Gas Chromatography

Gas chromatography was performed in a specially designed instrument. The major instrumental components consisted of a flowing mobile phase, an injector port, a separation column containing the stationary phase, a detector, and a data recording system as shown in Appendix Figure A1. Certain amount of gaseous mixture, 0.5 mL in this research, was injected into gas chromatograph at the injector port and was volatilized in a hot injection chamber before it was transported to the head of the chromatic column. Then, a flow of inert carrier gas (as a mobile phase) swept the injected mixture through a heated column which contained the stationary phase. The gaseous sample moved along the packing column whereas its component gas moved with different flow rates and thus separated into pure component. Before each component exited the instrument, it passed through a detector. The detector sent an electronic signal to the recorder and the analyzed results were printed out.

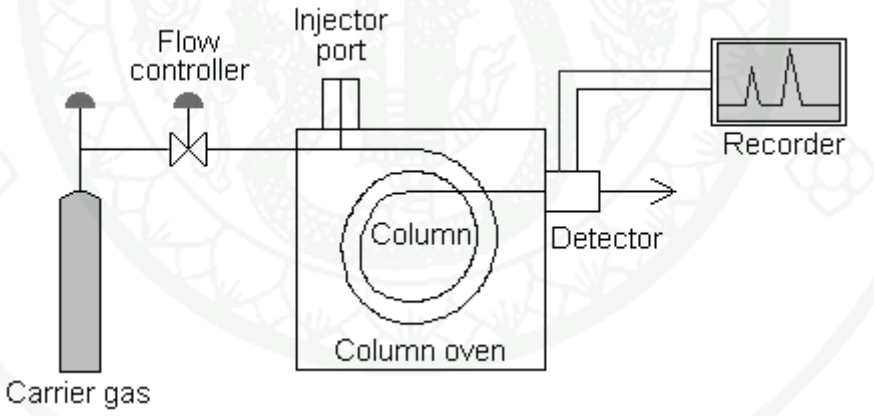

Appendix Figure A1 Schematic diagram of gas chromatograph.

In this work, the quantitative and qualitative data of product composition was obtained from TCD-gas chromatography as mention in the experimental chapter. Before analysis, the condition of operation was set and kept on running for about an hour to stabilize the based line. Certain volume of sample mixture (0.5 mL in this case) was injected into the injection port by gas syringe. After the mixture of sample gas was analyzed, the qualitative and quantitative data were interpreted from the peak

area obtained from the recorder. The component of injected gas mixture can be identified by using the value of retention time data compared with the retention time received from injected standard gas.

The quantitative analysis of gas samples were obtained from the calibration curves where the correlation between the amount of injected gas sample (mole) and the peak area of gas chromatograms were proposed. The correlation between these parameters (mole and area) was analyzed by a linear regression equation.

The calculation for the amount of each component in a standard-gas mixture can be calculated as follows:

$$\text{Amount of component}_i \text{ (mol)} = \frac{V_i \times T}{100 \times 22{,}400}$$

where V_i = % volume of component$_i$ (cm^3/cm^3)

T = volume of standard gases mixture (mL)

Appendix B

Small angle X-ray scattering (SAXS) of mesoporous silica-aluminosilicate

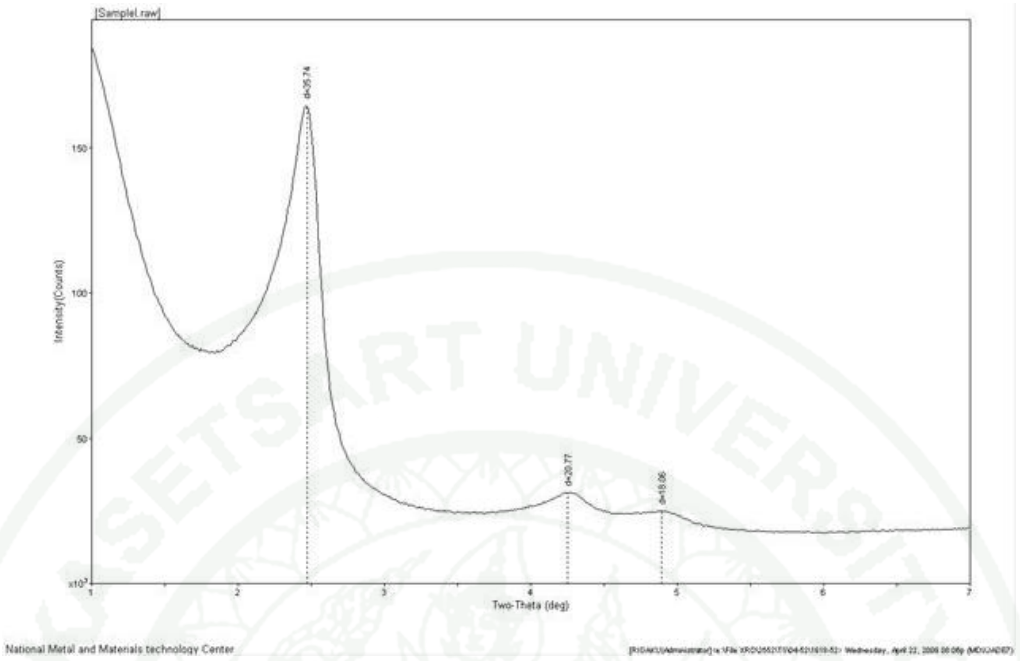

Appendix Figure B1 SAXS pattern of mesoporous silica-aluminosilicate (ASC11.5-11.5)

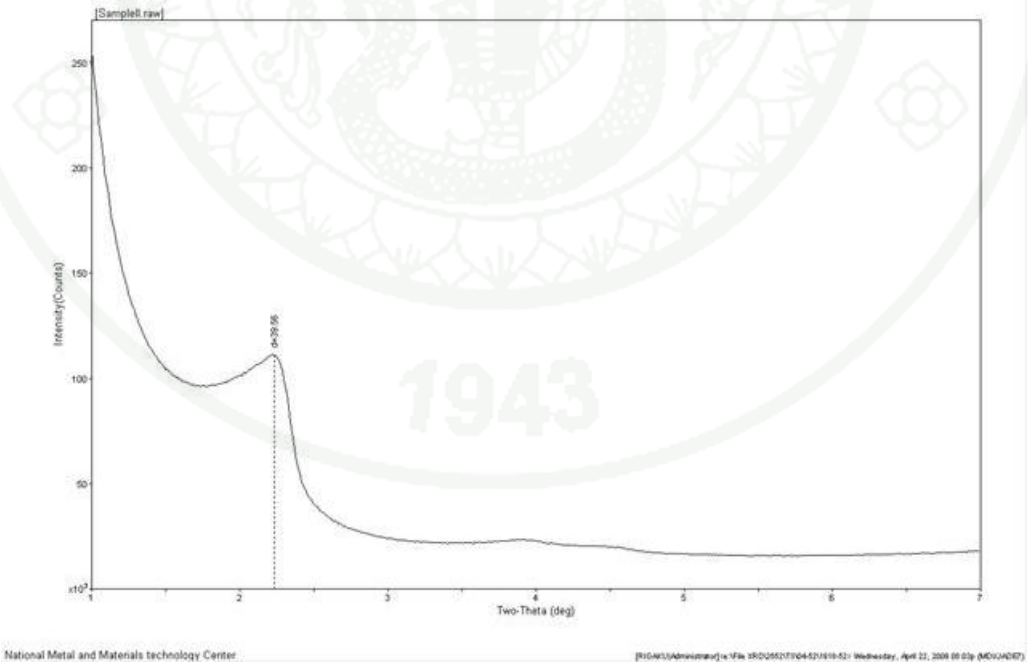

Appendix Figure B2 SAXS pattern of mesoporous silica-aluminosilicate (ASC11.5-6.5)

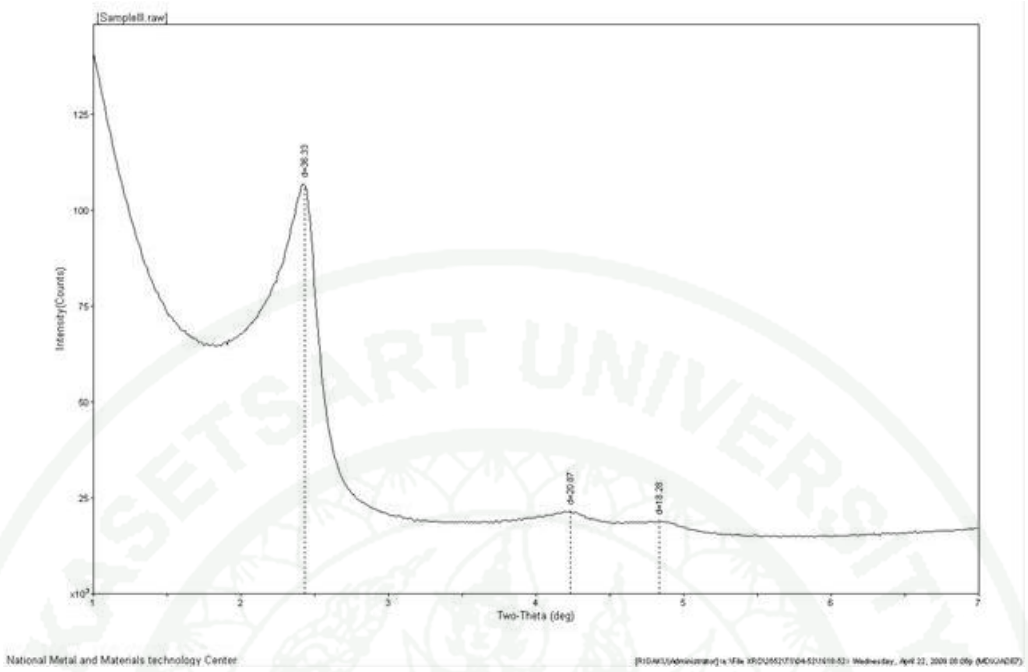

Appendix Figure B3 SAXS pattern of mesoporous silica-aluminosilicate (ASC6.5-6.5)

Appendix C

Small angle X-ray scattering (SAXS) of Cu-containing silica-aluminosilicate

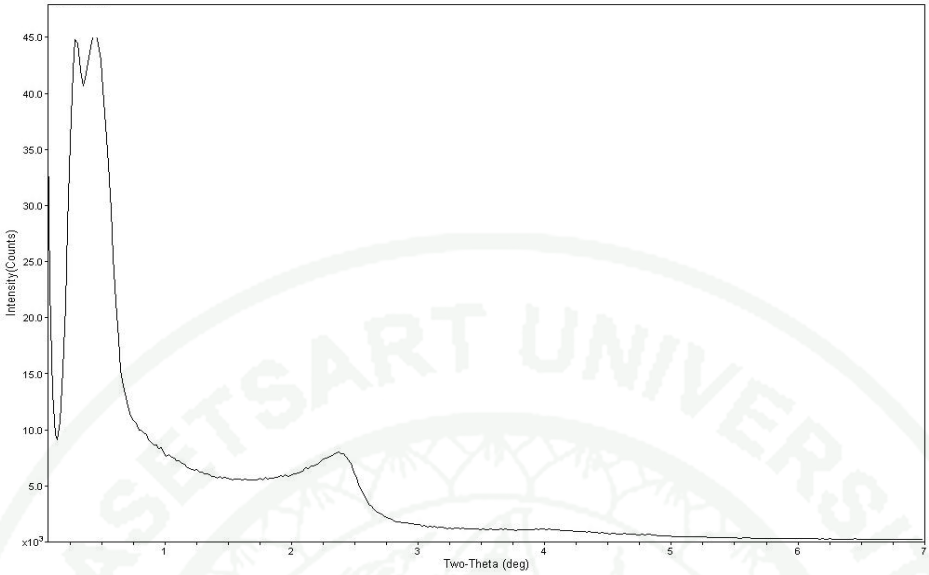

Appendix Figure C1 SAXS pattern of mesoporous silica-aluminosilicate prepared at pH 11.5 with chitosan addition and 1.5 wt % of Cu (SASC11.5 + 1.5)

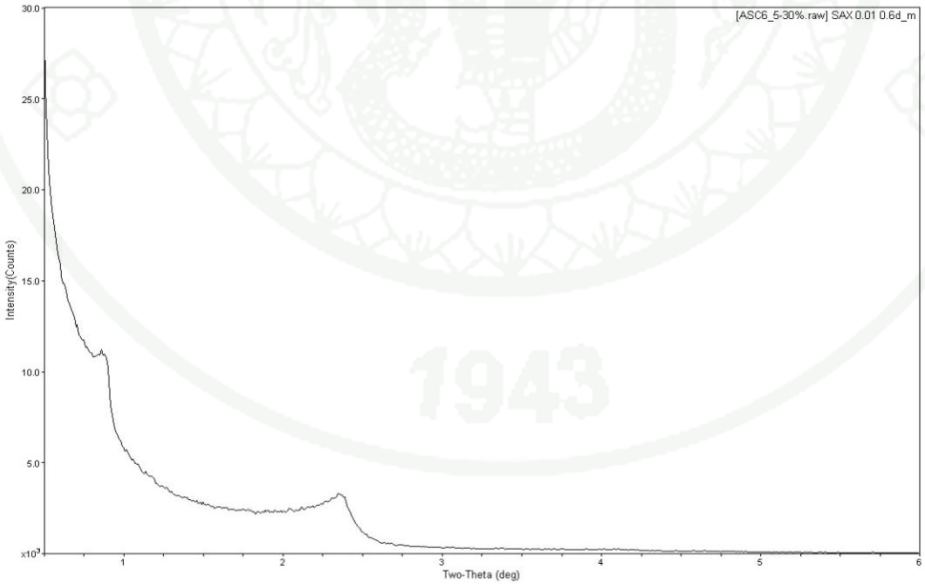

Appendix Figure C2 SAXS pattern of mesoporous silica-aluminosilicate prepared at pH 6.5 with chitosan addition and 1.5 wt % of Cu (SASC6.5 + 1.5)

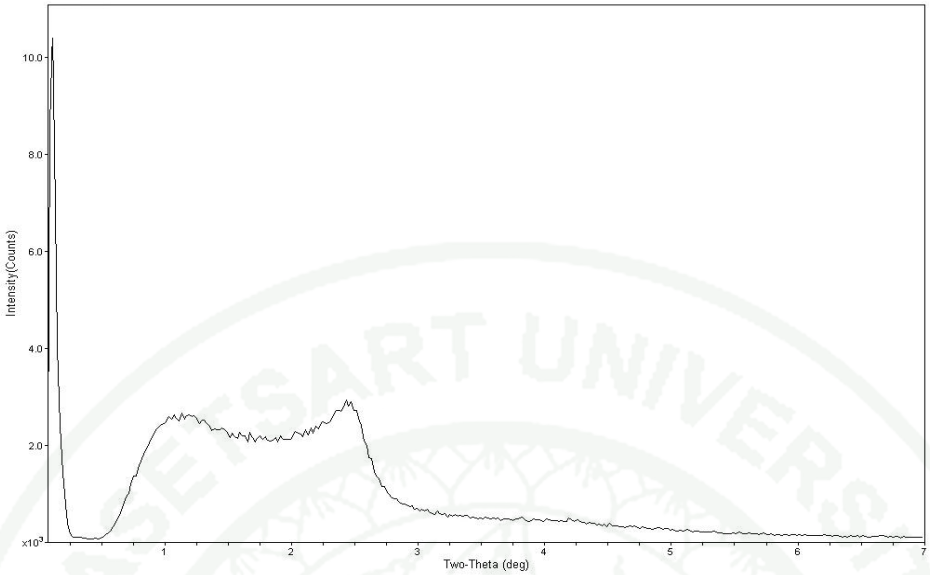

Appendix Figure C3 SAXS pattern of mesoporous silica-aluminosilicate prepared at pH 11.5 without chitosan addition and 1.5 wt % of Cu (SASP11.5 + 1.5)

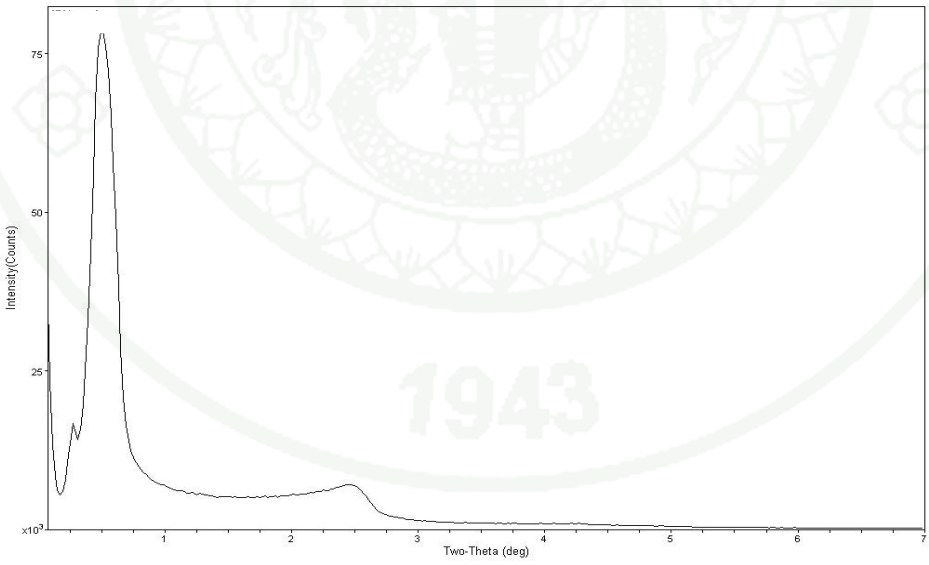

Appendix Figure C4 SAXS pattern of mesoporous silica-aluminosilicate prepared at pH 6.5 without chitosan addition and 1.5 wt % of Cu (SASP6.5 + 1.5)

Appendix D

Transmission Electron Microscopy (TEM) and
Elemental Dispersion X-ray Analysis (EDS) Results

Sample preparation for TEM-EDS

1. Embedding: Powder sample was embedded in epoxy resin, by using silicon embedding case (Cure temperature of resin ～60℃).

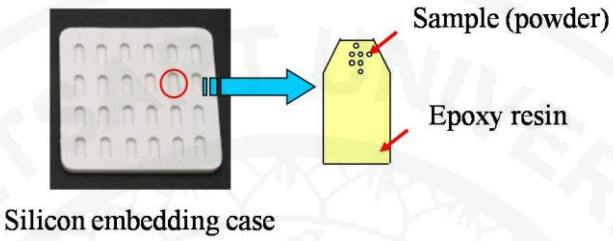

2. Sectioning: Resin block, including sample, was sliced to ultrathin sections (thickness <100 nm) by using ultramicrotome. The sections float off onto water in trough.

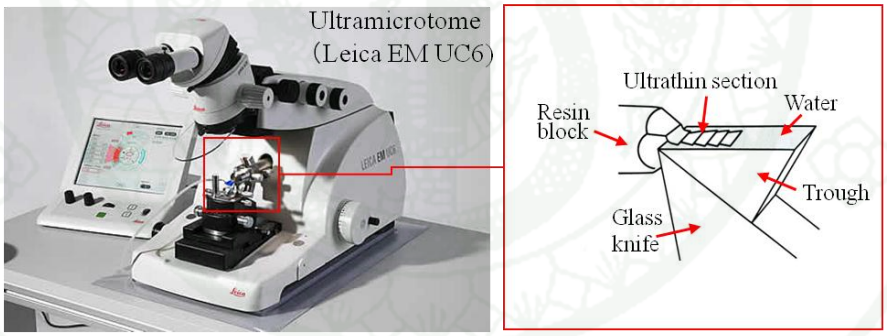

3. Mounting: Ultrathin sections was collected and mounted on a TEM grid by using tweezers

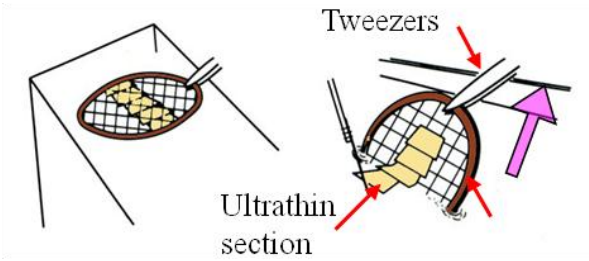

ASC6.5-6.5 Sample

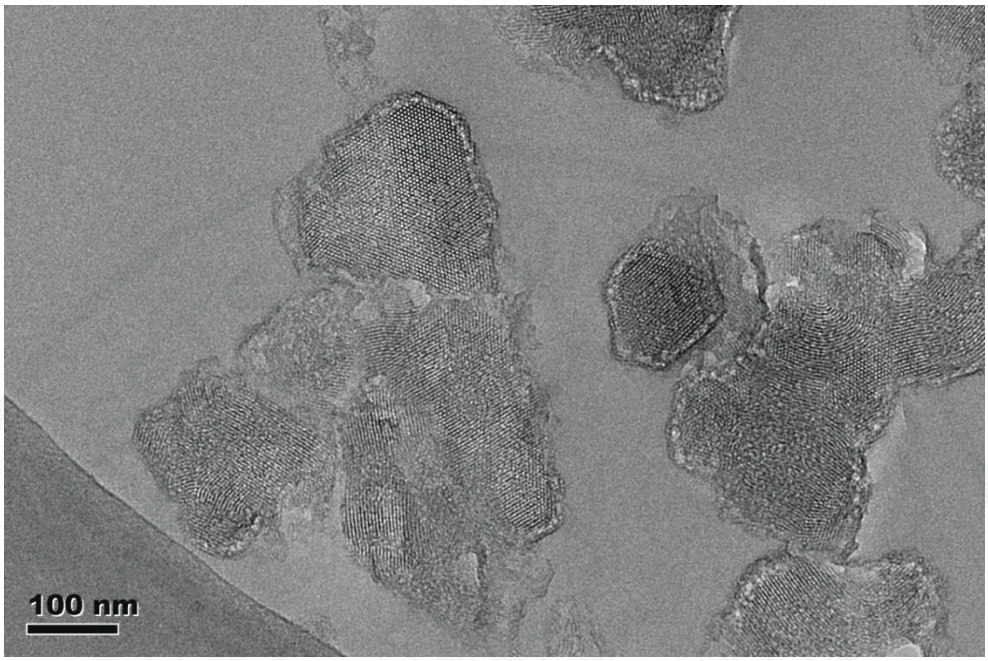

Appendix Figure D1 TEM image of ASC6.5-6.5

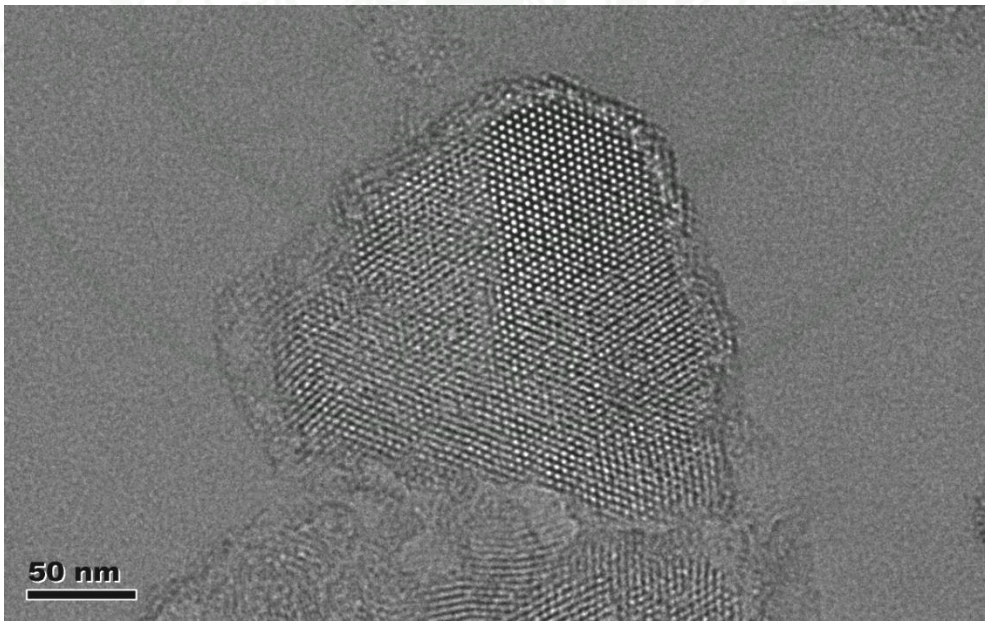

Appendix Figure D1 TEM image (high magnification) of ASC6.5-6.5

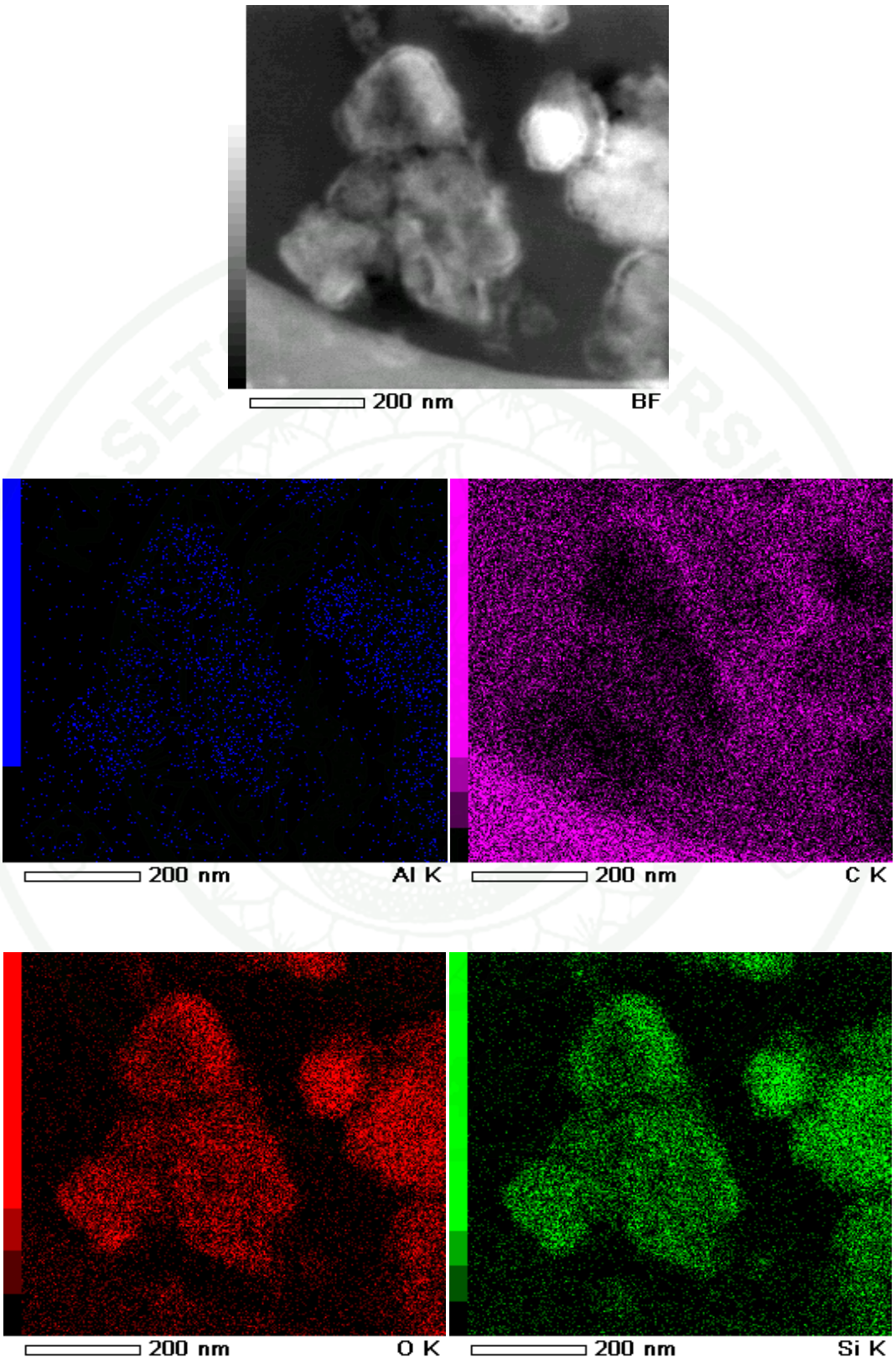

Appendix Figure D3 EDS X-ray mapping

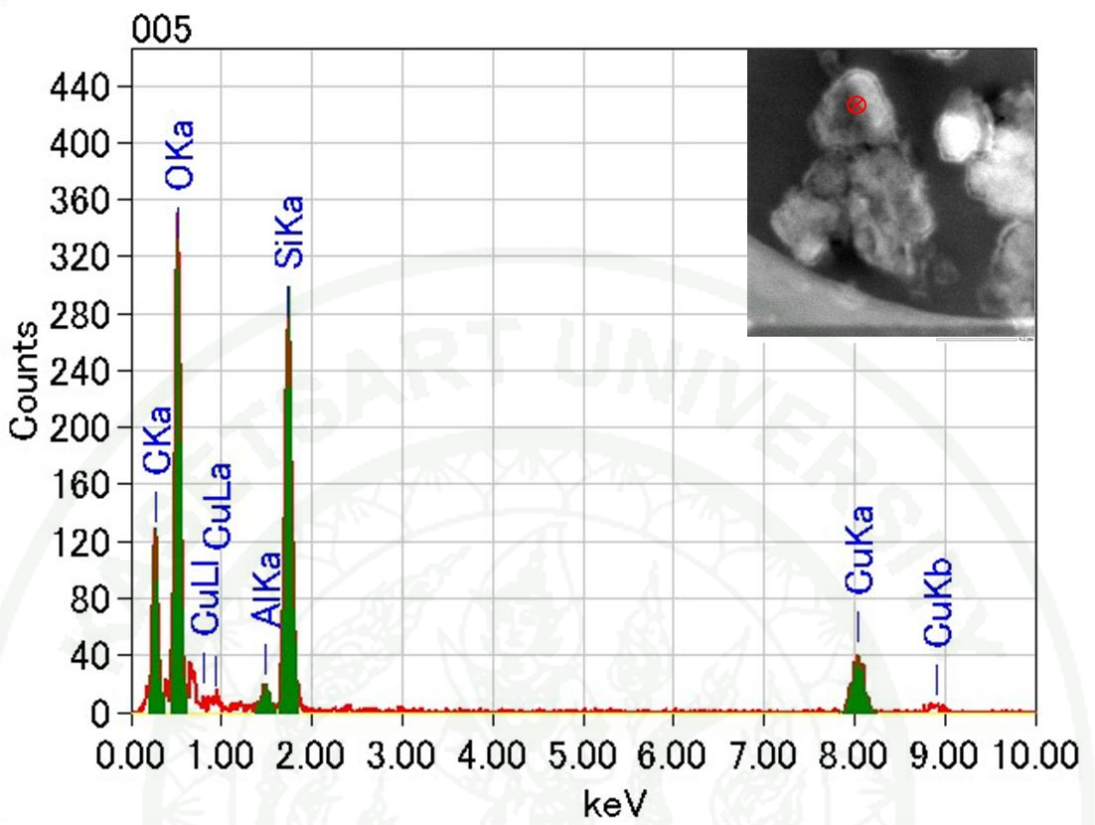

Appendix Figure D4 EDS X-ray point analysis of elements of ASC6.5-6.5

CURRICULUM VITAE

NAME : Miss Busaya Chamnankid

Date of Birth : April 5, 1984

BIRTH PLACE : Bangkok, Thailand

EDUCATION :

YEAR	**INSTITUTE**	**DEGREE**
2007	Thammasat Univ.	B.Sc. 2nd honor (Chemical)
2011	Kasetsart Univ.	D.Eng. (Chemical)

SCHOLARSHIP/AWARDS :
- Royal Golden Jubilee Ph.D. Scholarship (Grant No. PHD/0182/2008), Thailand Research Fund (TRF) 2009-2012
- : The Asian Development Bank (ADB) Scholarship 2007-2009
- : JASSO Short-Term Student Exchange Promotion Program (Inbound) Scholarship at University of Tsukuba Japan 2005-2006
- : Human Resource Development in Science Project (Science Achievement Scholarship of Thailand, SAST) 2003-2007